الجمهـــورية الجزائـــــرية الديمقـــــراطية الشعـــــــبية
People's Democratic Republic of Algeria
وزارة التعليم العالي والبحث العلمي
Ministry of Higher Education and Scientific Research
جـــامعة محمد بوضـــياف – بالمســـــيلة
Mohamed BOUDIAF University – M'Sila

جامعة محمد بوضياف - المسيلة
Université Mohamed Boudiaf - M'sila

كـلية التكنـــولـــوجيـا
Faculty of Technology

نيابة العمادة لما بعد التدرج والبحث العلمي والعلاقات الخارجية
Vice Deanship of Post-Graduation, Scientific Research and External Relations

رقم: 162/ ن.ع.ب.ع /ك.ت /2026

المسيلة في: 25 ماى 2026

شهادة ادارية

المصادقة على تقارير خبرة للموافقة على مطبوعة بيداغوجية

بعد الإطلاع على تقارير لجنة الخبراء للموافقة على المطبوعة البيداغوجية للأستاذ : **برابح فؤاد – أستاذ محاضر قسم أ** ، بقسم الهندسة المدنية بكلية التكنولوجيا بجامعة محمد بوضياف بالمسيلة والتي كانت كلها ايجابية.

تمّ تقرير التّالي:

1-المصادقة على تقارير لجنة الخبراء للموافقة المطبوعة البيداغوجية والمعنونة بـــ:

Soil Mechanics 2
Third year of License-Civil engineering

2- حيث تمّ تشكيل هذه اللجنة بناءاً على إجتماع اللجنة العلمية لقسم الهندسة المدنية المنعقد بتاريخ: 2026/04/27.
المكونة من السّادة الآتية أسماؤهم:

- **صديقي أحمد**، أستاذ محاضر "أ"، جامعة محمد بوضياف- المسيلة.
- **بكير نسيمة**، أستاذ محاضر "أ"، جامعة محمد بوضياف- المسيلة.
- **مفتاح عبد المجيد**، أستاذ محاضر "أ"، جامعة قسنطينة.

وتمت الموافقة بالاجماع على هذه المطبوعة.

رئيس المجلس العلمي للكلية

المجلس العلمي

د. علي جريوي

Mohamed Boudiaf University - M'sila

Faculty of Technology

Department of Civil Engineering

Lecture notes on:

Soil Mechanics 2

Course and exercises

by :

Dr. Fouad BERRABAH

Intended for:

3rd Year Civil Engineering Students

Academic Year 2025-2026

Preface

Soil behavior under loading is a fundamental concern in civil engineering, as it directly governs the performance and safety of structures. Unlike rigid materials, soils exhibit complex responses that depend on stress conditions, time effects, and environmental influences. Understanding how soils deform, consolidate, and fail under various loading conditions is therefore essential for the design and analysis of geotechnical structures.

This course, "**Soil Mechanics 2**", is intended for third-year civil engineering students. It focuses on the mechanical behavior of soils and provides the theoretical and practical tools required for analyzing engineering problems related to foundations, earthworks, and geotechnical structures.

The course is organized into four main chapters. The first chapter addresses stresses and strains in soils, introducing the concepts of stress distribution, effective stress, and soil deformation. The second chapter focuses on settlement and consolidation, examining time-dependent deformation and the mechanisms governing volume change in saturated soils. The third chapter is devoted to the shear strength of soils, which is essential for stability analysis of slopes, foundations, and retaining structures. The fourth chapter presents soil investigation and exploration methods, emphasizing field and laboratory techniques used to characterize soil properties and reduce uncertainties in design.

Each chapter is supported by examples and exercises aimed at developing analytical skills and preparing students for real-world engineering situations. This course constitutes a key step toward advanced studies in geotechnical engineering and provides essential knowledge for professional practice in civil engineering.

Fouad BERRABAH

M'sila, 2026

Contents

Chapter 1
Stresses and strains

1.1 Concept of stress – Basic notions

Let a solid body (S) be subjected to a system of surface forces. Consider a fictitious plane (P) that divides the solid in the vicinity of point M into two parts (I) and (II).

Let dS be a small surface element surrounding point M.

Let $\overrightarrow{dF}$ be the force exerted on dS by part (II) on part (I).

The stress vector at point M on the surface element dS is defined as:

$$\vec{f} = \frac{d\vec{F}}{dS}$$

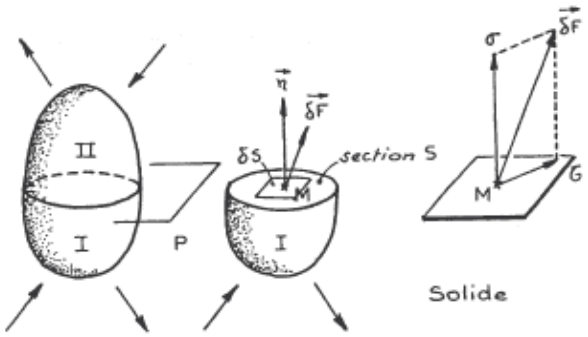

Figure 1.1 Stress in a medium

The stress vector can be decomposed into a normal component and a tangential component to plane (P):

$$\vec{f} = \sigma.\vec{n} + \tau.\vec{t}$$

Where:

$\vec{n}$: outward unit normal vector (positive orientation of space)

$\vec{t}$: unit tangent vector

σ: normal stress

τ: shear stress

The stress vector is a function of the considered point and of the orientation of the plane passing through this point (change of reference system):

$$\vec{f} = \vec{f}(M, \vec{n})$$

For a given point M, $\vec{f}$ therefore has a different expression depending on the plane considered (change of reference system).

This is a *fundamental remark*: it means that at a given point M, and for a given stress vector $\vec{f}$ relative to the considered plane, a soil may or may not have, for example, a tangential (shear) component. This is all the more important if the material does not have the same strength limits in tension, compression, or shear — which is often the case.

Note:

1. Asking for the stress at a point in soil without specifying with respect to which plane $\Longrightarrow$ has no meaning in terms of strength of materials (SOM), since a given material may have different strengths in tension, compression, or shear (for example: concrete, water, etc.).
2. Theory shows that, to determine the stresses acting on all the different planes around a point M, it is sufficient to know at this point the values of the six quantities:

   $$\sigma_x, \sigma_y, \sigma_z, \tau_{xy} = \tau_{yx}, \tau_{zx} = \tau_{xz} \text{ et } \tau_{zy} = \tau_{yz}$$

   That is, the components of the stresses acting on the faces of a cube centered at point M, with edges parallel to the axes Ox, Oy, Oz.

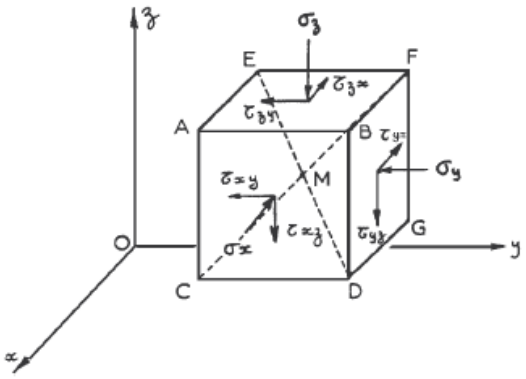

with:

$\tau_{xy} = \tau_{yx}$

$\tau_{yz} = \tau_{zy}$

$\tau_{zx} = \tau_{xz}$

Figure 1.2 State of stresses around a point M

3. At every point M, there exist three particular planes for which the stress is purely normal ($\tau = 0$). These are called *principal planes*; their normal directions are called *principal directions*, and the corresponding stresses are called *principal stresses*. They are denoted:

   $$\sigma_1, \sigma_2, \sigma_3 \ (\sigma_1 < \sigma_2 < \sigma_3)$$

   and are respectively called the *minor principal stress*, *intermediate principal stress*, and *major principal stress*.

In other words, by taking these three so-called principal directions as the reference system, the stress tensor becomes diagonal, and the stress vector $\vec{f}$ in this system of axes formed by the principal vectors can be written as:

$$\vec{f} = [\sigma].\vec{n} = \begin{bmatrix} \sigma_1 & 0 & 0 \\ 0 & \sigma_2 & 0 \\ 0 & 0 & \sigma_3 \end{bmatrix}$$

1.2 Mohr's circle of stresses at a point

1.2.1 Analytical method

In the coordinate system (Ox, Oz), the stress tensor is written as:

$$[\sigma] = \begin{bmatrix} \sigma_x & \tau_{xz} \\ \tau_{xz} & \sigma_x \end{bmatrix}$$

The condition of zero resultant moment requires:

$$\tau_{ij} = \tau_{ji} \text{ that is, } \tau_{xz} = \tau_{zx}$$

Knowing the stresses on the faces with normal directions Ox and Oz, one can determine the stresses on any other plane inclined at an angle θ.

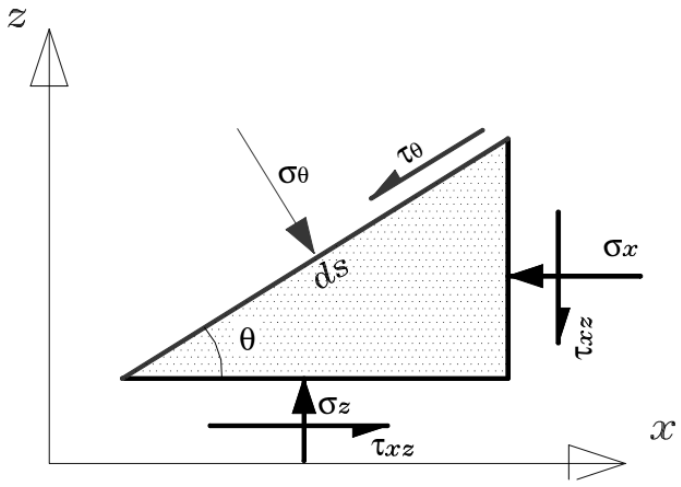

Figure 1.3 Stresses on an inclined plane

If we write the first equilibrium condition (sum of forces equals zero), we obtain the stress state on the plane inclined at angle θ:

$$\sigma_\theta = \frac{\sigma_x + \sigma_z}{2} + \frac{\sigma_z - \sigma_x}{2}\cos(2\theta) - \tau_{xz}\sin(2\theta)$$

$$\tau_\theta = \frac{\sigma_z - \sigma_x}{2}\sin(2\theta) + \tau_{xz}\cos(2\theta)$$

The locus of stresses in the (σ, τ) plane is defined by the relation:

$$\left(\sigma_\theta - \frac{\sigma_x + \sigma_z}{2}\right)^2 + {\tau_\theta}^2 = \left(\frac{\sigma_z - \sigma_x}{2}\right)^2 + {\tau_{xz}}^2$$

This is the equation of a circle (Mohr's circle):

- Center at coordinates: $(\frac{\sigma_x+\sigma_z}{2}, 0)$
- Radius: $R = \sqrt{\left(\frac{\sigma_z-\sigma_x}{2}\right)^2 + {\tau_{xz}}^2}$

The orientation of the principal planes is obtained for $\tau_\theta = 0$, that is:

$$\theta_1 = -\frac{1}{2} arc\tan\left(\frac{2\tau_{xz}}{\sigma_z-\sigma_x}\right), \theta_2 = \theta_1 + \frac{\pi}{2}$$

Thus, there are two principal planes whose orientations are given by θ_1 and θ_2. The *major and minor principal stresses* are determined from the circle equation:

$$\sigma_1 = \frac{\sigma_x + \sigma_z}{2} + \sqrt{\left(\frac{\sigma_z - \sigma_x}{2}\right)^2 + {\tau_{xz}}^2}$$

$$\sigma_3 = \frac{\sigma_x + \sigma_z}{2} - \sqrt{\left(\frac{\sigma_z - \sigma_x}{2}\right)^2 + {\tau_{xz}}^2}$$

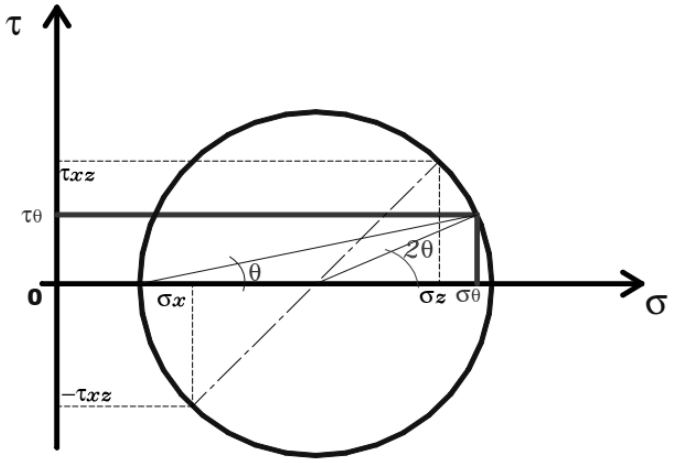

Figure 1.4 Mohr's Circle

Note that if the directions x and z are principal direction ($\sigma_x = \sigma_3$, $\sigma_z = \sigma_1$, $\tau_{xz} = 0$), we obtain:

$$\sigma_\theta = \frac{\sigma_1 + \sigma_3}{2} + \frac{\sigma_1 - \sigma_3}{2}\cos(2\theta)$$

$$\tau_\theta = \frac{\sigma_1 - \sigma_3}{2}\sin(2\theta)$$

1.2.2 Graphical method

To study the stress state at a point, a graphical representation of the vector $\vec{f}$ is generally used in a coordinate system (σ, τ). The points representing the principal stresses (τ = 0) therefore lie on the Oσ axis.

Each point of Mohr's stress circle corresponds to a possible plane around point O (see Figure 1.5). In the plane containing the principal axes P_1 and P_3, this circle has for its diameter $(\sigma_1 - \sigma_3)$, called the *stress deviator*, and for the abscissa of its center $(\sigma_1 + \sigma_3)/2$, called the *mean stress*. When the plane rotates by an angle θ with respect to a principal plane, the corresponding point on Mohr's circle rotates by 2θ in the opposite direction.

The *normal stress* σ and *shear stress* τ acting on a plane inclined at an angle θ with respect to the major principal plane are given by:

$$\sigma = \frac{\sigma_1 + \sigma_3}{2} + \frac{\sigma_1 - \sigma_3}{2}\cos(2\theta)$$

$$\tau = \frac{\sigma_1 - \sigma_3}{2}\sin(2\theta)$$

where θ is the angle measured from the major principal plane to the studied plane.

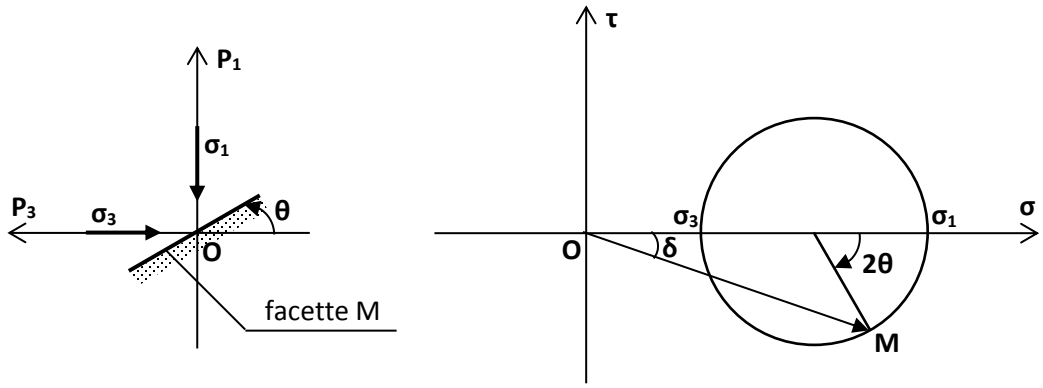

Figure 1.5 Mohr's Circle of stresses at point O

1.3 The equations of equilibrium in soil

The stress state in a solid may vary from one point to another, meaning that the six quantities we have defined, namely σ_x, σ_y, σ_z, τ_{xy}, τ_{yz}, τ_{zx}, are functions of the coordinates *x*, *y*, *z* of the considered point M.

Consider a cube of solid centered at M, with sides parallel to the axes Ox, Oy, and Oz. This cube, which may be taken as small as desired, is subjected to a body force $\vec{F}(X; Y; Z)$, with X(*x*, *y*, *z*), Y(*x*, *y*, *z*), Z(*x*, *y*, *z*).

The internal equilibrium of the solid (zero resultant of forces, $\sum \vec{F} = \vec{0}$) is expressed, in two dimensions, by the relations:

$$\begin{cases} \dfrac{\partial \sigma_x}{\partial x} + \dfrac{\partial \tau_{xy}}{\partial y} = X \\ \dfrac{\partial \tau_{yx}}{\partial x} + \dfrac{\partial \sigma_y}{\partial y} = Y \end{cases}$$

And, in the case of a solid in three dimensions, by the relations:

$$\begin{cases} \dfrac{\partial \sigma_x}{\partial x} + \dfrac{\partial \tau_{xy}}{\partial y} + \dfrac{\partial \tau_{yz}}{\partial z} = X \\ \dfrac{\partial \tau_{yx}}{\partial x} + \dfrac{\partial \sigma_y}{\partial y} + \dfrac{\partial \tau_{yz}}{\partial z} = Y \\ \dfrac{\partial \tau_{zx}}{\partial x} + \dfrac{\partial \tau_{zy}}{\partial y} + \dfrac{\partial \sigma_z}{\partial z} = Z \end{cases}$$

Note:

1. In soil mechanics, body forces are generally reduced to gravity forces, and the Oz axis is taken as vertically upward, thus:

$$X = 0, \qquad Y = 0, \qquad Z = -\gamma$$

2. The condition of zero resultant moments ($\sum \vec{M} = \vec{0}$) leads to the result:

$$\tau_{xy} = \tau_{yx}\ , \tau_{yz} = \tau_{zy}, \tau_{xz} = \tau_{zx}$$

1.4 Application to soils

1.4.1 Stresses in soils

Since soils develop very little tensile normal stress, in soil mechanics — unlike in continuum mechanics (strength of materials) — the following sign convention is adopted:

$\sigma < 0$: tension

$\sigma > 0$: compression

Consider the case of a saturated soil.

In such a soil, stresses are distributed between the soil skeleton and the water in the same way as in a composite bar made of rubber and metal: the compressive force F is shared between a compressive force F_1 in the rubber and a compressive force F_2 in the metal.

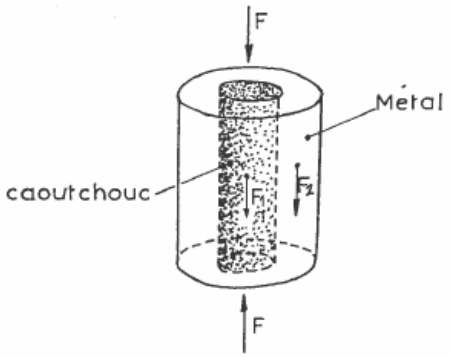

Figure 1.6 Analogy: water/soil & rubber/metal

The only difference is that, in soil, water and the solid skeleton are intimately mixed. Moreover:

1. We know that in a liquid at equilibrium — that is, in water at rest — stresses are only normal regardless of the plane considered (a liquid cannot "sustain" shear stress $\Longrightarrow$ whatever the plane considered at a point M in the water, $\tau = 0$). Stresses in water are thus reduced to the water pressure at the considered point M, called *pore water pressure* and denoted *u*.
2. In a solid skeleton (soil without water), on any plane, a normal stress denoted σ' and a shear stress denoted τ' act. These are called *effective stresses*.

Thus, if the total stresses acting in the two phases of the soil (skeleton + water) on the given plane are σ and τ, then we have the very important Terzaghi's relation:

$$\sigma = \sigma' + u$$

$$\tau = \tau'$$

where:

u: pore water pressure

σ' and τ': effective stresses

σ and τ: total stresses

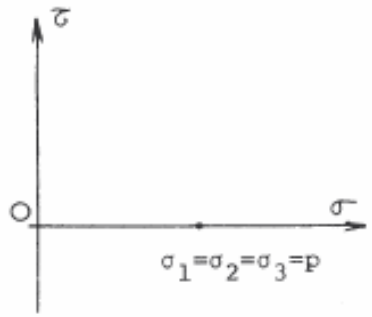

Figure 1.7 Mohr's Circle of water at a point M under pressure P ($\tau = 0$ for all planes)

1.4.2 Application of the equilibrium equations

1.4.2.1 Semi-infinite soil with horizontal ground surface

Consider a semi-infinite soil with a horizontal ground surface, subjected only to the action of gravity (total unit weight).

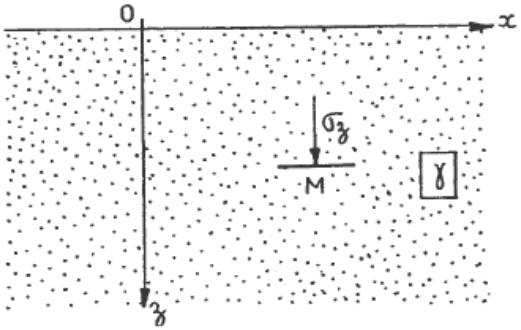

Figure 1.8 Semi-infinite soil with horizontal surface

From the symmetry of the problem, the total stresses σ_x and σ_z are principal stresses, therefore $\tau_{xy} = 0$.

Equilibrium equations

$$\begin{cases} \frac{\partial \sigma_x}{\partial x} = 0 \\ \frac{\partial \sigma_z}{\partial z} = \gamma \end{cases} \Rightarrow \begin{cases} \sigma_x = f(z) \\ \sigma_z = \gamma z + cte \end{cases}$$

Since the free surface of the soil is unloaded, no stress acts on it, which implies $cte = 0$. Hence:

$$\sigma_z = \gamma z$$

In the case of layered *soils* (Figure 1.9):

$$\sigma_z = \sum_{i=1}^{n} \gamma_i d_i$$

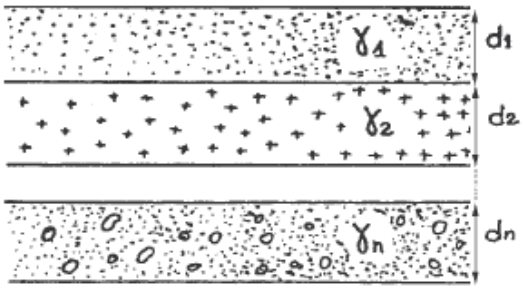

Figure 1.9 Case of layered soils

1.4.2.2 Semi-infinite soil with an inclined surface

Consider a semi-infinite soil whose planar surface makes an angle α with the horizontal.

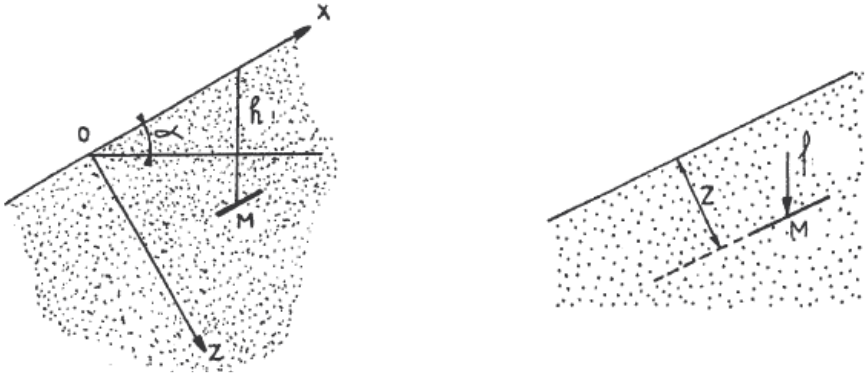

Figure 1.10 Semi-infinite soil with inclined surface: calculation of $\vec{f}$ for a facet parallel to the surface at point M

We seek the stress acting on a facet parallel to the surface.

The equilibrium equations are written as:

$$\begin{cases} \dfrac{\partial \sigma_x}{\partial x} + \dfrac{\partial \tau_{xz}}{\partial z} = -\gamma \sin\alpha \\ \dfrac{\partial \sigma_z}{\partial z} + \dfrac{\partial \tau_{xz}}{\partial x} = \gamma \cos\alpha \end{cases}$$

However, in this problem the stress state at a point, i.e., (σ_x ; σ_y ; σ_z), must be independent of *x*, which implies:

$$\frac{\partial \sigma_x}{\partial x} = 0 \quad \text{and} \quad \frac{\partial \tau_{xz}}{\partial x} = 0$$

Integrating the equilibrium equations then gives:

$$\begin{cases} \sigma_z = \gamma z \cos\alpha \\ \tau_{xz} = -\gamma z \sin\alpha \end{cases} \Longrightarrow \left\|\vec{f}\right\| = \gamma z = \gamma h \cos\alpha \text{ and } \vec{f} \text{ is vertical}$$

1.4.2.3 Example of stress calculation

Consider a semi-infinite soil with a horizontal surface, submerged, with water at a height *H* above the soil (Figure 1.11).

At depth *z*, the total vertical stress is:

$$\sigma_z = H\gamma_w + \gamma z$$

γ : total unit weight of the soil.

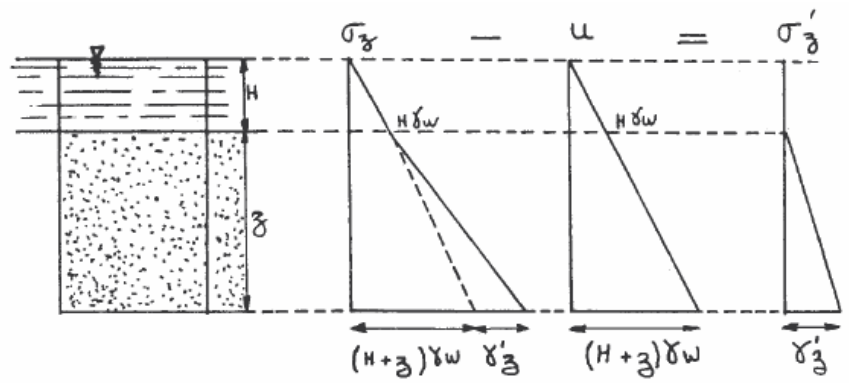

Figure 1.11 Stress calculation

The water pressure is:

$$u = (H + z)\gamma_w$$

Note:

The expression $u = z\gamma_w$ (water pressure) is only valid for a soil without seepage.

Thus, the effective stress is:

$$\sigma'_z = \sigma_z - u = (\gamma - \gamma_w)z = \gamma' z$$

1.5 Exercises

Exercise 1

Draw the Mohr's circle at a point M within a volume of water subjected to a pressure of 2 bar.

Solution

In a fluid at rest, the stress state is hydrostatic. The normal stress is equal in all directions and shear stresses are zero. Consequently, $\sigma_1 = \sigma_2 = \sigma_3 = -P$, and the Mohr circles collapse into a single point.

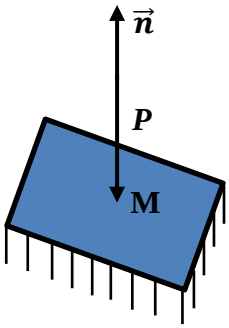

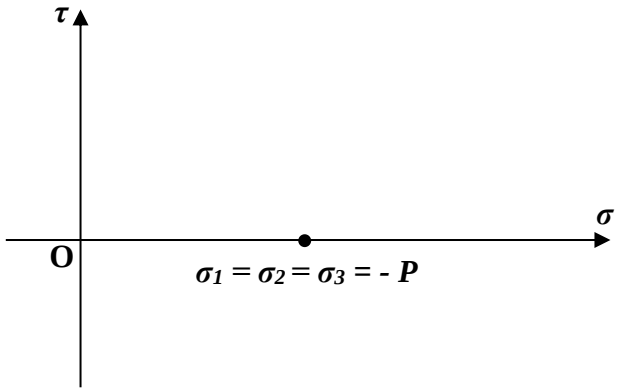

Exercise 2

At a point M, the normal and shear stresses are 100 kPa and 25 kPa on a horizontal plane, and 50 kPa and 25 kPa on a vertical plane.

Determine the Mohr circle, as well as the magnitude and orientation of the principal stresses.

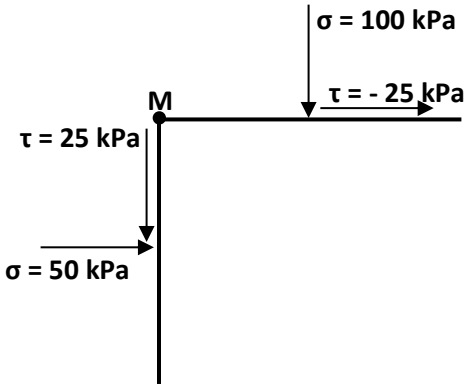

Solution

The major and minor principal stresses (σ_1, σ_3) are given by:

$$\sigma_1 = \frac{\sigma_x + \sigma_z}{2} + \sqrt{\left(\frac{\sigma_z - \sigma_x}{2}\right)^2 + {\tau_{xz}}^2} = \frac{50 + 100}{2} + \sqrt{\left(\frac{100 - 50}{2}\right)^2 + 25^2} = 110 \text{ kPa}$$

$$\sigma_3 = \frac{\sigma_x + \sigma_z}{2} - \sqrt{\left(\frac{\sigma_z - \sigma_x}{2}\right)^2 + {\tau_{xz}}^2} = \frac{50 + 100}{2} - \sqrt{\left(\frac{100 - 50}{2}\right)^2 + 25^2} = 40 \text{ kPa}$$

There are two principal planes, whose orientations are given by θ_1 and θ_2, such that:

$$\theta_1 = -\frac{1}{2} arc\tan\left(\frac{2\tau_{xz}}{\sigma_z - \sigma_x}\right) = \theta_1 = -\frac{1}{2} arc\tan\left(\frac{2 \times 25}{100 - 50}\right) = -22.5°$$

$$\theta_2 = \theta_1 + \frac{\pi}{2} = 67.5°$$

The Mohr circle has:

- Center:

$$\left(\frac{\sigma_x + \sigma_z}{2}, 0\right) = (75, 0)$$

- Radius:

$$R = \sqrt{\left(\frac{\sigma_z - \sigma_x}{2}\right)^2 + {\tau_{xz}}^2} = \sqrt{\left(\frac{100 - 50}{2}\right)^2 + 25^2} = 35 \text{ kPa}$$

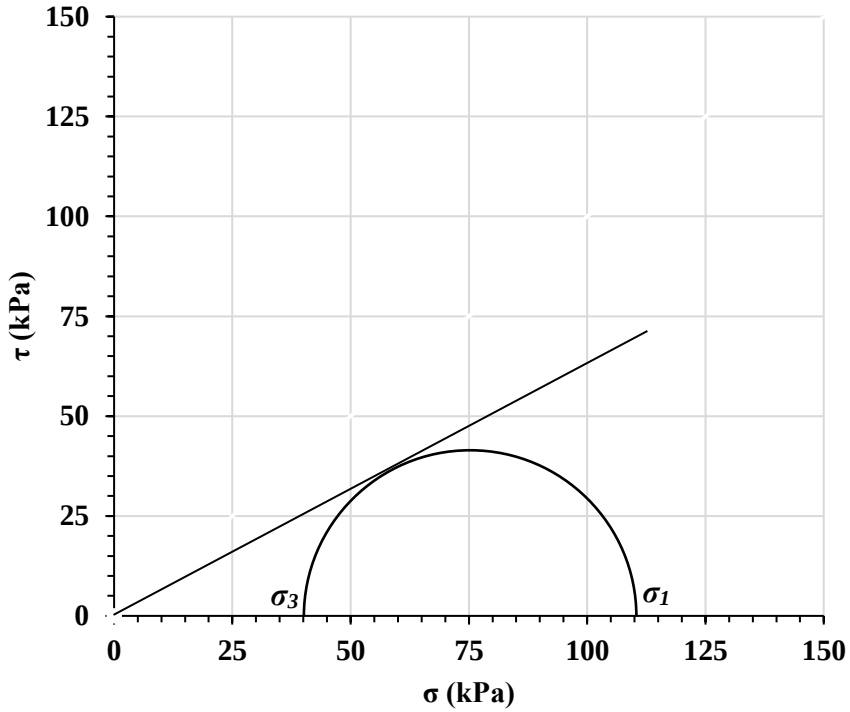

Exercise 3

Determine analytically and graphically the stresses acting on a plane inclined at 60°.

Solution

The normal and shear stresses σ_θ and τ_θ acting on a plane inclined at an angle $\theta = 60°$ are given by:

$$\sigma_\theta = \frac{\sigma_1 + \sigma_3}{2} + \frac{\sigma_1 - \sigma_3}{2}\cos(2\theta) = \frac{100 + 30}{2} + \left(\frac{100 - 30}{2}\right)\cos(120)$$

$$\sigma_\theta = 47.4 \text{ kPa}$$

$$\tau_\theta = \frac{\sigma_1 - \sigma_3}{2}\sin(2\theta) = \frac{100 - 30}{2}\sin(120)$$

$$\tau_\theta = 30.2 \text{ kPa}$$

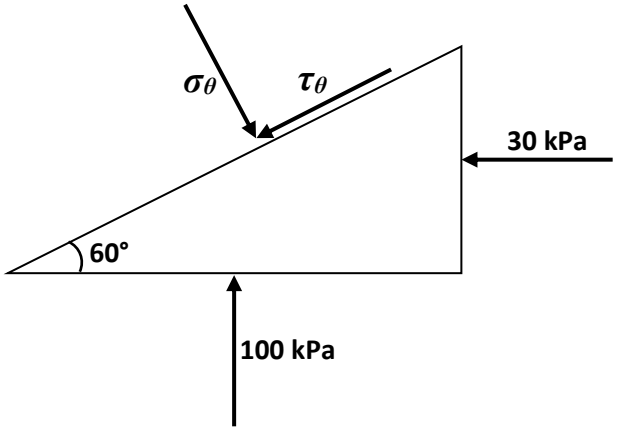

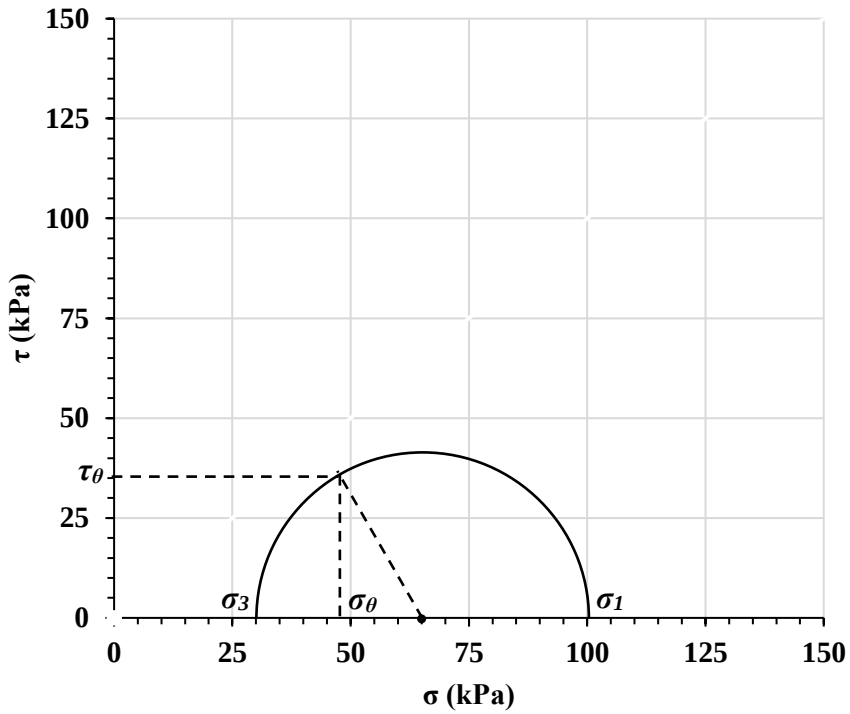

Exercise 4

Calculate the variation with depth of the stresses σ_z, u, and σ_z' for the case shown in the figure below.

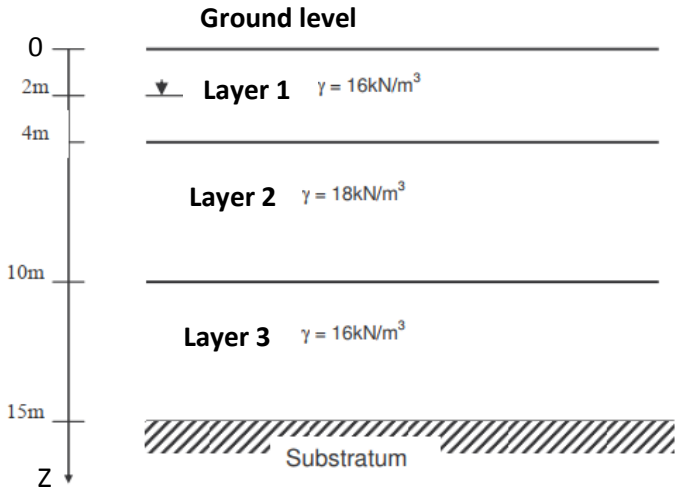

Solution

Note:

1. In this exercise, for Layer 1, the unit weight is assumed constant:

$$\gamma = \text{constant} = 16\ \text{kN/m}^3$$

regardless of whether the soil is located above or below the water table.

2. The symbol ∇ (or the indicated line in the figure) is conventionally used to represent the groundwater table.

We have:

$$\sigma_z = \gamma z$$

$$u = \gamma_w z_w$$

$$\sigma_z' = \sigma_z - u$$

where:

σ_z: total vertical stress

u: pore water pressure

σ_z': effective vertical stress

γ: unit weight of soil

γ_w: unit weight of water

z_w: depth below the groundwater table

The variation of σ_z, u, and σ_z' with depth z is summarized in the table below:

Depth z (m)	σ_z (kPa)	u (kPa)	σ_z' (kPa)
2	32	0	32
4	64	20	44
10	172	80	90
15	252	130	122

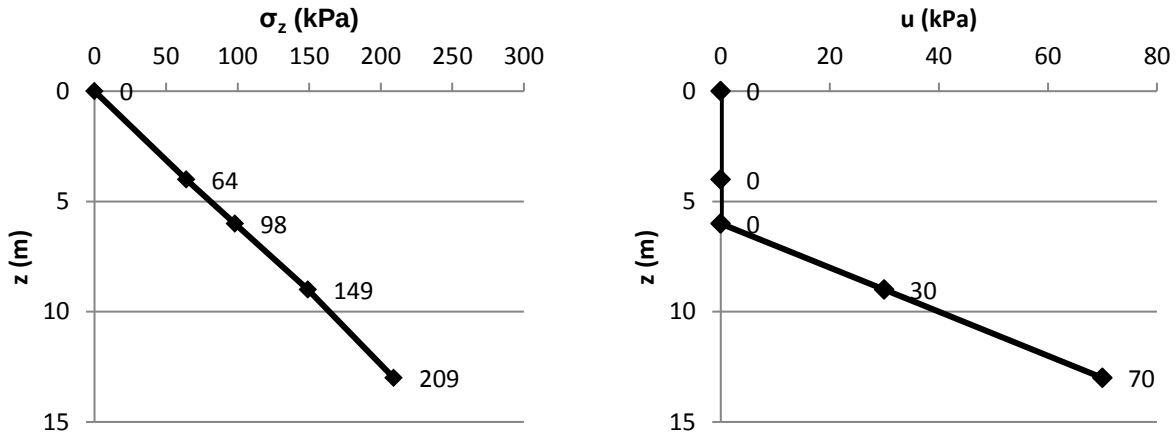

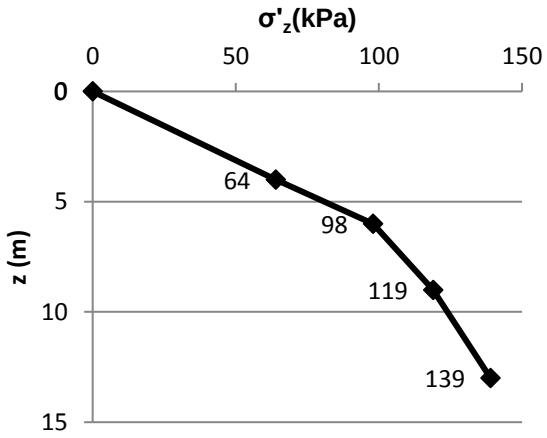

Exercise 5

Calculate and plot the variation with depth of σ_z, u, and σ'_z for the soil profile shown in the figure below.

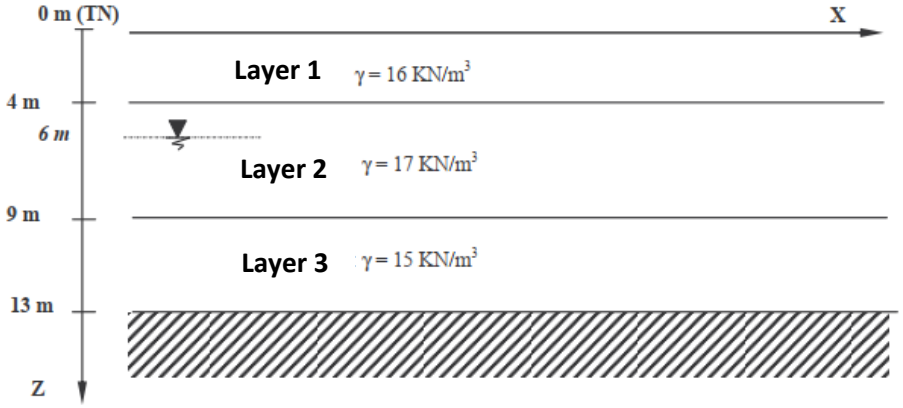

Solution

We have:

$$\sigma_z = \gamma z$$

$$u = \gamma_w z_w$$

$$\sigma'_z = \sigma_z - u$$

The variation of σ_z, u, and σ'_z with depth z is summarized in the table below:

Depth z (m)	σ_z (kPa)	u (kPa)	σ'_z (kPa)
4	64	0	64
6	98	0	98
9	149	30	119
13	209	70	139

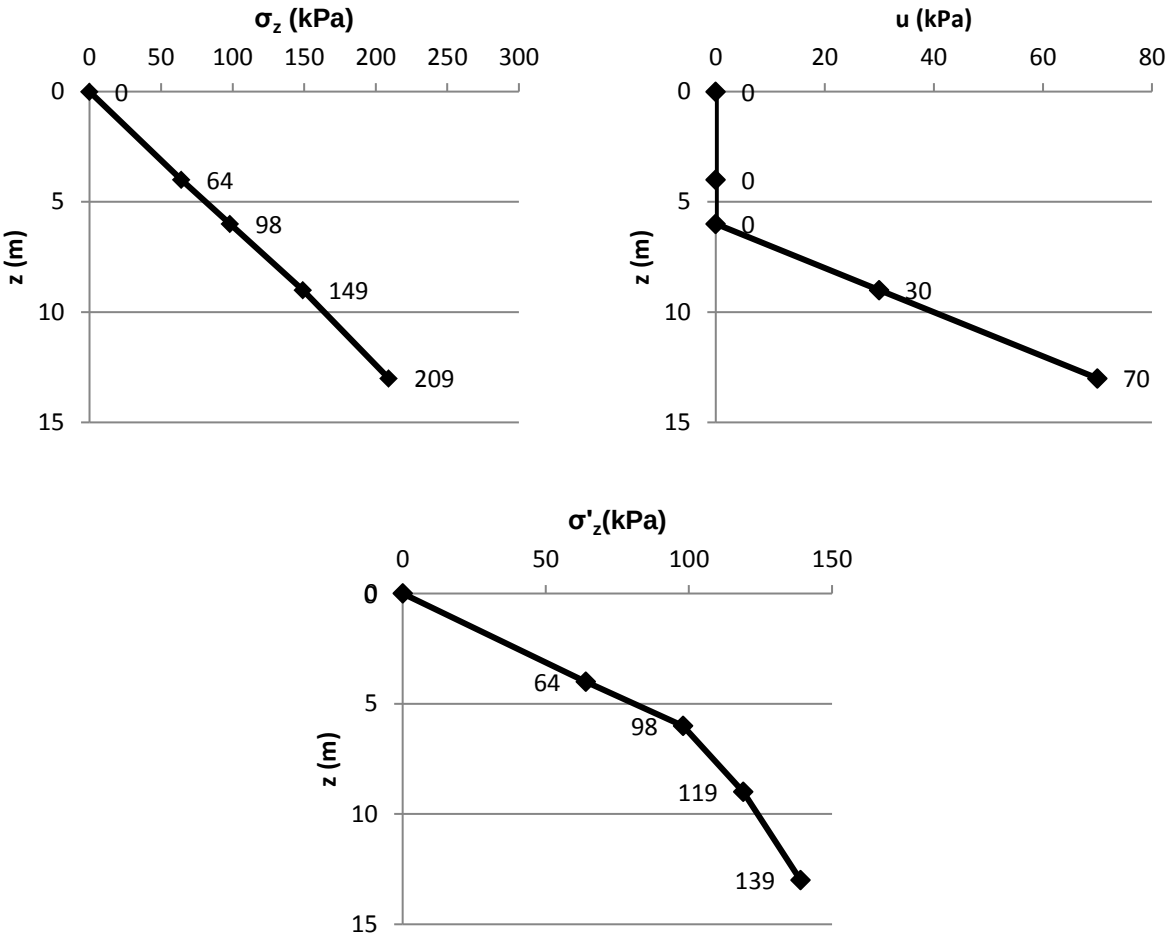

Exercise 6

The soil profile of a foundation extends from 0 to 22 m depth.

1) Plot the variation diagrams of total stress, effective stress, and pore water pressure from 0 to 22 m.
2) Calculate the change in stresses due to lowering of the groundwater table to a depth of 6 m below ground level.

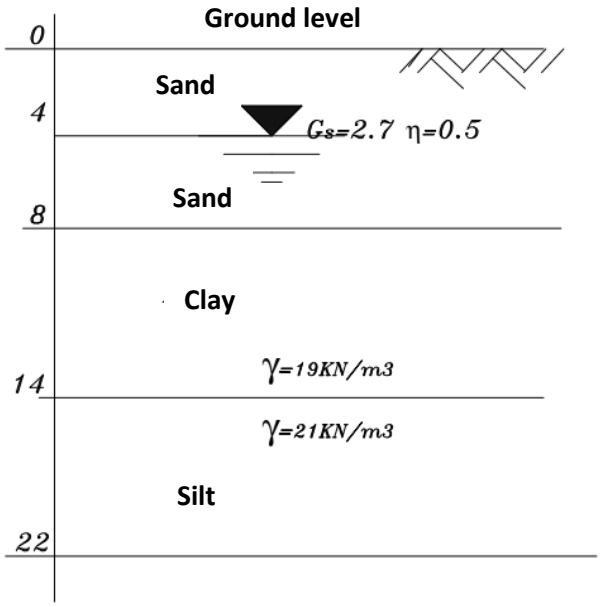

Solution

1) Stress distribution

Between 0 and 4 m, the sand is dry:

$$\gamma_d = (1-n)G_s\gamma_w = (1-0.5)\times 2.7 \times 10 = 13.5 \text{ kN/m}^3$$

Between 4 and 8 m, the sand is saturated:

$$\gamma_{sat} = [(1-n)G_s + n]\gamma_w = [(1-0.5)\times 2.7 + 0.5]\times 10 = 18.5 \text{ kN/m}^3$$

We have:

$$\sigma_z = \gamma z$$

$$u = \gamma_w z_w$$

$$\sigma'_z = \sigma_z - u$$

The variation of σ_z, u, and σ'_z with depth z is summarized in the table below:

Depth z (m)	σ_z (kPa)	u (kPa)	σ'_z (kPa)
4	54	0	54
8	128	40	88
14	242	100	142
22	410	180	230

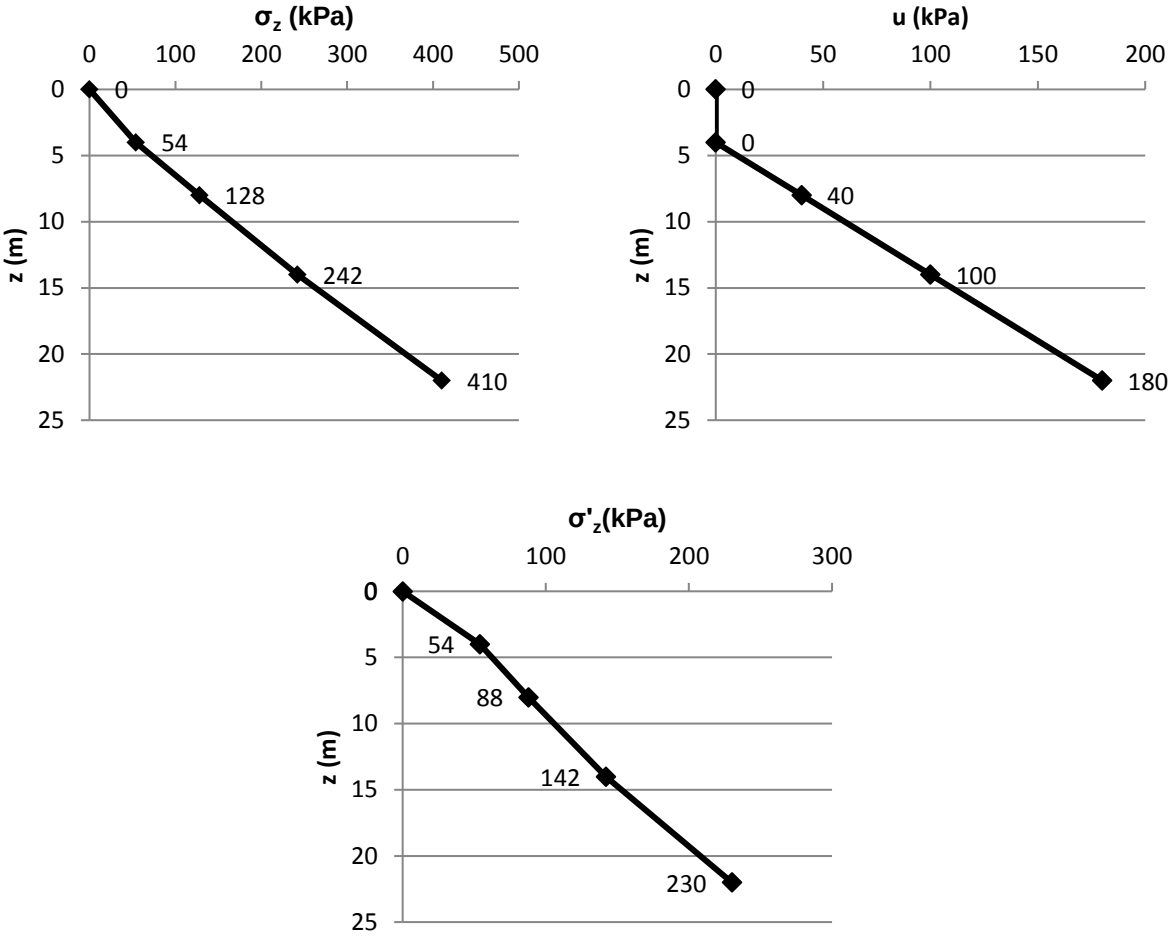

2) Effect of lowering the groundwater table

When the groundwater table is lowered by 2 m:

- σ_z remains unchanged (since the unit weights remain the same),
- u decreases by: $\gamma_w \times 2 = 20$ kPa,
- σ_v' decreases by: $\gamma_w \times 2 = 20$ kPa.

Chapter 2
Settlement and consolidation of soils

2.1 Generalities – Definitions

Under the action of applied loads, stresses develop within soils, leading to deformations. The vertical downward displacements are called settlements. In most cases, the applied loads are vertical and the ground surface is horizontal. Therefore, settlements are the predominant displacements. While uniform settlements can be inconvenient when they are excessive, differential settlements are particularly dangerous as they can cause serious damage — tilting or even overturning of structures, and significant increases in internal forces in hyperstatic (statically indeterminate) structures. Settlement is due to the compressibility of the soil, meaning its ability to decrease in volume. The compressibility of soil results from:

- Compression of the air filling the voids. Water is considered incompressible. Air, being highly compressible, causes an almost instantaneous settlement.
- Expulsion of the water contained in the voids. This is primary consolidation, which produces the largest part of the settlement: the soil undergoes a volume decrease equal to the volume of water expelled (the soil is assumed to be saturated).
- Compression of the soil skeleton. This is secondary consolidation, corresponding to the rearrangement of soil particles into a denser configuration. A slow deformation (creep) occurs due to the movement of adsorbed layers.

The total final settlement of a soil, $S_{t\infty}$, therefore has three components:

$$S_{t\infty} = S_i + S_c + S_s$$

where:

S_i : immediate settlement,

S_c: primary consolidation settlement,

S_s : secondary consolidation settlement.

In this chapter, we will focus on the main term — the consolidation settlement, which includes part of the secondary settlement.

In some highly organic soils, such as peat, the secondary compression component can no longer be neglected.

2.2 Calculation of stresses within a soil mass – General principles

In this section, we are concerned only with vertical stresses, since these are the ones that cause settlements.

2.2.1 Principle of superposition

This principle states that:

If, in a material, the stress state (σ_1) corresponds to the strain state (ε_1), and the stress state (σ_2) corresponds to the strain state (ε_2), then the combined stress state ($\sigma_1 + \sigma_2$) will correspond to the combined strain state ($\varepsilon_1 + \varepsilon_2$).

In general, for a soil with unit weight γ:

$$\sigma_z = \gamma \cdot h + \Delta\sigma_z$$

where:

$\gamma \cdot h$: stress due to the self-weight of the soil at depth h

$\Delta\sigma_z$: increase in stress due to the applied surface load at depth h

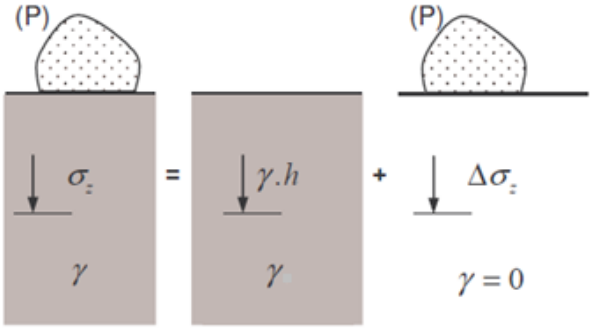

Figure 2.1 Principle of superposition

2.2.2 Case of a horizontally layered soil under uniform load

Consider a soil mass with a horizontal surface uniformly loaded by a surface pressure of intensity q.

According to the *principle of superposition*, the total stress at depth h is equal to the stress due to self-weight plus the stress due to the applied load:

$$\sigma_z = \gamma \cdot h + \Delta\sigma_z = \gamma \cdot h + q$$

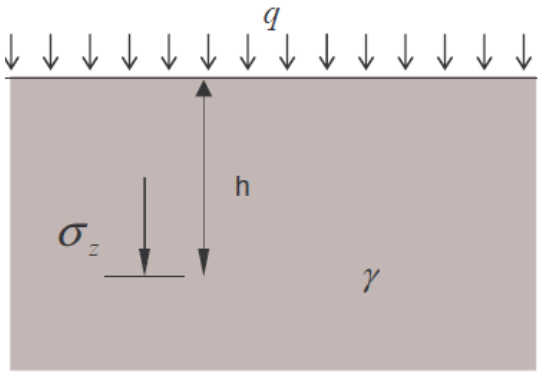

Figure 2.2 Uniformly loaded soil mass

2.2.3 Case of a point load

We use *Boussinesq's formula*, which gives the vertical stress at any point M in a weightless elastic medium loaded by a vertical point force *Q*:

$$\Delta\sigma_Z = \frac{3Q}{2\pi} \cdot \frac{z^3}{(r^2 + z^2)^{\frac{5}{2}}}$$

This relation can also be written as:

$$\Delta\sigma_z = \frac{Q}{z^2} \cdot N$$

where

$$N = \frac{3}{2\pi \left[1 + \left(\frac{r}{z}\right)^2\right]^{\frac{5}{2}}}$$

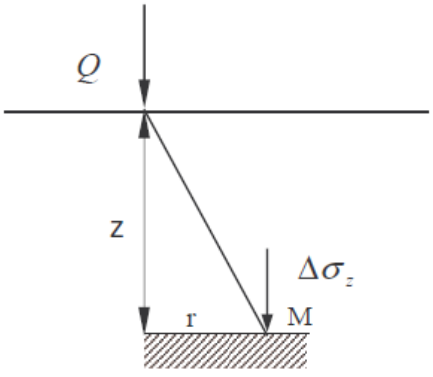

Figure 2.3 Point load

Chart No. 1 (see Appendix 1) shows the variations of *N* as a function of r/z.

2.2.4 Case of a uniform rectangular load

The increase in stress in a semi-infinite medium beneath the corner of a uniformly distributed rectangular load (q) is given by the relation:

$$\Delta\sigma_z = K \cdot q \qquad (q \text{ in kN/m}^2)$$

where

$K = K(m,n)$ with $m = \frac{a}{z}$; $n = \frac{b}{z}$ is a dimensionless influence factor given in Chart No. 2 (see Appendix 2).

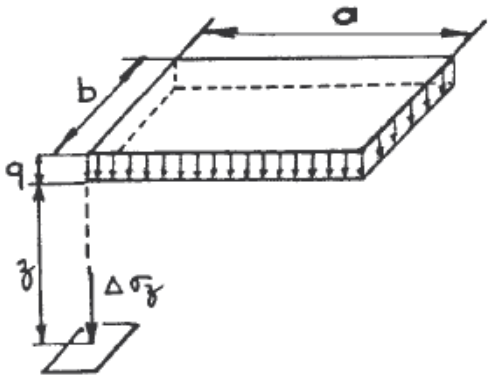

Figure 2.4 Uniform rectangular load

- If point A is *inside* the loaded rectangle (Fig. 2.5-a) : $\Delta\sigma_z = (K_1 + K_2 + K_3 + K_4) \cdot q$
- If point A is *outside* the loaded rectangle (Fig. 2.5-b) : $\Delta\sigma_z = \left(K_{(1,2,3,4)} - K_{(3,1)} - K_{(1,4)} + K_1\right) \cdot q$

where

k_i (i = 1, 2, 3, 4): *influence factor* of rectangle *i*.

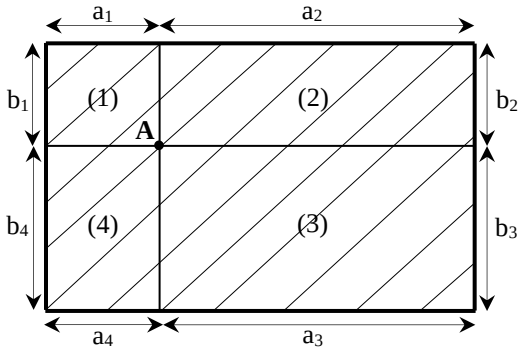

Figure 2.5-a Point inside the loaded rectangle

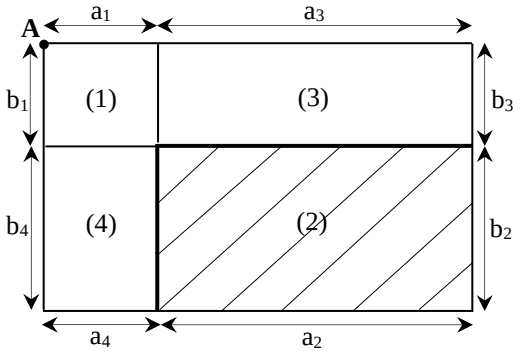

Figure 2.5-b Point outside the loaded rectangle

2.2.5 Case of a circular load

Along the axis of a uniformly distributed circular load of radius *r* (Figure 2.6), the increase in vertical stress at depth *z* is:

$$\Delta\sigma_z = J \cdot q$$

where

$$J = 1 - \left[\frac{1}{1 + \left(\frac{r}{z}\right)^2}\right]^{\frac{3}{2}}$$

is given by chart No. 3 (see Appendix 3)

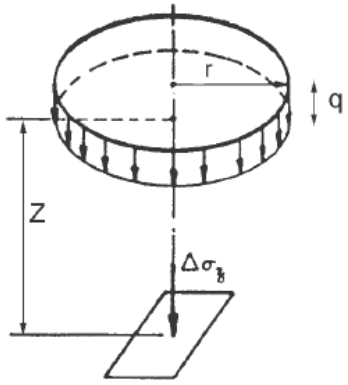

Figure 2.6 Circular load

2.2.6 Case of an embankment-shaped load of infinite length

The vertical stress beneath the edge of an infinitely long embankment-shaped load at depth *z* (Figure 2.7) is given by:

$$\Delta\sigma_z = I \cdot q$$

where

$$I = I\left(\frac{a}{z}, \frac{b}{z}\right)$$

is a dimensionless coefficient provided in Chart No. 4 (see Appendix 4).

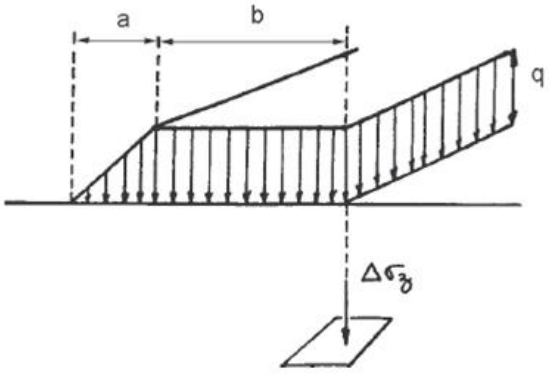

Figure 2.7 Embankment load

Note:

This value represents the stress beneath the corner of a load distribution. Therefore, when the embankment has two slopes, it is important to add the effect of the right-hand side to that of the left-hand side (see Figure 2.8)

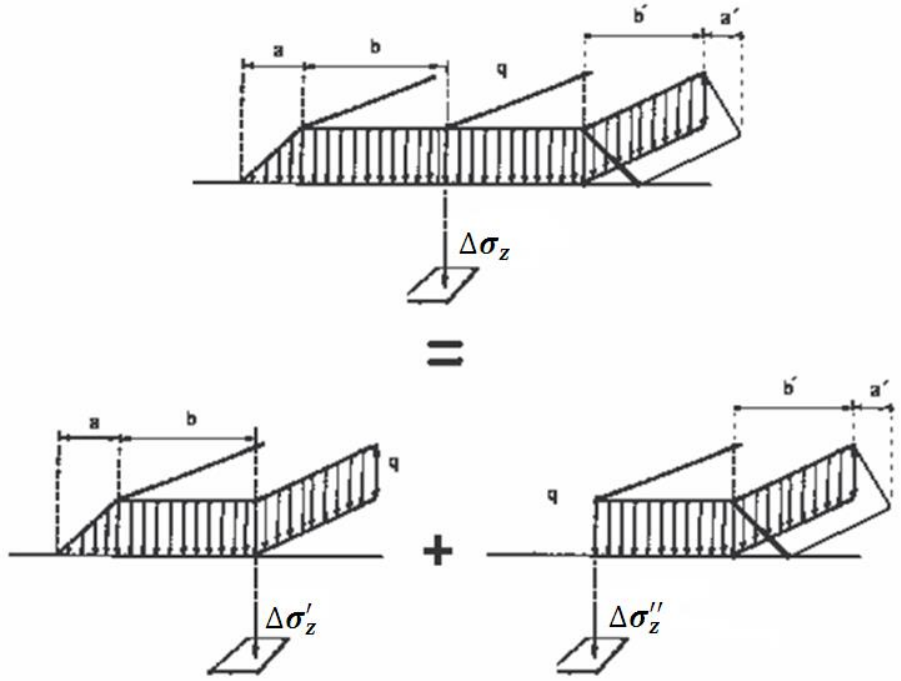

Figure 2.8. Contribution of the right-hand and left-hand parts of the embankment

2.2.7 Simplified stress distribution – Case of continuous footings

When only an approximate value of settlements and stresses is required, a simplified distribution of normal stresses can be used.

It is assumed that stress diffusion with depth is uniform and bounded by straight lines forming an angle α with the vertical.

In the case shown in Figure 2.9:

$$\begin{cases} (\Delta\sigma_z)_M = q \cdot \dfrac{a}{a + 2 \cdot z \cdot tg\alpha} \\ (\Delta\sigma_z)_P = 0 \end{cases}$$

Note:

The value of α is generally taken as 30°.

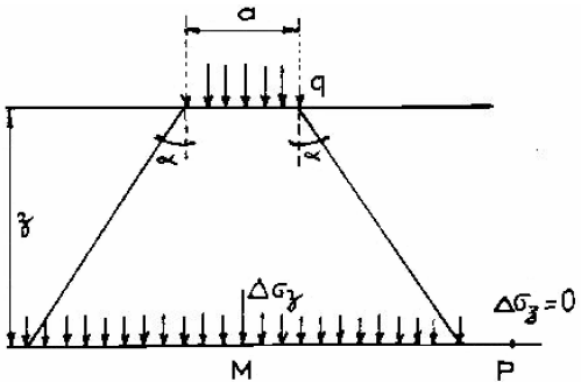

Figure 2.9 Simplified stress distribution

2.3 Settlements – General rules

2.3.1 Settlement of granular soils

Experience shows that:

- The compressibility of granular soils is due only to the compression of the solid skeleton.
- Settlements in these soils are almost instantaneous; they occur immediately when loads are applied.
- Settlements are the same whether the soil is dry, moist, or saturated.
- Deformations in granular soils are caused by two mechanisms:
  - A re-arrangement (interlocking) of the grains, which leads to a reduction in the void ratio (this occurs under stress levels typically encountered in geotechnical engineering).
  - Deformation of the grains themselves under the forces acting at their contact points (this occurs only under extremely high loads, very rarely encountered in practice).

2.3.2 Settlement of saturated soils – the consolidation phenomenon

2.3.2.1 Consolidation: mechanical analogy

In dry materials (dry sand, rock, etc.), deformation is almost instantaneous. However, in a fully saturated medium (fine soil or granular soil), the situation is different: at the beginning, the *water*

initially carries all the applied load. The water then begins to move according to *Darcy's law (v = K·i)* and flows at a rate that depends on the soil's permeability.

Gradually, the solid grains take over from the water in transmitting the applied stresses. After some time, *all the load is transmitted directly from grain to grain*, and the pore water pressure at every point returns to its initial value, as it was before the load was applied. At this stage, the soil is said to be *consolidated* under the effect of the applied external forces.

This process is illustrated by the analogy shown in Figure 2.10, and its evolution is summarized in Table 1.

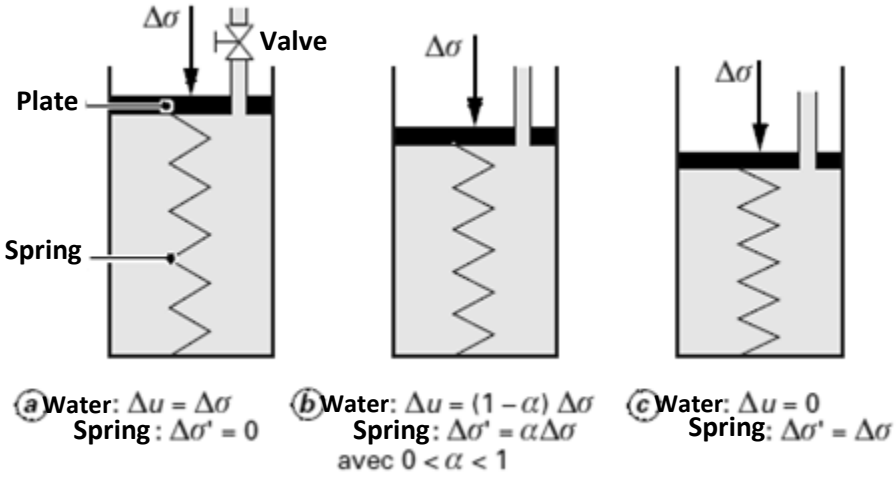

Figure 2.10 Schematic diagram of the consolidation phenomenon

In this analogy:

- The soil is loaded through a plate with a small orifice equipped with a valve.
- The mechanical behavior of the soil skeleton is represented by a *spring*.
- The liquid phase is represented by *water*.
- The low permeability of the soil is simulated by restricting the opening through which water can escape from the loading plate.
- The downward movement *ΔH* of the plate corresponds to the *settlement* of the soil.

The stages of the phenomenon are as follows:

- At the initial instant (a), $t = 0$ (valve closed): The applied load $\Delta\sigma$ is carried entirely by the water, and the spring (soil skeleton) is not loaded.
- After opening the valve (b): Water escapes slowly over time, and the spring gradually takes up the load as pore pressure decreases.

- At the end of consolidation (c): The excess pore water pressure is fully dissipated, water flow stops, and the entire load is transferred to the spring**,** which represents the soil skeleton.

Table 2.1 Evolution of stresses during consolidation

Time	**Total stress (applied laod)**	**Effective stress**	**Pore water pressure**	**Settlement**	**State of the consolidation process**
0	$\Delta\sigma_v$	*0*	$\Delta\sigma_v$	*0*	Beginning ($\alpha = \beta = 0$)
t	$\Delta\sigma_v$	$\alpha\,\Delta\sigma_v$	$(1-\alpha)\,\Delta\sigma_v$	$\beta\,\Delta H$	In progress ($0 < \alpha < 1$) ($0 < \beta < 1$)
t_{100}	$\Delta\sigma_v$	$\Delta\sigma_v$	*0*	ΔH	End ($\alpha = \beta = 1$)

2.3.2.2 Primary consolidation and secondary consolidation

The lowering of the plate at the end of primary consolidation corresponds to the final settlement of the soil, or *primary settlement*.

Beyond this phase, the entire load is carried by the spring, that is, by the soil skeleton. The pore water pressure within the soil mass becomes equal to the hydrostatic pressure. The excess pore pressure *u* induced by the loading becomes zero.

Experience shows that the soil continues to settle even after primary consolidation is completed. This new phase of settlement is called *secondary consolidation*. It is due to changes in the arrangement of the solid particles within the soil skeleton (see settlement of granular soils).

Settlements due to secondary consolidation are generally small (especially in fine soils), and their effect can be neglected compared to the settlements from primary consolidation.

Conclusion

For settlement analysis, only the settlement of saturated fine soils is of major importance, since it is responsible for the largest portion of total settlement—specifically its primary consolidation component. Fine soils are therefore highly sensitive to the consolidation phenomenon.

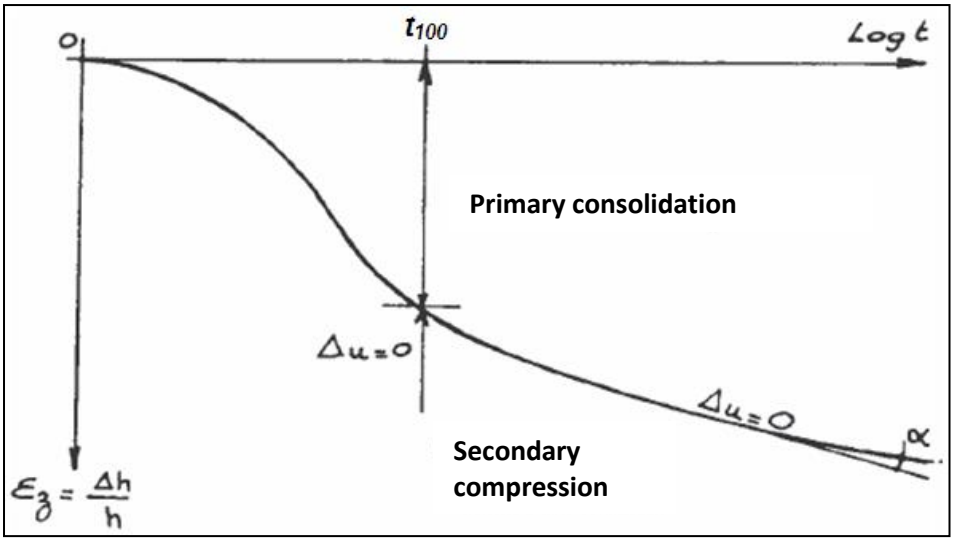

Figure 2.11 Vertical deformation of a saturated soil as a function of time

2.3.3 Main settlement calculation methods

The calculation of settlements is carried out using different methods depending on the pair (type of structure/nature of the soil). Two main methods are distinguished:

Oedometer Method	**Pressuremeter Method**
Structures Concerned ▪ Large embankments, ▪ Raft foundation 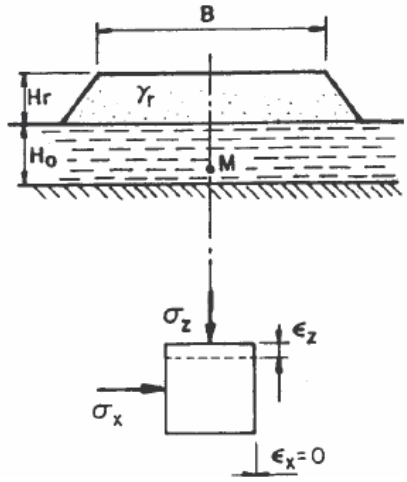	*Structures Concerned* ▪ Point or strip foundations 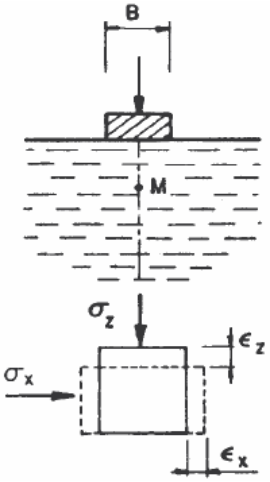
Soil Type ▪ Soft soils (clay) & stiff soils (sand)	*Soil Type* ▪ Soft soils (clay) & stiff soils (sand)
Criterion (Key Parameter) ▪ Deformations at non-constant volume, i.e., lateral deformation is negligible	*Criterion (Key Parameter)* ▪ Involves constant-volume deformations, i.e., including lateral deformations

Test Type ▪ Laboratory test using Terzaghi's oedometer	*Test Type* ▪ In-situ test using the Menard pressuremeter
Calculation Type ▪ Settlement calculations using the oedometer method	*Calculation Type* ▪ Calculations using Menard's formula
Mechanical Parameters Used (Behavior Law) ▪ Module oediométrique E' (parfois noté E_0) ▪ Oedometer modulus E' (sometimes noted E_0)	*Mechanical Parameters Used (Behavior Law)* ▪ Poisson's ratio v ▪ Soil structure coefficient α ▪ Deformation modulus for settlement E_d ▪ Deformation modulus for consolidation E_c

Note:

The boundary between the oedometer method and the pressuremeter method is not always very clear (due to soil diversity, foundation stiffness, edge effects for wide loads, etc.). The choice of one method over the other is most often based on experience. The "criterion" parameter is decisive.

2.4 Terzaghi's oedometer

This device allows for the evaluation of the magnitude of settlements as well as their evolution over time for structures built on saturated soils. It specifically measures oedometer-type settlements (settlements without lateral deformation).

2.4.1 Description of the device

The apparatus includes (Figure 2.12):

- A cell containing the soil sample,
- A loading frame.

The essential components of the cell are:

- A metal cylinder containing the soil sample,
- Two porous stones ensuring drainage on both faces of the sample,
- Dial gauges measuring piston displacements with a precision of 1/100,
- The soil sample, typically 70 mm in diameter and an initial thickness of around 24 mm (most common oedometer configuration).

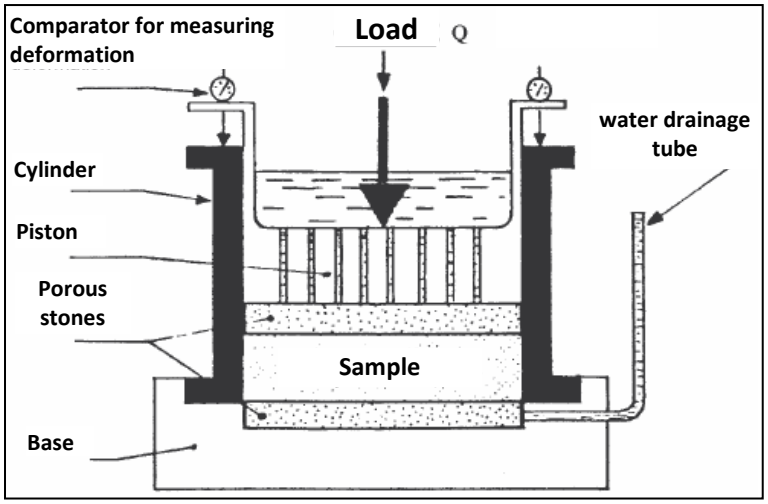

Figure 2.12 Terzaghi's Oedometer

The loading frame allows vertical loads *Q* to be applied on the piston, corresponding to pressures σ ranging from 5 to 2500 kPa.

2.4.2 Use of Terzaghi's oedometer

The associated tests allow the establishment of two types of curves:

1. **Compressibility curves**, which indicate the total settlement as a function of the applied stress,
2. **Consolidation curves**, which determine the settlement of the sample over time when a constant stress is applied.

2.5 Soil compressibility

2.5.1 Compressibility curve

The compressibility curve is established as follows: Normal stresses are applied to the sample in successive increments in the presence of water. Settlement is measured under each load increment until stabilization is practically achieved. The duration of each load application is generally 24 hours.

The results are presented as variations of the soil void ratio *e* as a function of $\log \sigma'$ (Fig. 2.13). These variations are related to the relative settlement by the relation:

$$\frac{\Delta H}{H_0} = \frac{\Delta e}{1 + e_0}$$

where:

H_0 : initial thickness of the sample

e_0 : void ratio corresponding to H_0

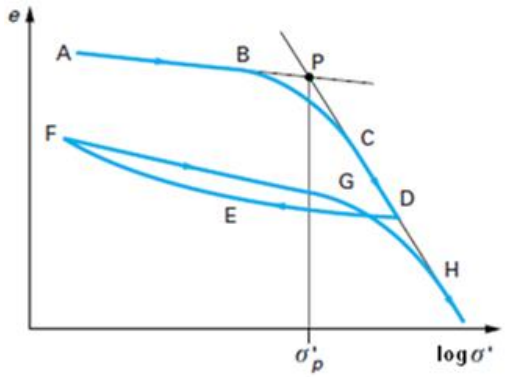

Figure 2.13 Compressibility Curve

The compressibility curve consists of two approximately straight segments connected by a curved portion. After reaching the desired maximum load (point D), an unloading-reloading cycle can be performed. The curve has two roughly linear portions: AB with a small slope and CD with a steep slope, connected by a curved segment.

Observations:

- Segments AB and FD are approximately parallel.
- Beyond point D, the straight portion continues in the extension of CD (same slope).

2.5.2 Compressibility characteristics

The compressibility curve makes it possible to determine four characteristics of the studied soil:

- The preconsolidation pressure,
- The compression index,
- The swelling index,
- The oedometer modulus.

2.5.2.1 Preconsolidation pressure σ'_p

The compressibility curve allows the graphical determination of the preconsolidation pressure σ'_p (Figure 2.14).

The simplest method consists of taking the abscissa of the intersection point of the two asymptotic straight lines.

Casagrande proposed a method based on the bisector Tc of an angle whose vertex is point T, corresponding to the point of minimum radius of curvature (Figure 2.14).

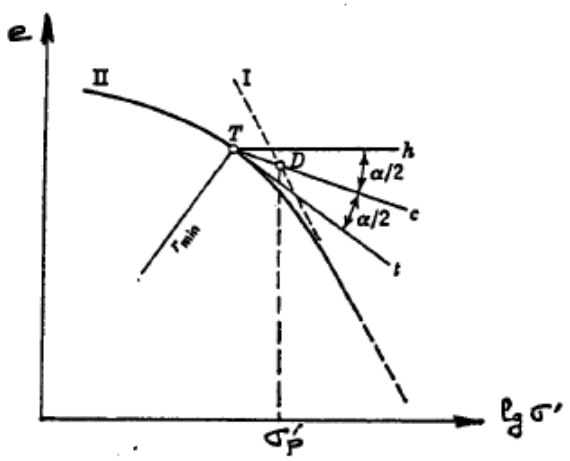

Figure 2.14 Determination of σ'_p (Casagrande method)

We observe that:

For $\sigma'_v < \sigma'_p$, the soil deforms very little because it has already been consolidated in its past under a pressure whose maximum value was equal to σ'_p.

For $\sigma'_v > \sigma'_p$, the soil becomes much more deformable because it is subjected to stresses higher than any it has previously experienced. The corresponding portion of the curve is called the *virgin compression curve*.

2.5.2.2 Compression index C_c

The compression index, denoted C_c, is defined as the (negative) slope of the virgin compression curve:

For $\sigma' \geq \sigma'_p$:

$$C_c = -\frac{\Delta e}{\Delta(log\sigma')} \qquad (C_c \text{ is a dimensionless number})$$

with:

$$\Delta(log\sigma') = log(\sigma' + \Delta\sigma') - log\sigma' = log\left(1 + \frac{\Delta\sigma'}{\sigma'}\right)$$

For an initial effective stress $\sigma'_{v0} = \sigma'_p$ and a stress increment $\Delta\sigma'$, we obtain:

$$\Delta e = -C_c log\left(1 + \frac{\Delta\sigma'}{\sigma'_{v0}}\right)$$

and since:

$$\frac{\Delta H}{H_0} = \frac{\Delta e}{1 + e_0}$$

we can write:

$$\Delta H = -H_0 \frac{C_c}{1+e_0} \cdot log\left(1 + \frac{\Delta\sigma'}{\sigma'_{v0}}\right)$$

This equation makes it possible to calculate the change in thickness ΔH of a soil layer of initial thickness H_0 when the effective vertical stress increases from σ'_{v0} to $\sigma'_{v0} + \Delta\sigma'$ (provided that $\sigma'_{v0} = \sigma'_p$).

Since the layer thickness decreases, ΔH is negative; the settlement S is therefore equal to $|\Delta H|$.

Table 2.2 Typical values of the compression index for various soils

Soil type	**Range of C_c**
Sand	$0.01 < C_c < 0.10$
Kaolinites	$0.10 < C_c < 0.25$
Illites	$0.25 < C_c < 0.80$
Montmorillonites	$0.80 < C_c < 2.50$

Table 2.3 Compressibility classification based on C_c

Compressibility	**Criterion**	**Typical soil**
incompressible	$C_c < 0.02$	Sands
very slightly compressible	$0{,}02 < C_c < 0{,}05$	
slightly compressible	$0.05 < C_c < 0.10$	
moderately compressible	$0.10 < C_c < 0.20$	Kaolinites
fairly highly compressible	$0.20 < C_c < 0.30$	Illite
very compressible	$0.30 < C_c < 0.50$	
extremely compressible	$0.50 < C_c$	Montmorillonites

Indirect estimation of the compression index:

When oedometer tests are not available at certain depths, empirical correlations can be used:

$$C_c = \frac{W_n}{100}$$

Initially used for peat, but applicable to clays as well.

$$C_c = 0.009(W_L - 10)$$

Proposed by Skempton, valid for normally consolidated clays (with W_L expressed in percent).

2.5.2.3 Swelling index C_s

The swelling index, denoted C_s, is the (negative) average slope of the unloading–reloading cycle of the compression curve.

2.5.2.4 Oedometer modulus

A modulus is a parameter in a constitutive law that links stresses to strains.

In the case of an oedometer loading condition (i.e., one-dimensional deformation), we write:

$$\Delta\sigma' = -E_{oed} \cdot \frac{\Delta H}{H}$$

The oedometer modulus E_{oed} has the dimensions of stress.

$$E_{oed} = -\frac{\Delta\sigma'}{\frac{\Delta H}{H}} = -\frac{\Delta\sigma'(1+e)}{\Delta e} = \frac{(1+e)}{C_c} \cdot \frac{\Delta\sigma'}{log\left(1+\frac{\Delta\sigma'}{\sigma'}\right)} = \frac{1}{m_v}$$

where :

$m_v = -\frac{\Delta e}{(1+e)\Delta\sigma'}$ is called the *coefficient of compressibility*.

Remarks:

The oedometer modulus is *not constant*, unlike Young's modulus for a linear elastic material. It depends on:

- the *initial stress state* σ', and
- the *stress increment* $\Delta\sigma'$.

2.6 Calculation of consolidation settlement – oedometer method

Let an undisturbed soil sample be taken at depth *z* (Figure 2.15). We can calculate the natural effective vertical stress σ'_{v0} acting at depth *z*, and determine the preconsolidation pressure σ'_p in the oedometer. Depending on the respective values of σ'_{v0} and σ'_p, three cases may occur (Figure 2.15).

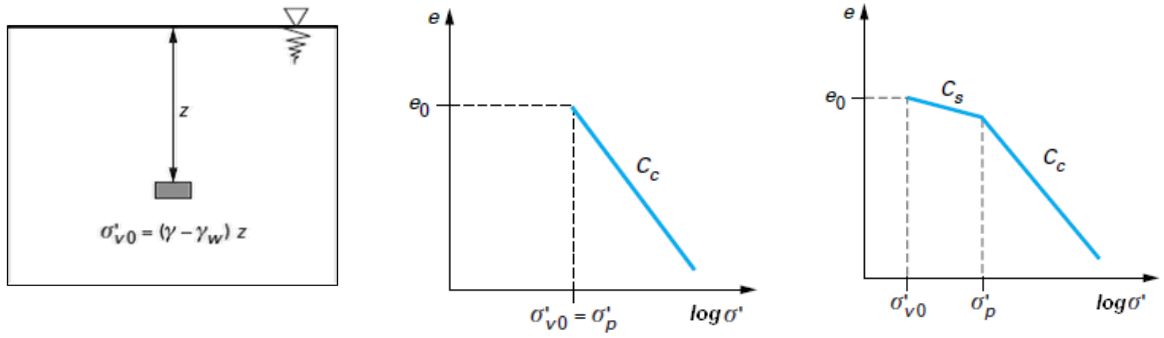

a- initial effective stress b- normally consolidated soil c- overconsolidated soil

Figure 2.15 Soil compressibility according to its in-situ consolidation state:

2.6.1 Normally consolidated soil

When $\sigma'_{v0} = \sigma'_p$, the soil is said to be *normally consolidated*.

The soil has never been subjected to a stress greater than the current geostatic stress. It has only been consolidated under the weight of the overlying layers, following the virgin compression curve. The settlement due to an increment of effective stress $\Delta\sigma'$ follows the virgin curve and is given by:

$$S = H_0 \frac{C_c}{1+e_0} \cdot log\left(1 + \frac{\Delta\sigma'}{\sigma'_{v0}}\right)$$

where:

H_0: initial thickness of the compressible layer

e_0: initial void ratio

2.6.2 Overconsolidated soil

When $\sigma'_{v0} < \sigma'_p$, the soil is *overconsolidated*.

In the past, it was subjected to a pressure greater than the current overburden stress.

Case 1: $\sigma'_{v0} + \Delta\sigma' > \sigma'_p$

$$S = H_0 \frac{C_s}{1+e_0} \cdot log\left(\frac{\sigma'_p}{\sigma'_{v0}}\right) + H_0 \frac{C_c}{1+e_0} \cdot log\left(\frac{\sigma'_{v0} + \Delta\sigma'}{\sigma'_p}\right)$$

Often, the settlement corresponding to the stress increase from σ'_{v0} to σ'_p is neglected, because this portion of the compression curve has a very low slope.

Thus, settlement is approximated by:

$$S = H_0 \frac{C_c}{1+e_0} \cdot log\left(\frac{\sigma'_{v0} + \Delta\sigma'}{\sigma'_p}\right)$$

Overconsolidation may be caused by:

- overburden from geological layers that were later eroded,
- temporary loads such as the weight of a glacier that has since disappeared.

Case 2 : $\sigma'_{v0} + \Delta\sigma' < \sigma'_p$

$$S = H_0 \frac{C_s}{1+e_0} \cdot log\left(\frac{\sigma'_{v0} + \Delta\sigma'}{\sigma'_{v0}}\right)$$

The corresponding settlement is generally very small.

2.6.3 Underconsolidated soil

When $\sigma'_{v0} > \sigma'_p$, the soil is *underconsolidated*. This occurs in soils that are still consolidating under their own weight (recent fills, poorly compacted fills, newly formed clays, silts, peats). The primary consolidation process is not complete, meaning excess pore water pressure has not fully dissipated.

Such soils are generally unsuitable for construction, as they continue deforming even without additional loading.

2.6.4 Expansive (swelling) soils

These are soils for which the unloading-reloading curve shows a marked slope under low stress. They are particularly dangerous for the foundations of lightweight structures.

2.7 Decomposition of the soil into homogeneous layers

Natural sites rarely consist of a fully homogeneous and isotropic compressible soil over the entire thickness. We consider the final settlement: the soil is fully consolidated, and the stress variation caused by the applied loads is taken up by the soil skeleton.

The soil is divided into *n* layers of height h_i (Figure 2.16).

Oedometer tests are performed on samples taken from the middle of each layer. For each sample, the swelling and compression indices, C_s and C_c, as well as the preconsolidation pressure σ'_p, are determined. At the middle of each layer, the initial vertical effective stress before construction σ'_{v0} and the stress increment due to the construction $\Delta\sigma'_z$ are calculated.

A simplifying assumption is made that the values of these two parameters remain constant throughout the thickness of the considered layer.

The settlement S_i of each of the *n* layers is then calculated using the formulas presented in the previous section. The total settlement is equal to the sum of the settlements of all *n* layers:

$$S = \sum_{i=1}^{i=n} S_i$$

Note:

- The approximation of S_i is more accurate when h_i is small.
- h_i can be chosen larger when the depth increases.
- If the soil consists of several layers with different properties, the settlement for each identified layer must be calculated separately.

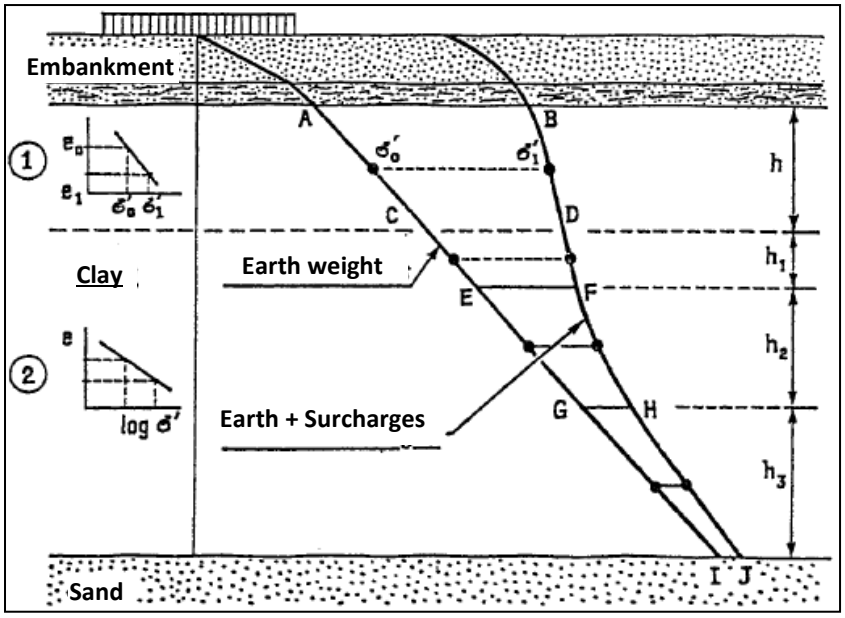

Figure 2.16 Layered soil

2.8 Secondary consolidation

Following primary consolidation, also called hydrodynamic consolidation, a delayed phenomenon occurs, known as *secondary consolidation* (Figure 2.11). It corresponds to *creep of the soil's solid mineral skeleton*. The settlement approximately follows a *linear law with respect to the logarithm of time*, meaning it continues to occur long after primary consolidation has dissipated. This phenomenon is particularly pronounced in peats and recently deposited silts.
Secondary settlement occurs *with almost no loss of load* (since it is very slow). It is determined by simple geometric scaling (homothety) from the results of the compressibility test. The most commonly used method is the *Buisman and Koppejan (1948)* method.

For $t \leq t_{100}$, the settlement follows a law that involves, in particular, the theory of consolidation.

For $t > t_{100}$, the settlement law is written as:

$$S_f = \Delta\sigma \cdot h \cdot \alpha \cdot log\left(\frac{t}{t_{100}}\right)$$

where:

$\Delta\sigma$: uniformly distributed applied stress

h: initial thickness of the compressible layer

α: proportionality coefficient determined in the oedometer (long-term test)

t_{100}: time corresponding to the end of primary consolidation

2.9 Differential settlements and allowable settlements

With regard to the structures supported by the soil, the absolute magnitude of settlements is generally of secondary importance: the stresses induced in buildings and civil engineering structures depend on the difference in settlement between points of the structure. This difference in settlement between two points A and B is called the *differential settlement*:

$$S_{AB} = S_A - S_B$$

Differential settlements can have several origins:

- **Origins related to loading:**
  - Unequal load intensity from one support to another,
  - Non-uniform load distribution under a support,
  - Different loaded surface areas from one support to another.
- **Origins related to the supports:**
  - Geometry of the supports (dimensions, depth),
  - Stiffness of the supports.
- **Origins related to the site:**
  - Variations in geometric characteristics of the layers (notably thickness),
  - Variations or heterogeneity in soil properties.

The *angular distortion* ω, equal to the differential settlement between two points divided by their horizontal distance, is often used to describe the allowable differential settlements for buildings and civil engineering structures.

See Appendix 5: *Order of magnitude of allowable settlements*.

2.10 Rate of consolidation

The one-dimensional consolidation theory proposed by Terzaghi in the early 20th century deals with the consolidation of a layer in which deformations and flow occur *only in the vertical direction*, and where the load is applied instantaneously at the initial moment. This theory corresponds to the conditions of the oedometer test, under each loading increment, and to the configuration of horizontal compressible soil layers without horizontal displacements. Despite assumptions that significantly simplify some aspects of soil behavior, this theory remains the reference for consolidation calculations because it incorporates the main components of the

phenomenon and correctly represents the behavior observed in saturated compressible soils under structures.

Consider a compressible soil layer of thickness *H*, extending infinitely in the horizontal direction, on the surface of which a uniform pressure σ is applied (Figure 2.17).

The problem is to study the *time-dependent evolution of settlements* under the following assumptions:

- The compressible layer is homogeneous, isotropic, and saturated,
- The upper boundary of the layer is drained, allowing pore water to escape, while the lower boundary is an impermeable substratum,
- Darcy's law is applicable,
- The permeability coefficient *K* is constant in the compressible layer and constant in time,
- The medium is infinite in the horizontal direction. In other words, due to symmetry, flow lines are vertical and equipotential lines are horizontal,
- The surcharge σ causing consolidation is uniform and applied instantaneously.

The differential equation governing the consolidation phenomenon is:

$$\frac{\partial u}{\partial t} = C_v \frac{\partial^2 u}{\partial z^2}$$

where:

u: pore pressure at any point located at elevation *z* in the layer, at time *t*,

C_v : coefficient of consolidation of the soil, defined as:

$$C_v = \frac{K \cdot E_{oed}}{\gamma_w}$$

C_v is expressed in cm²/s and depends on the soil's permeability and compressibility.

To solve the problem, this partial differential equation must be supplemented with boundary conditions and an initial condition.

Solving the problem leads to the definition of a dimensionless number T_v, called the time factor:

$$T_v = \frac{C_v}{H^2} \cdot t$$

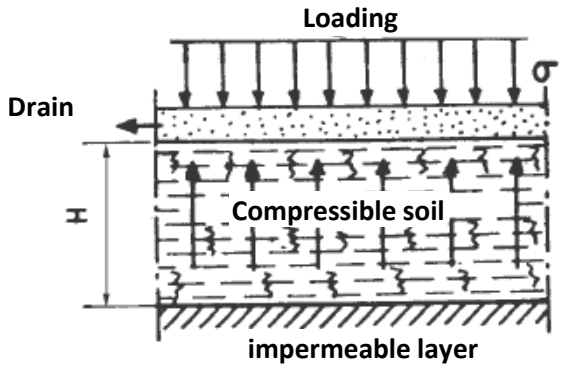

Figure 2.17 Layer drained on one side

2.10.1 Average degree of consolidation

The average degree of consolidation of a compressible layer is defined as the ratio of the settlement S_t at time t to the final settlement S_∞; it is denoted by U. It is a dimensionless number.

$$U(t) = \frac{S_t}{S_\infty}$$

where:

S_t : settlement at time t

S_∞ : final primary settlement

The degree of consolidation is a well-defined function of the time factor:

$$U = f(T_v)$$

This function is independent of the applied load σ and the geometric (H), hydraulic (K), and mechanical (E_{oed}) characteristics of the problem. These parameters only affect the calculation of the time factor.

In practice, the function $U = f(T_v)$ is presented as a graph or table (see Appendix 6).

Approximate formulas:

$$U = \left(\frac{T_v^3}{T_v^3 + 0.5}\right)^{\frac{1}{6}}$$ (Brinch- Hansen relation)

and

$$\begin{cases} U < 60\ \% \ \longrightarrow \ T_v = \frac{\pi}{4}\left(\frac{U}{100}\right)^2 \\ U > 60\ \% \ \longrightarrow \ T_v = 1.781 - 0.933log(100 - U) \end{cases}$$ (Casagrande et Taylor relations)

2.10.2 Consolidation of a layer drained on both sides

Let *H* be the thickness of the layer. Figure 2.18 shows the direction of flow toward the drains during the consolidation process. By symmetry, the behavior is similar to that shown in Figure 2.17, but with an effective thickness equal to *H*/2.

The upper half of the compressible layer drains through the top drain, and the lower half drains through the bottom drain. As a result, the time factor is given by:

$$T_v = \frac{4C_v}{H^2} \cdot t$$

Let the drainage length be the maximum distance between any point in the soil and the nearest drain. The consolidation time is proportional to the square of the drainage length.

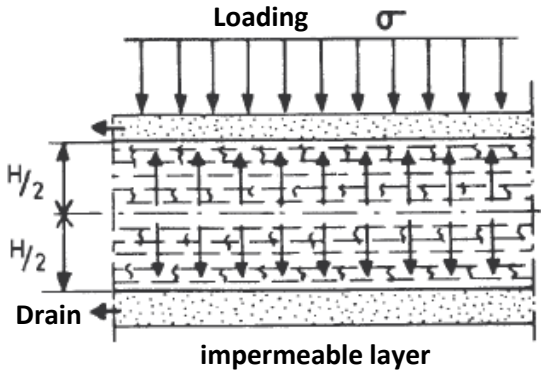

Figure 2.18 Layer drained on both side

2.10.3 Duration of settlements

Granular soils settle in very short times (simultaneously with the application of the load); therefore, the question of settlement duration concerns only fine soils (delayed phenomenon).
The time factor is defined by the relation:

$$T_v = \frac{C_v}{H^2} \cdot t$$

Knowing the consolidation coefficient C_v, it allows the determination of the time *t* required to reach a chosen degree of consolidation *U*: for a given $U \rightarrow T_v$ is determined $\rightarrow t = \frac{H^2}{C_v} \cdot T_v$ is calculated.

2.10.4 Determination of C_v in the oedometer – Casagrande method

The consolidation coefficient C_v is determined from the consolidation curve (*S* - *logt*) or (*H* - *logt*), where *S* (or *H*) is the settlement (or height) of the sample under a given load (Figure 2.19).

$$C_v = \frac{T_v \cdot d^2}{t}$$

It is calculated for a mean degree of consolidation U = 0.5. For $U = 0.5$, $T_v = 0.197$, which gives:

$$C_v = \frac{0{,}197 \cdot d^2}{t_{50}}$$

where t_{50} is the time required to achieve 50% of primary consolidation, and $d = H$ is the half-thickness of the sample drained on both faces at time t_{50}, called the drainage path.

Determination of t_{50}:

Knowing H_0, the initial height of the sample at the start of the loading step, we successively determine:

Steps	**Time**	**Sample Heigh**	**Description**
1°	t_{100}	H_{100}	End of primary consolidation
2°	-	H_{50}	Middle of the segment H_0H_{100}
3°	t_{50}	-	Abscissa of the point corresponding to ordinate H_{50}

Table 2.4 Typical orders of magnitude of the consolidation coefficient $\underline{C_v}$ (in m²/s):

Soil Type	**C_v (m²/s)**
Kaolinites	$2.10^{-7} < C_v < 4.10^{-7}$
Illites	$10^{-7} < C_v < 2.10^{-7}$
Montmorillonites	$2.10^{-8} < C_v < 10^{-7}$
Sandy clays	Around 10^{-7}
Silts	Around 5.10^{-6}

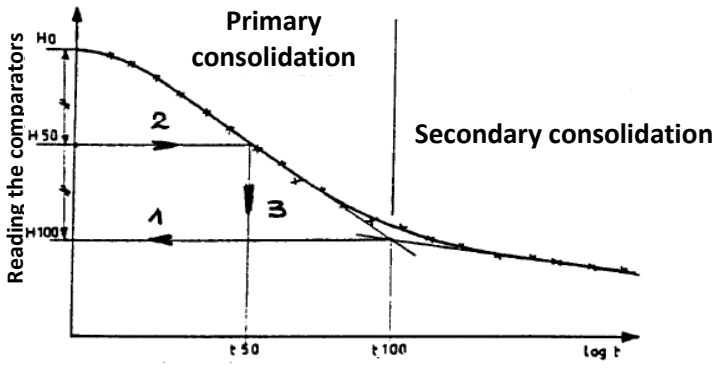

Figure 2.19 Consolidation curve

2.10.5 Time required to reach final settlement

The final settlement is considered reached when U = 99.42%. At this point, T_v = 2.00. The time required to achieve the final settlement is calculated using this T_v value (see Appendix 6).

2.10.6 Consolidation of a soil composed of multiple layers

For a soil composed of several layers subjected to one-dimensional consolidation under a uniformly distributed load (Figure 2.20), an equivalent single homogeneous layer of thickness H and consolidation coefficient C_{ve} can be considered:

$$C_{ve} = \frac{H^2}{\left(\sum_i \frac{h_i}{\sqrt{C_{vi}}}\right)^2} \qquad \text{(Absi's relation)}$$

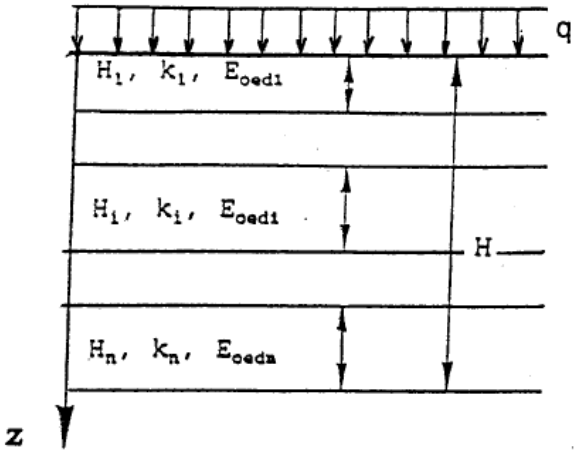

Figure 2.20 Case of a stratified soil

2.11 Exercises

Exercise 1

Calculate the vertical stress increase produced by the concentrated loads Q_1, Q_2, and Q_3 shown in the figure below, at points A, B, and C, using the Boussinesq method.

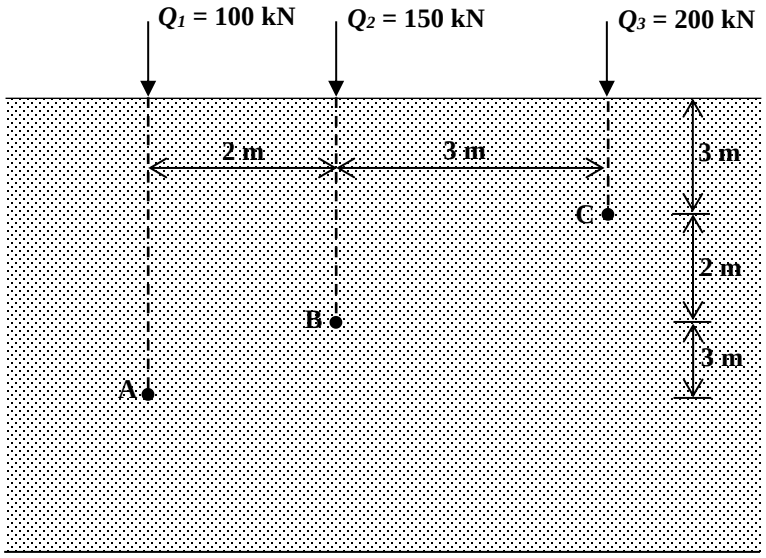

Solution

The concentrated loads Q_1, Q_2, and Q_3 are assumed to be transmitted by an isolated footing resting on the ground surface. The resulting stress distribution within the soil mass is assumed to be equivalent to that produced by these forces acting at the surface of a semi-infinite, homogeneous, and elastic medium.

Under these conditions, at a depth *z*, at a radial distance *r* from the load *Q*, the vertical stress acting on a horizontal plane is given by Boussinesq's equation:

$$\Delta\sigma_Z = \frac{3Q}{2\pi} \cdot \frac{z^3}{(r^2 + z^2)^{\frac{5}{2}}}$$

or equivalently:

$$\Delta\sigma_z = \frac{Q}{z^2} \cdot N$$

with:

$$N = \frac{3}{2\pi \left[1 + \left(\frac{r}{z}\right)^2\right]^{\frac{5}{2}}}$$

Calculation at point A

$$\Delta\sigma_{ZA} = \Delta\sigma_{Z1} + \Delta\sigma_{Z2} + \Delta\sigma_{Z3}$$

- For Q_1:

$$\Delta\sigma_{Z1} = \frac{3Q_1}{2\pi} \cdot \frac{z^3}{(r_1^2 + z^2)^{\frac{5}{2}}} = \frac{3 \times 100}{2\pi} \times \frac{8^3}{(0^2 + 8^2)^{\frac{5}{2}}} = 0.746$$

- For Q_2:

$$\Delta\sigma_{Z2} = \frac{3Q_2}{2\pi} \cdot \frac{z^3}{(r_2^2 + z^2)^{\frac{5}{2}}} = \frac{3 \times 150}{2\pi} \times \frac{8^3}{(2^2 + 8^2)^{\frac{5}{2}}} = 0.961$$

- For Q_3:

$$\Delta\sigma_{Z2} = \frac{3Q_3}{2\pi} \cdot \frac{z^3}{(r_3^2 + z^2)^{\frac{5}{2}}} = \frac{3 \times 200}{2\pi} \times \frac{8^3}{(5^2 + 8^2)^{\frac{5}{2}}} = 0.654$$

Thus:

$$\Delta\sigma_{ZA} = 0.746 + 0.961 + 0.654 = 2.361$$

The same procedure is followed to calculate $\Delta\sigma_{ZB}$ and $\Delta\sigma_{Zc}$ at points B and C.

Summary of Results

Point	Q_i	r_i	z	$\Delta\sigma_{zi}$ (kPa)	$\Delta\sigma_z$ (kPa)
A	100	0	8	0.746	2.361
	150	2	8	0.961	
	200	5	8	0.654	
B	100	2	5	1.318	5.954
	150	0	5	2.865	
	200	3	5	1.771	
C	100	5	3	2.124	14.14
	150	3	3	1.406	
	200	0	3	10.61	

Exercise 2

The foundation shown in the figure below is subjected to a uniform load of 15 kN/m².

Calculate the vertical stress increase at points A, B, and C, located at a depth of 4 m below the ground surface.

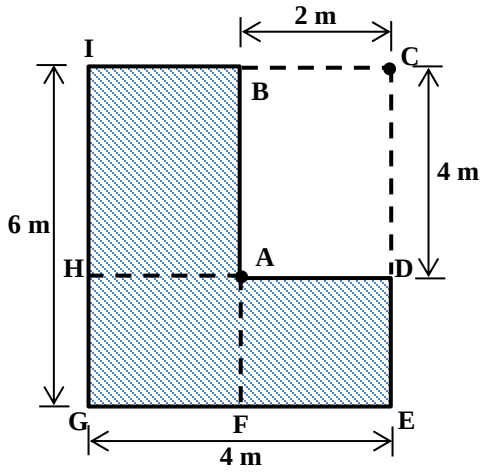

Solution

The increase in vertical stress in a semi-infinite medium beneath the corner of a uniformly loaded rectangular area q is given by:

$$\Delta\sigma_z = K \cdot q$$

where $K = K(m, n)$ is a dimensionless influence factor, with:

$m = \frac{a}{z}, \qquad n = \frac{b}{z}$

The value of *K* is obtained from influence charts (see Chart No. 2 in Appendix 2).

Calculation at Point A

To compute the stress increase at point A, the loaded area is divided into three rectangles: ABCD, ADEF, and AFGH.

$$\Delta\sigma_z = \Delta\sigma_{z1} + \Delta\sigma_{z2} + \Delta\sigma_3 = (K_1 + K_2 + K_3)q$$

- Rectangle ABCD:

$$\frac{a}{z} = 0.5, \quad \frac{b}{z} = 1 \quad \Longrightarrow \quad K_1 = 0.12$$

- Rectangle ADEF:

$$\frac{a}{z} = 0.5, \quad \frac{b}{z} = 0.5 \quad \Longrightarrow \quad K_1 = 0.085$$

- Rectangle AEGH:

$$\frac{a}{z} = 0.5, \quad \frac{b}{z} = 0.5 \quad \Longrightarrow \quad K_1 = 0.085$$

Thus:

$$\Delta\sigma_z = (K_1 + K_2 + K_3)q = (0.12 + 0.085 + 0.085) \times 15 = 4.35 \text{ kPa}$$

The same procedure is followed to calculate the stresses at points B and C (see table below).

Point	Rectangle	*a/z*	*b/z*	*K*	$\Delta\sigma_{zi}$ (kPa)	$\Delta\sigma_z$ (kPa)
A	ABIH	0.5	1	0.12	1.8	4.35
	AHGF	0.5	0.5	0.085	1.275	
	AFED	0.5	0.5	0.085	1.275	
B	BIGF	0.5	1.5	0.13	1.95	2.1
	BFEC	0.5	1.5	0.13	1.95	
	BADC	0.5	1	0.12	1.8	
C	CIGE	1	1.5	0.194	2.91	1.11
	CBAD	0.5	1	0.12	1.8	

Exercise 3

A clay specimen is subjected to an oedometer test, which yields the following results:

Stress σ (daN/cm²)	0	0.1	0.2	0.4	0.8	1.6	3.2	6.4	12.8	1.6	0.4	0.1
Settlement ΔH (mm)	0	0.02	0.03	0.05	0.10	0.19	0.43	1.09	1.78	1.58	1.43	1.22

At the beginning of the test, the specimen height is 25 mm and its initial void ratio is e_0 = 1.01.

Construct the oedometer curve $e - log\sigma$, and determine:

- the compression index C_c,
- the preconsolidation pressure σ'_p,
- the oedometer modulus E_{oed} corresponding to the stress interval [6.4 daN/cm^2 −12.8 daN/cm^2] during loading.

Solution

1) Oedometer curve $e - log\sigma$

$$\frac{\Delta H}{H_0} = \frac{\Delta e}{1 + e_0}$$

$$\Delta e = \frac{1 + e_0}{H_0}\Delta H = \frac{1 + 1.01}{25}\Delta H$$

$$\Delta e = 8.04 \times 10^{-2}\Delta H$$

σ (daN/cm²)	ΔH (mm)	Δe ($\times 10^{-4}$)	$e = e_0 - \Delta e$
0	0	0	1.010
0.1	0.02	16.1	1.0084
0.2	0.03	24.1	1.0076
0.4	0.05	40.2	1.006
0.8	0.10	80.4	1.002
1.6	0.19	152.8	0.995
3.2	0.43	345.7	0.975
6.4	1.09	876.4	0.922
12.8	1.78	1431.1	0.867
1.6 (unloading)	1.58	1270.3	0.883
0.4 (unloading)	1.43	1149.7	0.895
0.1 (unloading)	1.22	980.9	0.912

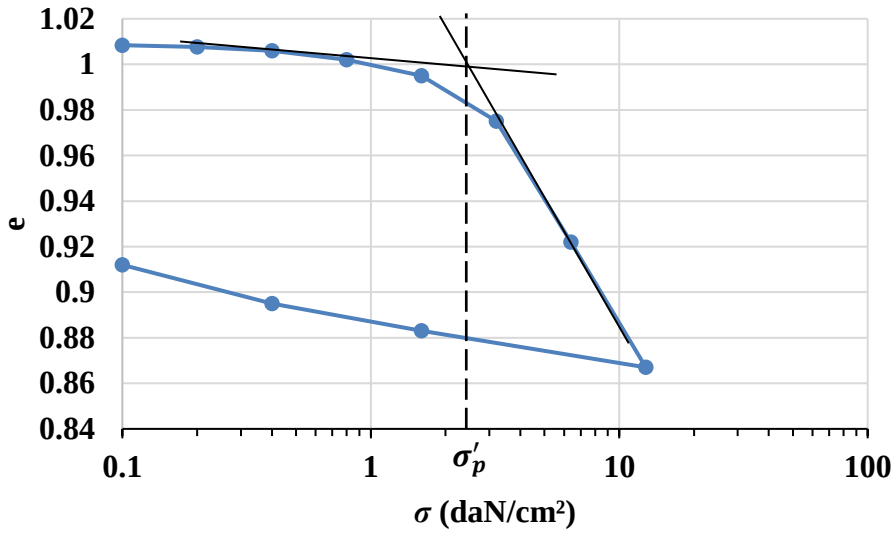

2) Compression index C_c

$$C_c = -\frac{\Delta e}{\Delta log\sigma}$$

The curve may be approximated by a straight line for: $3.2 \leq \sigma \leq 12.8$ daN/cm²

$$C_c = -\frac{0.867 - 0.975}{log12.8 - log3.2} = 0.18$$

3) Oedometer modulus E_{oed}

$$E_{oed} = -\frac{\Delta\sigma}{\Delta H/H}$$

Where:

H: specimen height at σ = 6.4 daN/cm²

ΔH: settlement between 6.4 and 12.8 daN/cm²

H = 25 – 1.09 = 23.91 mm

ΔH = – (1.78 – 1.09) = – 0.68 mm

$\Delta\sigma$ = 12.8 – 6.4 = 6.4 daN/cm²

Thus :

$$E_{oed} = \frac{6.4}{0.69/23.91} = 222 \text{ daN/cm}^2$$

4) Preconsolidation pressure σ_p'

The preconsolidation pressure is determined graphically using the Casagrande method:

$$\sigma_p' = 2.4 \text{ daN/cm}^2$$

Exercise 4

The consolidation of a clay layer, drained on both sides and having a thickness of 8 m, is studied. The clay has a coefficient of permeability $K = 3 \times 10^{-9}$ cm/s and an oedometer modulus $E_{oed} = 400$ daN/cm². Determine the time required to reach a degree of consolidation of 40% and 80%.

Solution

According to Terzaghi's consolidation theory, the degree of consolidation U is a function of the time factor T_v:

$$T_v = \frac{C_v t}{H^2} \qquad \Rightarrow \qquad t = \frac{H^2 T_v}{C_v}$$

where:

$$C_v = \frac{K E_{oed}}{\gamma_w}$$

Thus:

$$t = \frac{\gamma_w H^2 T_v}{K E_{oed}}$$

The function $T_v = f(U)$ is given in table 2 (Appendix 6).

For U = 40%, T_v = 0.127

$$t_{40\%} = \frac{0.127 \times 16 \times 9.81 \times 10^3}{3 \times 10^{-11} \times 4 \times 10^7} = 0.127 \times 13.08 \times 10^7 \text{ seconds}$$

$$t_{40\%} = \frac{0.127 \times 13.08 \times 10^2}{0.864} = 192 \text{ days}$$

Thus:

$$t_{40\%} = 6 \text{ months}, 12 \text{ days}$$

For U = 80%, T_v = 0.567

$$t_{80\%} = \frac{0.567 \times 16 \times 9.81 \times 10^3}{3 \times 10^{-11} \times 4 \times 10^7} = 0.567 \times 13.08 \times 10^7 \text{ seconds}$$

$$t_{80\%} = \frac{0.567 \times 13.08 \times 10^2}{0.864} = 858 \text{ days}$$

Thus:

$$t_{80\%} = 2 \text{ years}, 4 \text{ months}, 8 \text{ days}$$

Exercise 5

Consider a 10 m thick clay layer with single drainage, which undergoes a settlement of 90 mm in 3.5 years. The coefficient of consolidation of this clay is $C_v = 0.544 \times 10^{-6}$ m²/s.

Determine:

- the final consolidation settlement S_c,
- the time required to reach a settlement equal to 90% of this value.

Solution

1) Final consolidation settlement S_c

$$T_v = \frac{C_v t}{H^2}$$

where :

H is the drainage path, equal to the full thickness for single drainage.

Convert C_v to m²/year:

$$C_v = 0.544 \times 10^{-6} \frac{\text{m}^2}{\text{s}} = 0.544 \times 10^{-6} \times 3.1536 \times 10^7 \text{ m}^2/\text{ans} = 17.155 \text{ m}^2/\text{ans}$$

Then:

$$T_v = \frac{17.155 \times 3.5}{10^2} = 0.6$$

From the table of the function $U = f(T_v)$ (Appendix 6):

$$T_v = 0.6 \quad \Rightarrow \quad U = 81.6\%$$

$$U = \frac{S(t)}{S_c}$$

$$S_c = \frac{S(t)}{U} = \frac{90}{0.8156} = 110 \text{ mm}$$

2) Time required to reach 90% of S_c

$$t = \frac{H^2 T_v}{C_v}$$

$$U = 90\% \quad \Rightarrow \quad T_v = 0.848$$

$$t = \frac{0.848 \times 10^2}{0.544 \times 10^{-6}} = 1.559 \times 10^8 \text{ seconds} = \frac{1.559 \times 10^8}{3.1536 \times 10^7} \text{ years}$$

Thus:

$$t = 4.94 \text{ years}$$

Exercise 6

An undisturbed specimen of saturated clay, 20 mm thick, is subjected to an oedometer test, which yields the following results:

Applied effective stress (kN/m²)	50	100	200
Specimen height (mm)	20	19.62	19.24

The initial water content is 40%, and the specific gravity of solids is G_s = 2.7.

1) Determine the compression index C_c and the coefficient of volume compressibility m_v for each stress increment.
2) The specimen was taken from a 4 m thick clay layer resting on an impermeable rock substratum and overlain by a sand layer. The initial average effective vertical stress in this layer is 75 kN/m². This stress increases to 150 kN/m² due to a surface load. Using these stress values, calculate the total settlement of the clay layer using the appropriate value of C_c.

Solution

1) Compression index C_c and coefficient of volume compressibility m_v

$$C_c = -\frac{\Delta e}{\Delta log\sigma}$$

$$\Delta e = \frac{1 + e_0}{H_0} \Delta H$$

From the oedometer test results:

At σ = 50kPa, the specimen thickness remains unchanged:

$$H_{50} = 20 \text{ mm}$$

$$e_{50} = e_0 = wG_s = 0.4 \times 2.7 = 1.08$$

$$\Delta e = \frac{1 + 1.08}{20}\Delta H = 0.104\Delta H$$

$$\Delta log\sigma = log\left(\frac{100}{50}\right) = log\left(\frac{200}{100}\right) = log(2) = 0.301$$

$$\Delta H = 19.62 - 20 = 19.24 - 19.62 = -0.38 \text{ mm}$$

Thus, the compression index is the same for both increments:

$$C_{c1} = C_{c2} = \frac{0.38 \times 0.104}{0.301} = 0.131$$

The coefficient of volume compressibility is:

$$m_v = -\frac{\Delta H/H}{\Delta\sigma}$$

Thus:

$$m_{v1} = \frac{0.38/20}{100 - 50} = 3.8 \times 10^{-4} \text{ m}^2/\text{kN}$$

$$m_{v2} = \frac{0.38/19.62}{200 - 100} = 1.9 \times 10^{-4} \text{ m}^2/\text{kN}$$

2) Total settlement of the clay layer ΔH

The average effective vertical stress remains within the range 50-200 kN/m², for which C_c = 0.131.

This value is therefore used to calculate settlement.

From 50 to 75 kN/m²:

$$\Delta e = -C_c\Delta log\sigma$$

$$\Delta e = -0.131log\left(\frac{75}{50}\right) = -0.023$$

$$e_{75} = \Delta e + e_{50} = 1.08 - 0.023 = 1.057$$

From 75 to 150 kN/m²:

$$\Delta e = -0.131log\left(\frac{150}{75}\right) = -0.039$$

$$\frac{\Delta H}{H} = \frac{\Delta e}{1 + e_{75}}$$

$$\Delta H = \frac{\Delta e}{1 + e_{75}} H$$

$$\Delta H = \frac{-0.039 \times 4 \times 10^3}{1 + 1.057} = -76.7 \text{ mm}$$

Thus:

$$\Delta H \approx 77 \text{ mm}$$

Exercise 7

A 3 m high embankment is constructed on a 6 m thick layer of normally consolidated clay, which rests on an impermeable rock. The groundwater is at the surface.

1) Calculate the total primary consolidation settlement under the center of the embankment.
2) How many years will it take for 50% consolidation to occur?

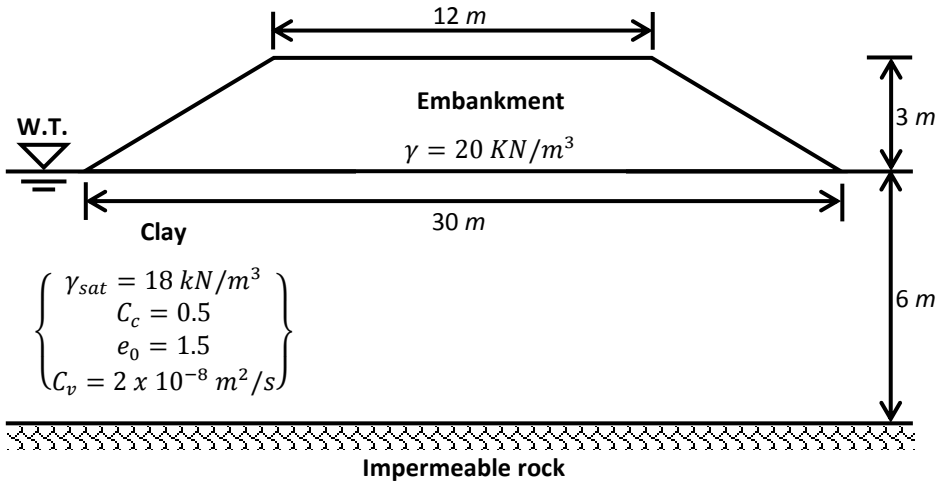

Solution

1) Primary consolidation settlement S_c

The clay layer is normally consolidated, therefore:

$$S_c = \frac{C_c}{1 + e_0} H_0 log\left(1 + \frac{\Delta\sigma'_z}{\sigma'_{v0}}\right)$$

The initial effective vertical stress is:

$$\sigma'_{v0} = (\gamma_{sat} - \gamma_w)z = (18 - 10) \times 3 = 24\ kPa$$

$$\sigma'_{v0} = 24\ kPa$$

The increase in vertical stress is:

$$\Delta\sigma'_z = 2Iq$$

From Osterberg's influence chart (Appendix 4):

For *a/z* = 3 and *b/z* = 2

I = 0.494

Thus:

$$\Delta\sigma'_z = 2 \times 0.494 \times 20 \times 3 = 59.28\ kPa$$

Then:

$$S_c = \frac{C_c}{1+e_0} H_0 log\left(1 + \frac{\Delta\sigma'_z}{\sigma'_{v0}}\right) = \frac{0.5 \times 6}{1+1.5} log\left(1 + \frac{59.28}{24}\right) = 0.65\ m$$

$$S_c = 0.65\ m$$

2) Consolidation time $t_{50\%}$

$$T_v = \frac{C_v t}{H^2}$$

For:

$$U = 50\% \quad \Rightarrow \quad T_v = 0.197$$

$$t_{50\%} = \frac{T_v H^2}{C_v} = \frac{0.197 \times 6^2}{2 \times 10^{-8}} = 3.546 \times 10^8 \text{ secondes}$$

Convert to years:

$$t_{50\%} = \frac{3.546 \times 10^8}{3.1536 \times 10^7} = 11.25 \text{ years}$$

Chapter 3
Shear strength of soils

3.1 Introduction

In practice, the solution of a soil mechanics problem consists successively in:

- verifying that stability against failure is ensured with a satisfactory factor of safety,
- ensuring that the design of the structure is compatible with the allowable settlements.

The second verification was the subject of the previous chapter; the first is the subject of the present chapter.

3.2 Basic concepts of soil failure

When the experimental stress path permits large deformations, a stress–strain curve (behavior law) of the form shown in Figure 3.1 is obtained.

The following approximations are made:

- in the small-strain range, the behavior is assumed to be linear, and the theory of linear elasticity is applied;
- in the large-strain range, the behavior is irreversible, and it is assumed that the theory of perfect plasticity can be used.

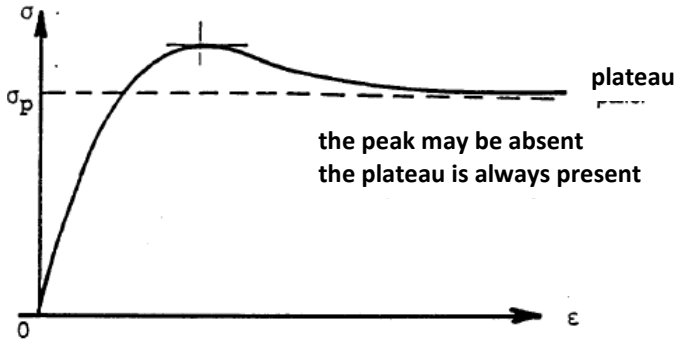

Figure 3.1 Typical stress–strain curve

Let us consider a loaded soil mass and the stresses induced at a point M within it. As the applied loads increase, the stresses increase accordingly. These stresses, however, cannot increase without limit. On certain planes, called *slip planes* or *failure surfaces*, the shear stresses eventually reach a limiting value beyond which the soil particles begin to slide relative to one another (Figure 3.2).

Failure in soil occurs by relative sliding of the grains with respect to one another, and not by breakage of the grains themselves.

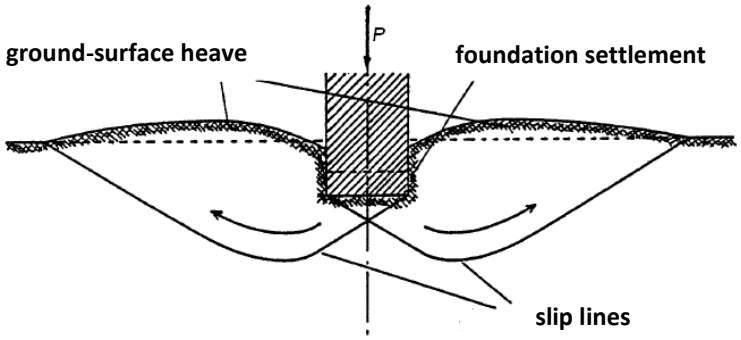

Figure 3.2 Failure mechanism in a soil mass showing slip lines

3.3 Review of continuum mechanics

3.3.1 State of stress at a point

The stress at a point M located within a continuous medium is defined with respect to an elemental plane passing through that point.

The stress vector $\vec{f}$ acting on a given plane can be resolved into (Figure 3.3):

- σ: normal stress
- τ: shear stress

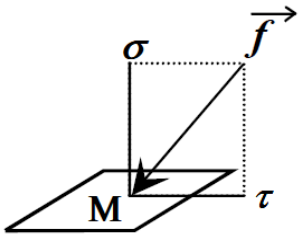

Figure 3.3 Stress components acting on an elemental plane

The state of stress at point M is defined by a tensor called the stress tensor. At every point, there exist three particular planes on which the stress is purely normal ($\tau = 0$). These are called the principal planes, and they are mutually orthogonal; the corresponding normal stresses are the principal stresses, denoted by σ_1, σ_2, σ_3.

In what follows, we will restrict ourselves to the common cases to which engineers usually reduce practical problems:

- cases where $\sigma_2 = \sigma_3$ (axisymmetric conditions),
- or cases where $\sigma_2 = 0$ (two-dimensional conditions).

3.3.2 Mohr's diagram

To study the state of stress at a point, a graphical representation of the stress vector f is generally used in a system of axes (σ, τ). The points representing the principal stresses ($\tau = 0$) therefore lie on the σ-axis. It can be shown that, when the plane rotates about a principal

direction, the tip of the stress vector traces a circle in the (σ, τ) plane, called Mohr's circle (Figure 3.4).

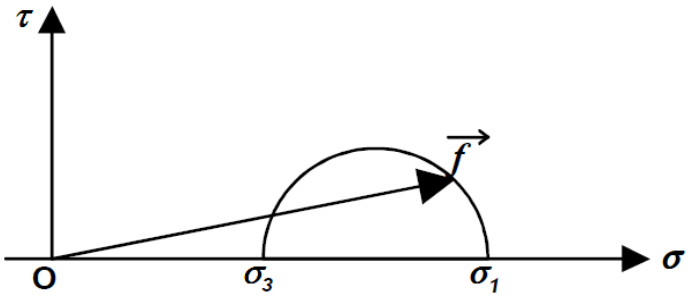

Figure 3.4 Mohr's circle for stress

It can also be shown that when the plane rotates through an angle α, the tip of the stress vector rotates through an angle 2α on Mohr's circle.

Remark: In the particular case of a liquid, τ is always zero and $\sigma_1 = \sigma_2 = \sigma_3$ (hydrostatic pressure). In this case, Mohr's representation is obviously of no practical interest.

3.4 Coulomb's law (1775)

3.4.1 Concept of the intrinsic curve

In soil mechanics, the concept of the intrinsic curve, introduced by Caquot, is commonly used. This theory applies to a homogeneous and isotropic material.

In the Mohr plane (σ, τ), the yield limit is represented by a curve, called the *failure envelope curve*, which separates the region of possible stress states from the region of stress states that cannot develop in the material, since yielding occurs before such states can be reached (Figure 3.5).

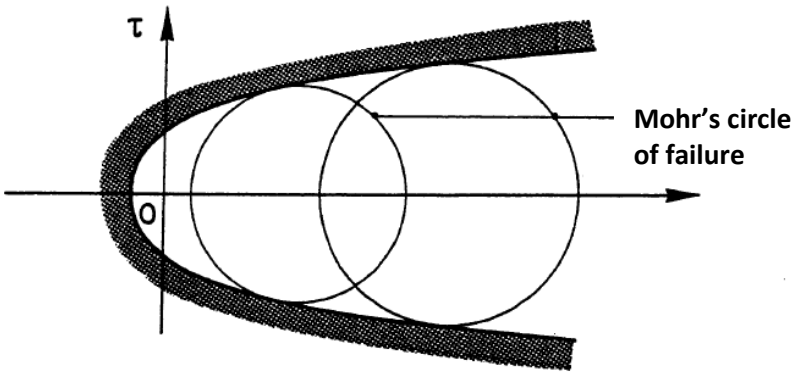

Figure 3.5 Failure envelope curve

The intrinsic curve is the envelope of the Mohr circles for which yielding of the material begins (failure Mohr circles). When a circle is tangent to the intrinsic curve, yielding occurs by sliding in the direction of the plane corresponding to the point of contact between the circle and the curve. For soils, its experimental determination is relatively straightforward.

3.4.2 Coulomb criterion

Experimental evidence shows that the failure envelope curve of a soil consists of two straight half-lines symmetrical with respect to the axis $(\overrightarrow{O\sigma'})$, called the *Coulomb lines*.

- **Cohesionless soils**: the half-lines pass through the origin of the axes.
- **Cohesive soils**: the half-lines do not pass through the origin of the axes; therefore, there exists a shear strength under zero normal stress, called the *cohesion*, denoted by c'.

The angle made by these half-lines with the axis $(\overrightarrow{O\sigma'})$, denoted by φ', is called the *angle of internal friction*.

The equations of the lines are:

For cohesionless soils:

$|\tau'_f| = \sigma' \cdot tg\varphi'$ (Figure 3.6-a)

For cohesive soils:

$|\tau'_f| = c' + \sigma' \cdot tg\varphi'$ (Figure 3.6-b)

where:

τ'_f : shear stress at failure

The two half-lines forming the intrinsic curve are also called the Coulomb failure lines. This corresponds to a perfectly plastic law known as the Coulomb criterion.

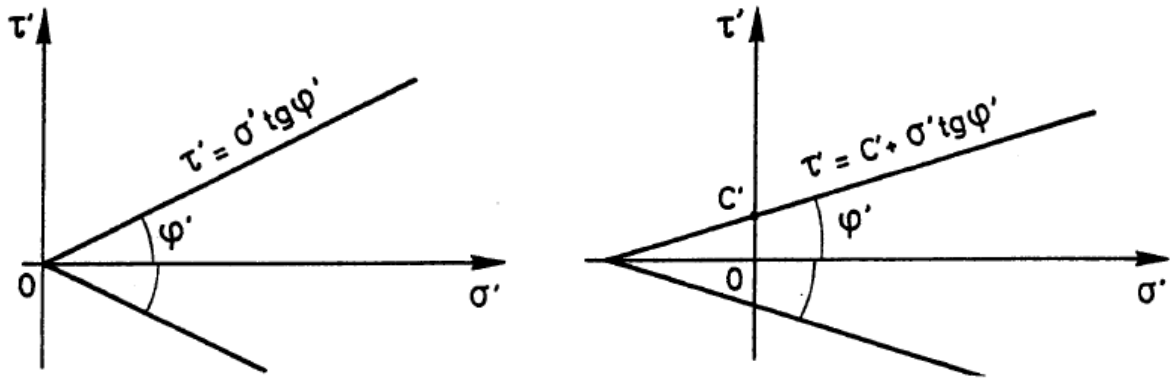

(a) cohesionless soil (b) cohesive soil

Figure 3.6 Mohr plane — Coulomb lines

3.4.3 Relationships between principal stresses at failure

Let us express the condition that the Mohr circle is tangent to the intrinsic curve (Figure 3.7):

$$\overline{IT} = \overline{IR} + \overline{RT} \implies$$

Hence,

$$\frac{\sigma_1' - \sigma_3'}{2} = \frac{\sigma_1' + \sigma_3'}{2}\sin\varphi' + c'\cos\varphi'$$

which gives

$$\sigma_1'(1 - sin\,\varphi') = \sigma_3'(1 + sin\,\varphi') + 2c'\cos\varphi'$$

therefore,

$$\sigma_1' = \frac{1 + sin\,\varphi'}{1 - sin\,\varphi'}\sigma_3' + 2c'\frac{\cos\varphi'}{1 - sin\,\varphi'}$$

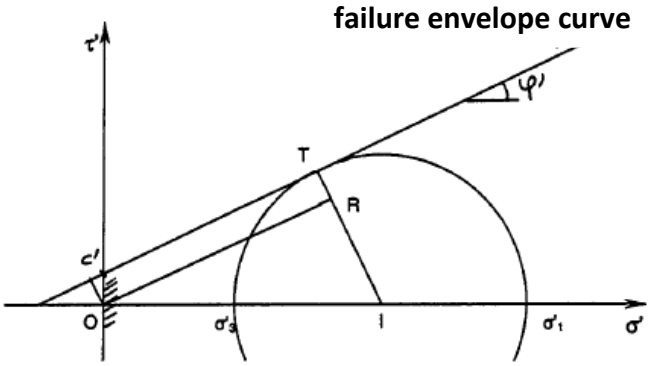

Figure 3.7 Representation of Mohr's circle

Let

$$\tan\frac{\varphi'}{2} = t$$

Then,

$\sin\varphi' = \frac{2t}{1+t^2}$ and $\cos\varphi' = \frac{1-t^2}{1+t^2}$

Hence,

$$\sigma_1' = \tan^2\left(\frac{\pi}{4} + \frac{\varphi'}{2}\right)\sigma_3' + 2c'\tan\left(\frac{\pi}{4} + \frac{\varphi'}{2}\right)$$

Similarly,

$$\sigma_3' = \frac{1 - sin\,\varphi'}{1 + sin\,\varphi'}\sigma_1' - 2c'\frac{\cos\varphi'}{1 + sin\,\varphi'}$$

Since it can be shown that:

$$\frac{1 - sin\,\varphi'}{1 + sin\,\varphi'} = \tan^2\left(\frac{\pi}{4} - \frac{\varphi'}{2}\right)$$

and

$$\frac{\cos\varphi'}{1 - sin\,\varphi'} = \tan\left(\frac{\pi}{4} - \frac{\varphi'}{2}\right)$$

it follows that:

$$\sigma_3' = \tan^2\left(\frac{\pi}{4} - \frac{\varphi'}{2}\right)\sigma_1' - 2c'\tan\left(\frac{\pi}{4} - \frac{\varphi'}{2}\right)$$

3.5 Laboratory measurement of shear strength parameters

The tests are performed on specimens taken from borehole cores. The sample is therefore unloaded, since it is subjected to zero total stress. The pore water is then placed in tension. For a given test, the specimens must be made as nearly identical as possible.

A reconsolidation stage is carried out so that, by restoring the in-situ conditions of pore pressure and effective stress, the values of the parameters that may influence the shear strength are altered as little as possible. This reconsolidation is performed before any shear strength test, particularly in the case of slow, that is, drained, tests.

To determine the Coulomb failure lines, two types of apparatus are commonly used:

- the direct shear apparatus or Casagrande shear box,
- the triaxial apparatus.

3.5.1 Direct shear apparatus (Casagrande shear box)

The specimen is placed between two halves of a shear box: an upper half C_1, which can slide horizontally over a lower half C_2 (Figure 3.8).

The soil is placed between two porous stones, which allow drainage. The porous stones may be replaced by solid plates, in which case the soil can no longer drain, at least theoretically.

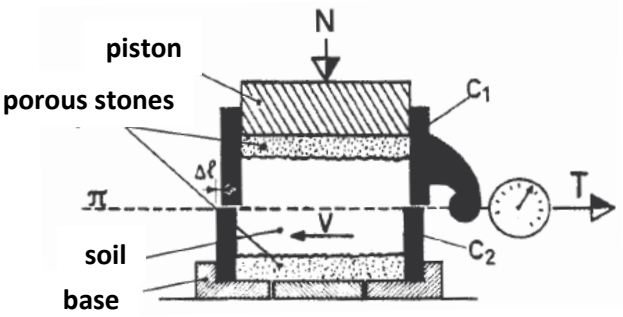

Figure 3.8 Casagrande direct shear box

The apparatus includes a loading device that makes it possible to apply a vertical load *N* through a piston. The test consists of pulling the upper half-box horizontally so as to shear the soil along plane π. The horizontal force *T* is measured as a function of the horizontal displacement Δl (Figures 3.9 and 3.10).

The test is carried out at a controlled displacement rate *V*. Let:

- *S*: cross-sectional area of the specimen along plane π,
- $\sigma_i = \frac{N}{S}$: normal stress applied to the specimen,
- $\tau_i = \frac{T}{S}$: shear stress measured at failure.

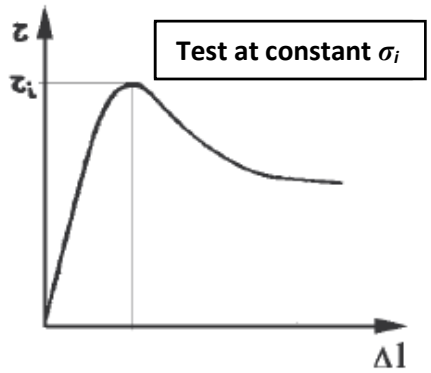

Figure 3.9 Shear stress–horizontal displacement curve

If this test is performed on several specimens of the same soil under different normal stresses, for example $\sigma_{i(i=1,2,3,4)}$, the intrinsic curve of the soil can be determined by plotting, on the Coulomb diagram (τ, σ), the points corresponding to the measured values $\tau_{i(i=1,2,3,4)}$ (Figure 3.10).

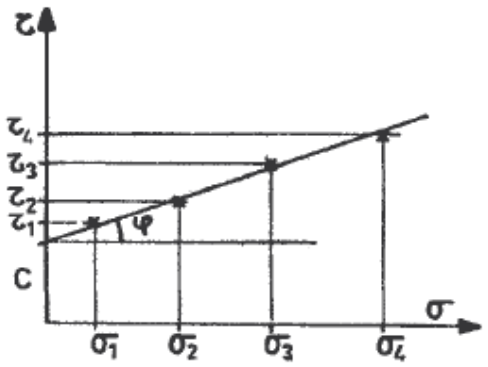

Figure 3.10 Determination of cohesion, *c*, and angle of internal friction, φ

Remark: The values of c and φ depend on the test conditions (rate of displacement, whether drainage is allowed or prevented, etc.).

3.5.2 Triaxial apparatus

The soil specimen has the shape of a right circular cylinder. It is placed inside a chamber called the triaxial cell.

The specimen is enclosed in a watertight, perfectly flexible elastic membrane. Its lower end, or both ends depending on the test arrangement, is in contact with a porous stone.

The cell is filled with water. The testing device makes it possible to apply pressure to this water, thereby subjecting the specimen to an isotropic stress σ_3 (here, $\sigma_2 = \sigma_3$).

In addition, the specimen may be compressed vertically by means of a piston. Let *P* be the load thus applied.

The vertical deformation Δl of the specimen is measured by means of a dial gauge.

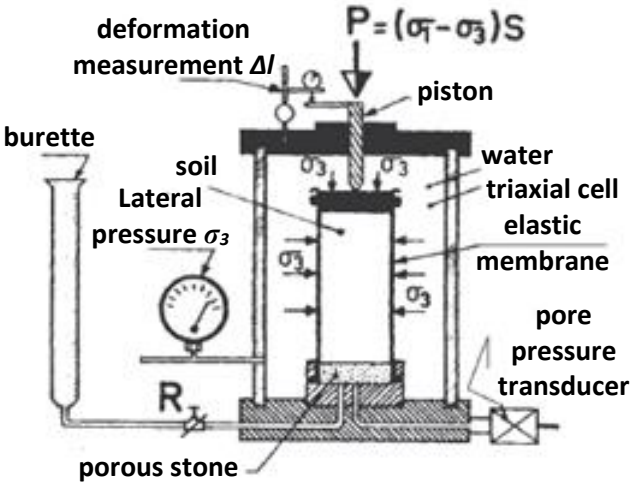

Figure 3.11 Triaxial compression apparatus

A valve R, when open, allows drainage of the specimen through the porous stones; the test is then said to be drained. When it is closed, the soil cannot drain, and the test is said to be undrained.

If R is closed and the soil is saturated, the pore water pressure may be measured by means of a pressure transducer.

If R is open, a burette makes it possible to measure the quantity of water expelled from or absorbed by the specimen.

For tests involving measurement of pore pressure, the entire system must be fully saturated.

The actual test consists, for a constant pressure σ_3, in gradually increasing *P*. By symmetry, the principal stresses σ_1 and σ_3 are respectively vertical and horizontal. Since σ_3 also acts on the upper face of the specimen, we have:

$$\sigma_1 = \frac{P}{S} + \sigma_3$$

with *S*: cross-sectional area of the specimen

At failure, the maximum stress deviator $(\sigma_1 - \sigma_3)$, corresponding to the Mohr circle tangent to the failure envelope, is therefore known (Figure 3.12).

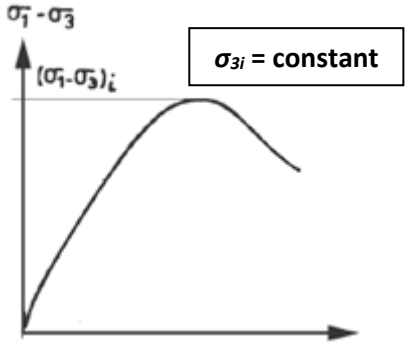

Figure 3.12 Stress–strain curve for a triaxial test

If the test is repeated for different values of σ_3, several Mohr circles are obtained, and it then becomes possible to plot the failure envelope (Fig. 3.13).

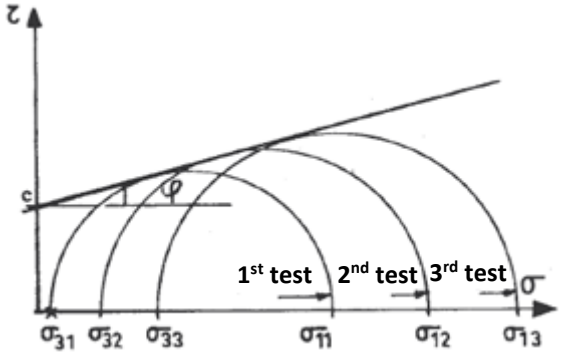

Figure 3.13 Determination of the failure envelope of a soil

Remark: As in the case of direct shear, the values of *c* and φ depend on the test conditions.

3.6 Shear strength of cohesionless soils

Since these soils are permeable, it is generally assumed that no excess pore water pressure develops in them. Experimental evidence shows that, in the Mohr plane, the failure envelope can be satisfactorily represented by a straight line passing through the origin. The angle φ that this line makes with the σ-axis is called the angle of internal friction of the soil (Figure 3.14). Shear failure occurs when:

$$\tau = \sigma tg\varphi$$

where:

τ: shear stress

σ: normal stress

φ: angle of internal friction

For a given sand, it has been observed experimentally that:

$$tg\varphi = \frac{K}{e}$$

Where, the coefficient K = 0.45 to 0.55 depends on the shape of the grains and on their particle-size distribution.

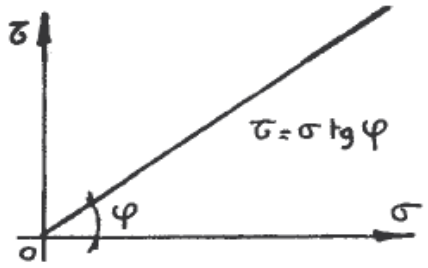

Figure 3.14 Coulomb failure line for a cohesionless soil

3.7 Shear strength of cohesive soils

Whereas, for cohesionless soils, attention is generally focused only on the drained shear strength parameters, for cohesive soils it is necessary to examine both the drained and undrained shear strength parameters. Three types of triaxial tests are commonly used to determine the parameters of the failure envelope.

- In the *consolidated-drained test (CD)*, pore water pressures are allowed to dissipate continuously during shearing. This is a slow test, corresponding to the long-term behavior of the soil. Thus, no excess pore water pressure develops during shearing. This test is classically interpreted using the Coulomb failure criterion: the failure envelope is a straight line of equation

$$\tau = c' + \sigma' tg\varphi'$$

where φ', the effective angle of internal friction, and c', the drained cohesion, are the intergranular strength parameters of the soil (Figure 3.15, CD test).

- In the *consolidated-undrained test with pore pressure measurement (CU)*, the specimen is first consolidated under an isotropic confining stress until the excess pore water pressures have dissipated. The drainage is then closed, and the axial stress is increased until failure while the pore water pressure is measured. This test, which is faster than the consolidated-drained test, still allow the determination of the intergranular parameters c' and φ', provided that it is interpreted in terms of *effective stresses* (Figure 3.15, CU test).
- In the *unconsolidated-undrained test (UU)*, pore water pressures are not allowed to dissipate. This rapid test corresponds to the short-term behavior of the soil. The test is interpreted in terms of *total stresses* and allows the estimation of c_u, the undrained cohesion. The angle of internal friction φ_u is generally assumed to be zero (Figure 3.15, UU test).

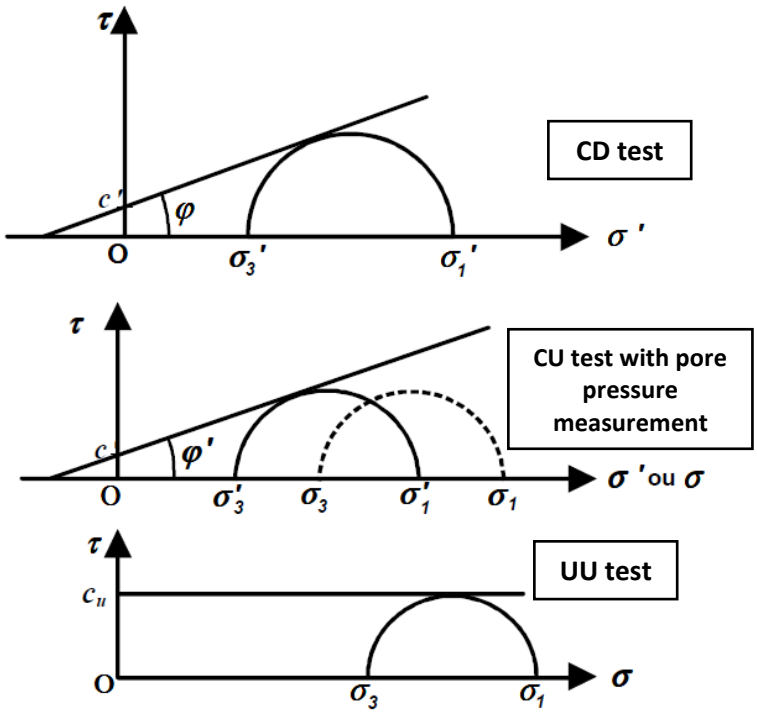

Figure 3.15 Interpretation of different types of triaxial tests

The triaxial test is the most commonly used, but other tests are also available:

– isotropic compression (triaxial test for which $\sigma_1 = \sigma_2 = \sigma_3$ throughout the test);

– direct shear;

– unconfined compression ($\sigma_2 = \sigma_3 = 0$).

The last test is easy to interpret in terms of total stresses. Since the Mohr circle passes through the origin and has σ_1 as its diameter, it follows that:

$$c_u = \frac{\sigma_1}{2}$$

3.8 Short-term and long-term conditions

In soil mechanics, the mechanical behavior of soils is commonly idealized by considering two situations:

- **short-term conditions:** this is the initial stage, usually corresponding to the construction phase, during which the soil is subjected to loading without drainage, that is, at constant volume (assuming the soil is saturated);

Short term ⇔ undrained conditions

- **long-term conditions:** this is the final stage, after the establishment of the final hydraulic regime.

Long term ⇔ final hydraulic regime

The time required for the transition from short-term to long-term conditions depends mainly on the permeability of the soil.

- **Case of coarse-grained soils:** the permeability is high enough for any local excess pore water pressure to dissipate almost instantaneously compared with the rate of construction. The soil is therefore considered to be immediately under long-term conditions. Stress analyses are performed in terms of effective stresses, using the parameters c' and φ'.
- **Case of fine-grained soils:** the transition from short-term to long-term conditions may take several months or even several years. It is therefore necessary to distinguish between two regimes:
  - in *the short term*, under undrained conditions, stress analyses are carried out in terms of total stresses, using c_u and φ_u; in practice, the undrained shear strength c_u, determined from tests simulating these loading conditions, is used;
  - in *the long term*, analyses are carried out in terms of effective stresses, using the parameters c' and φ', in the same way as for coarse-grained soils.

The stability analysis of geotechnical structures must therefore be performed for both situations. The external loads remain the same, but the manner in which the soil resists shear is different. Thus, short-term analysis is carried out in terms of total stresses, whereas long-term analysis is carried out in terms of effective stresses.

3.9 Exercises

Exercise 1

A dry sample of compacted sand is subjected to a triaxial test. It is assumed that the angle of internal friction, φ, is approximately 36°. If the minimum principal stress σ_3 is 300 kPa, what is the value of the maximum principal stress σ_1 at which the sample will fail?

Solution

For the given sand, the failure envelope is formed by two straight lines making an angle of 36° with the σ-axis, passing through the origin of the axes.

Let d and R represent the abscissa of the center and the radius of the Mohr circle at failure. We have (Figure below):

$$\frac{R}{d} = \sin\varphi$$

Thus:

$$\sigma_3 = d - R = \frac{R}{\sin\varphi} - R = R\frac{1-\sin\varphi}{\sin\varphi}$$

$$\sigma_1 = d + R = \frac{R}{\sin\varphi} + R = R\frac{1+\sin\varphi}{\sin\varphi}$$

Therefore:

$$\frac{\sigma_1}{\sigma_3} = \frac{1+\sin\varphi}{1-\sin\varphi} = \tan^2\left(\frac{\pi}{4}+\frac{\varphi}{2}\right)$$

$$\sigma_1 = \sigma_3 \tan^2\left(\frac{\pi}{4}+\frac{\varphi}{2}\right)$$

Substituting the values:

$$\sigma_1 = 300\tan^2(45+18) = 1160 \text{ kPa}$$

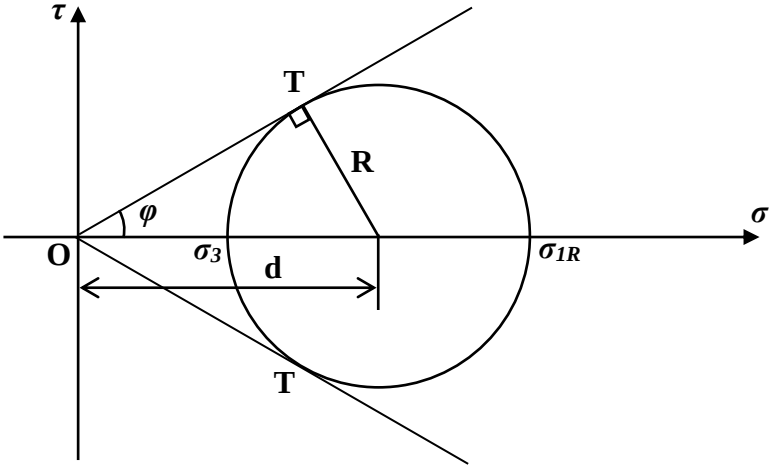

Exercise 2

Solve the previous problem assuming that the sand has a slight cohesion of 12 kPa.

Solution

In this case, the failure envelope is still formed by two straight lines, symmetric with respect to the σ-axis, making angles of 36° with the axis. However, due to the cohesion, these two lines no longer pass through the origin but through the points where $\sigma = 0$ and $\tau = \pm c$.

A calculation similar to the one performed in the previous problem gives us, by setting:

$$H = c\cot\varphi$$

$$\sigma_1 + H = (\sigma_3 + H)\tan^2\left(\frac{\pi}{4}+\frac{\varphi}{2}\right)$$

Thus:

$$\sigma_1 = (\sigma_3 + H)\tan^2\left(\frac{\pi}{4}+\frac{\varphi}{2}\right) - H$$

Given that:

$$H = 12\cot 36 = 16.5 \text{ kPa} \approx 17 \text{ kPa}$$

Now,

$$\sigma_{1R} = (300 + 17)\tan^2\left(45 + \frac{36}{2}\right) - 17 = 1203 \text{ kPa}$$

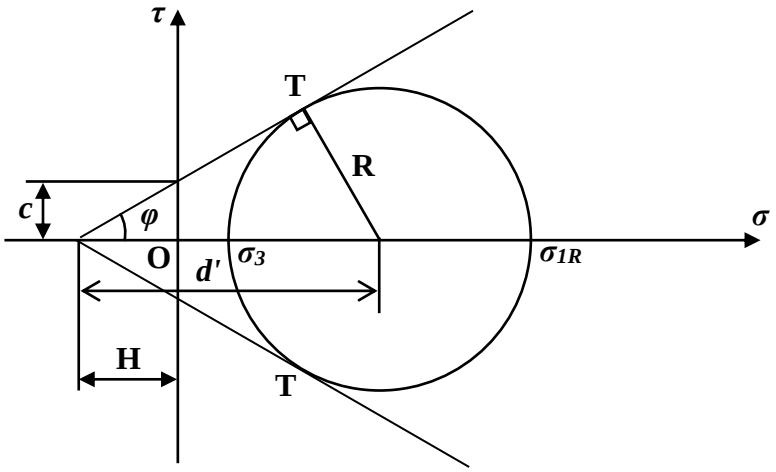

Exercise 3

Two triaxial tests are performed on a cohesive material. In the first test, the lateral pressure is 200 kPa, and failure occurs when an additional vertical pressure of 600 kPa is applied. In the second test, the lateral pressure is 300 kPa, and failure occurs when an additional vertical pressure of 800 kPa is applied.

What values can be assigned to c and φ for the material based on these tests?

Solution

Each of the two tests provides a Mohr circle at failure, which leads to the relationship established in the previous exercise:

$$\sigma_1 = (\sigma_3 + H)\tan^2\left(\frac{\pi}{4} + \frac{\varphi}{2}\right) - H$$

Let:

$$K = \tan^2\left(\frac{\pi}{4} + \frac{\varphi}{2}\right)$$

For the first test, we have:

$$\sigma_3 = 200 \text{ kPa}, \qquad \sigma_1 = 200 + 600 = 800 \text{ kPa}$$

For the second test, we have:

$$\sigma_3 = 300 \text{ kPa}, \qquad \sigma_1 = 300 + 800 = 1100 \text{ kPa}$$

We now have the following equations:

$$800 - 200K = H(K - 1) \qquad (1)$$

$$1100 - 300K = H(K - 1) \qquad (2)$$

From this, we can solve for *K*:

$$K = 3$$

Thus,

$$\tan^2\left(\frac{\pi}{4} + \frac{\varphi}{2}\right) = 3$$

Therefore:

$$\frac{\pi}{4} + \frac{\varphi}{2} = 60°$$

Which gives: $\varphi = 30°$

Equation (1) then gives:

$$H = \frac{800 - 200K}{K - 1} = 100$$

Thus:

$$c \cot \varphi = 100$$

From which we get:

$$c = 100 \tan \varphi = 100 \tan 36 = 57.7 \text{ kPa}$$

So:

$$c \approx 58\ kPA$$

Note: The result can also be obtained graphically by constructing the two Mohr circles and drawing their common tangent, as shown in the figure below.

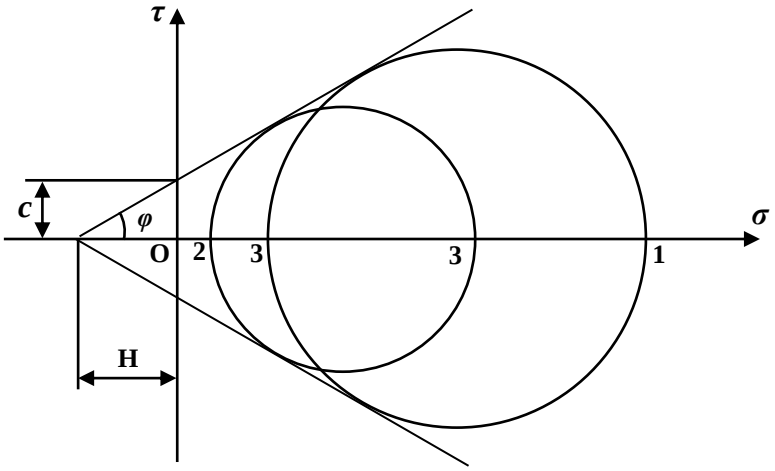

Exercise 4

Define the type of behavior, the mechanical properties involved, and the mechanical tests you would recommend for the following projects:

Project 1: A building resting on dry sand.

Project 2: The body of a dam to be built on a layer of saturated soft clay.

Project 3: A reservoir built on a saturated sandy layer continuous within an impermeable rock mass.

Project 4: Saturated silty soil with low undrained cohesion to be improved by consolidation using a fill.

Solution

Table 3.1 summarizes the behavior of each soil receiving the structure's load, the mechanical properties used in the calculations, and the shear tests to be performed in the laboratory.

It should be noted that in Project 2, it is possible to conduct a consolidated-undrained test with pore pressure measurement, which allows for obtaining both the short-term and long-term mechanical properties simultaneously.

Table 3.1 Soil behavior in the 4 projects

Project	**Consolidation**	**Mechanical behavior**	***c***	***φ***	**Type of test**
1	No	Drained	0	φ'	CD
2	Yes	Short-term (at t = 0)	c_u	0	UU
		Long-term (for $t \geq t_{100\%}$)	c'	φ'	CD
3	No	Undrained	0	φ	UU
4	Yes	Short-term	c_{cu}	φ_{cu}	C

Exercise 5

A triaxial compression test was performed on three samples of dense, dry, and clean silica sand. The results are provided in Table 3.2.

1) From the Mohr circles, graphically deduce the mechanical properties of this soil.
2) Determine the orientation of the failure plane.
3) Determine the stresses σ and τ acting on this plane in test 2, as well as the obliquity of the stress vector on this plane.
4) The study of the behavior of a plastic silty material in a triaxial test showed that it has the same friction angle as the previous sand and that it failed under σ_v = 486.5 kPa and σ_h = 25 kPa. Using the corresponding state theorem for sand, deduce the cohesion of the silt.

Table 3.2 Results of the drained triaxial test

Test	1	2	3
σ_h (kPa)	50	100	150
σ_v (kPa)	203.8	407.7	611.15

Solution

1) The cohesion of this dry, clean sand is zero. Plotting the three Mohr circles at failure allows us to fit the Mohr-Coulomb failure lines, which have the equation:

$$\tau = \pm(c + \sigma \tan \varphi)$$

For this type of soil, the lines pass through the origin while being tangent to the Mohr circles. Each tangency point actually represents a possible failure plane in the specimen. Figure below illustrates the Mohr circles and the line corresponding to the positive τ stresses, with the slope $\tan \varphi' = 0.761$; hence, φ' = 37.3°.

2) From the Mohr circles, it is clear that the failure planes are oriented at an angle $\theta = \pm(\pi/4 + \varphi/2)$ relative to the major plane, which is horizontal in this type of test. Thus: $\theta = \pm 63.6°$.

3) We have:

$$\sigma = \frac{\sigma_1 + \sigma_3}{2} - \frac{\sigma_1 - \sigma_3}{2} \sin \varphi = 160\ kPa$$

$$\tau = \pm \frac{\sigma_1 - \sigma_3}{2} \cos \varphi = \pm 122.4\ kPa$$

$$\tan \delta = \frac{\tau}{\sigma} = \pm \tan \varphi$$

Thus:

$$\delta = \pm 37.3°$$

4) To study the resistance of the silty soil (c, φ) , we can use the results from the sand test, provided we add an isotropic pressure $c/\tan \varphi$ to each failure plane. Therefore, we have:

Silty soil: σ_1 = 486.5 kPa, et σ_3 = 25 kPa,

Equivalent cohesionless soil: : $\sigma_1^* = \sigma_1 + c/\tan \varphi$ et $\sigma_3^* = \sigma_3 + c/\tan \varphi$.

Now:

$$\sigma_1^* - \sigma_3^* = \sigma_1 - \sigma_3 = 461.5\ kPa$$

Thus, using the results from test 3:

$$c/\tan \varphi = \sigma_1^* - \sigma_1 = 611.5 - 486.5 = 125\ kPa$$

So:

$$c = 125 \times \tan \varphi = 125 \times \tan 36 = 95.2 \text{ kPa}$$

Note: This result can also be obtained graphically by constructing the two Mohr circles and drawing their common tangent, as shown in the figure below.

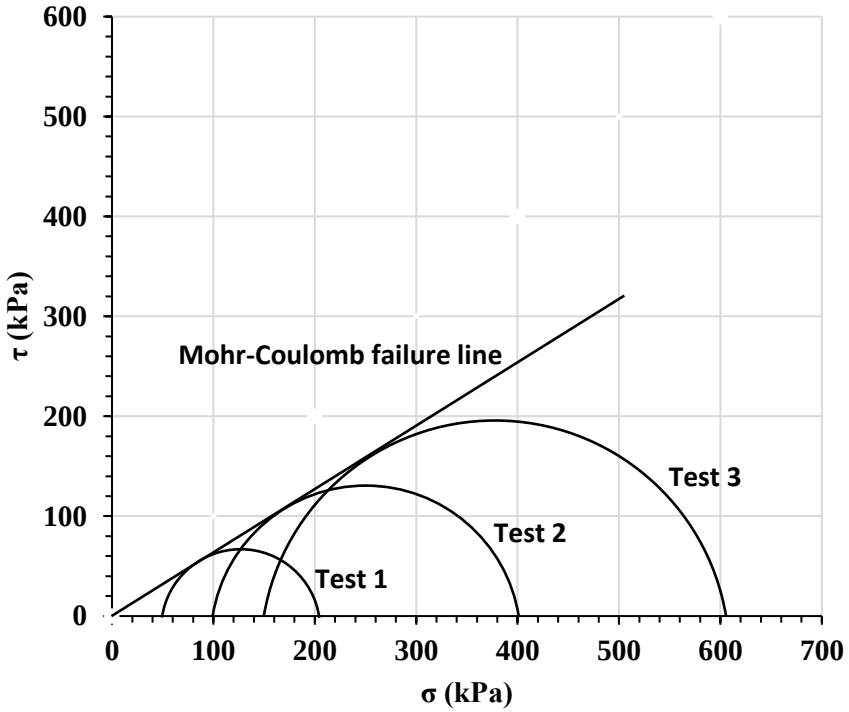
600
500
400
300
200
100
0
τ (kPa)
Mohr-Coulomb failure line
Test 3
Test 2
Test 1
0
100
200
300
400
500
600
700
σ (kPa)

Chapter 4
Soil investigation and exploration

4.1 Introduction

After learning the basic concepts of soil mechanics in the preceding chapters, this chapter introduces site or soil investigations. To design foundations for buildings and other civil engineering structures, including both shallow and deep foundations, as well as to assess the stability of slopes, it is crucial to understand the site conditions and the engineering properties of the soils present.

The purpose of this chapter is to:

- Plan a soil investigation.
- Describe soils in the field.
- Recognize the limitations of a soil investigation.
- Provide adequate engineering design parameters for the design of foundations and earth structures.

4.2 Importance and purposes of a soils investigation

A soils investigation is crucial in civil engineering as geological forces create complex formations that can affect the stability and costs of construction projects. These investigations are necessary to assess site conditions influenced by factors such as geological hazards (e.g., earthquakes and volcanic activity) and groundwater conditions. They help prevent structural failures that have historically led to significant loss of life and property due to unrecognized geotechnical issues. During a soils investigation, soil types are identified, observed, and sampled, although typically only a portion of a proposed site is examined to manage costs effectively. The limited data obtained necessitates estimations and judgments that greatly impact the design, performance, and financial viability of structures.

The primary objectives of a soils investigation include evaluating the suitability of the site for the intended project, facilitating the design process to ensure it is both effective and cost-efficient, and identifying potential construction challenges linked to local ground conditions. This comprehensive approach not only aids in the design and construction phases but also supports environmental assessments and overall project due diligence. Thus, a well-conducted soils investigation is integral to the successful implementation of any engineering project.

4.3 Phases of a soil investigation

The scope of a soil investigation depends on factors like the structure type, size, importance, the engineer's familiarity with the site, and local building codes. Sensitive structures, such as machine foundations and high-use buildings, generally require more thorough investigations. A simple investigation may suffice for familiar sites, but reducing the investigation below desired levels can increase risk.

A soil investigation typically has three components: *pre-design*, *during design*, and *during construction*. The pre-design component is more extensive and involves several phases:

- **Phase I (Desk Study):** This phase includes collecting available information such as site plans, structure details, previous reports, and maps (topographic, geologic, aerial, etc.). GIS tools and platforms like Google Earth can help visualize spatial data.
- **Phase II (site visit):** A visit to the site to observe the topography and geology. Observations should include photographs, sketches, and notes on existing structures, utility services, and geological features. Occasionally, boreholes may be dug for further exploration.
- **Phase III (detailed soils exploration):** A thorough examination to determine the geological structure, groundwater conditions, and to obtain soil samples for laboratory tests. In situ tests are also conducted.
- **Phase IV (laboratory testing):** Tests to classify the soil and determine its strength, permeability, and other critical parameters for the project.
- **Phase V (report writing):** A detailed report on the soils at the site, including exploration methods, test results, soil stratigraphy, groundwater conditions, and any potential construction challenges.

4.4 Soils exploration program

A soils exploration program usually involves test pits and/or soil borings (boreholes). During the site visit (Phase II), you should work out most of the soils exploration program. A detailed soils exploration consists of:

- Determining the need for and extent of geophysical exploration.
- Preliminary location of each borehole and/or test pit.
- Numbering of the boreholes or test pits.
- Planned depth of each borehole or test pit.
- Methods and procedures for advancing the boreholes.

- Sampling instructions for at least the first borehole. The sampling instructions must include the number of samples and possible locations. Changes in the sampling instructions often occur after the first borehole.
- Determining the need for and types of in situ tests.
- Requirements for groundwater observations.

4.5 Geophysical methods

There are several geophysical exploration methods available. They are nondestructive techniques used to provide spatial information on soils, rocks, and hydrological and environmental conditions.

4.5.1 Ground penetration radar survey

Ground penetration radar (GPR) sends high-frequency (10 to 1000 MHz) electromagnetic radiation pulses into the ground and detects refracted signals from subsurface objects and boundaries between different materials. It produces underground cross-sectional, two-dimensional images of the soils and subsurface features.

4.5.2 Seismic surveys

In this method, seismic vibrations (mostly done by mechanical impulses) are sent to the ground and the propagated wave signals are monitored by geophones as shown in Figure 4.1.

- **Seismic reflection survey:** As seen in Figure 4.1(a), impulse signals are sent from a ground surface and direct arrivals of P waves (compression waves) through the upper soil media and reflected ones on the lower material boundaries are detected on the ground surfaces at several locations. By knowing the distances and the arrival times of waves between the source and the receiver, the thickness and P wave velocity of the top soil layer are calculated.
- **Seismic refraction survey:** As seen in Figure 4.1(b), critically refracted signals on the material boundaries are the ones to arrive earlier than direct P wave arrivals at a geophone on the ground surface if lower layer materials are denser and have higher P wave velocities. In this method, thicknesses of sublayers and P wave velocities of each sublayer can be computed by the measured wave arrival time at several geophones located at different distances from the impulse.
- **Cross-hole seismic test:** As seen in Figure 4.1(c), two adjacent boreholes are used for impulses and geophones at several different depths. When the distance between two boreholes and measuring P wave arrival times are known, P wave velocities of each sublayer are obtained.

- **Downhole (or uphole) seismic test:** As seen in Figure 4.1(d), multiple geophones that are placed inside the wall of a borehole receive P wave signals from the ground surface. When the depth of geophone locations and measuring P wave arrival times are known, soil stratification can be prepared. The uphole test (not shown in Figure 4.1) is the reversed technique to the downhole method; impulses are given at several depths in the borehole and a geophone receiver is placed on the ground surface.
- **Surface wave seismic survey:** Involves generating body and surface waves through impulses at ground points. Rayleigh waves, a type of surface wave, are recorded at two distant locations, with their velocities influenced by near-surface soil properties. Initially, shear wave velocities for each soil layer are assumed, then Rayleigh wave propagation is computed. After comparing computed and measured velocities, new shear wave velocities are assigned iteratively. This method, known as spatial analysis of surface wave (SASW), allows for quick surveys without boreholes, reaching depths greater than 100 m and facilitating soil stratification.

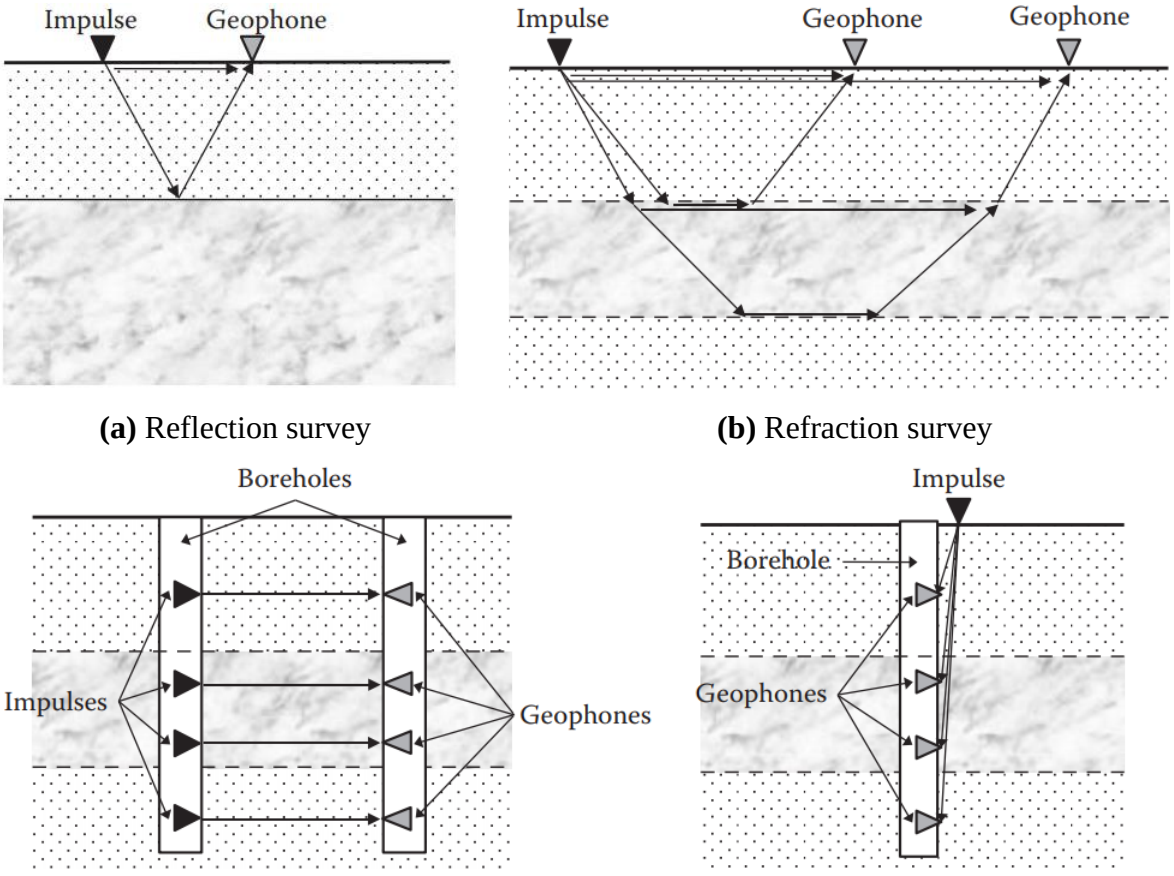

(a) Reflection survey **(b)** Refraction survey

(c) Cross-hole seismic test **(d)** Downhole seismic test

Figure 4.1 Seismic surveys

4.5.3 Electrical resistivity

Electrical resistivity measurements are essential for identifying groundwater depth, detecting clays, and assessing groundwater conductivity. Soil resistivity, measured in ohm-centimeters, decreases with increased moisture content, with wet fine-grained soils exhibiting lower resistivity than wet coarse-grained ones. The measurement process involves placing four electrodes in the ground and applying an AC current; resistance is calculated from the voltage and current, adjusted by a geometric factor. Electrodes are typically spaced to measure depths under 10 m and for deeper investigations, spacings of up to 150 m are used. Water is added to enhance the electrical contact during measurements. A resistivity profile is created through successive measurements at varying electrode spacings.

4.5.4 Additional geophysical techniques in geotechnical engineering

Other geophysical methods of interest in geotechnical engineering include gamma density, which estimates soil density and porosity, and neutron porosity that measures hydrogen density for porosity below groundwater levels. Sonic-VDL assesses seismic velocity to determine soil stiffness and bedrock elevation, while microgravity detects subsurface density changes and cavities through small gravity anomalies measured by a gravimeter.

4.6 Borehole drilling

In order to obtain parameters for foundation design, drilling boreholes at the site is essential. Disturbed or undisturbed samples are collected for soil classification and various laboratory tests. Field tests are also performed directly to obtain these parameters. The number of borings and the termination depth are determined by the engineer's judgment based on the size of the project, type of the structure, structural load, spatial variation of soil conditions at the site, existence of problematic soils, site exploration budget, etc.

Table 4.1 Guideline for spacing of borings

Structure or Project	**Spacing of Borings (m)**
Highway (subgrade survey)	60-600
Earth dam, dikes	15-60
Borrow pits	30-120
Multistory buildings	15-45
One-story manufacturing plants	30-90

4.6.1 Number of borings

At least one boring under the heaviest location of the structure should be made. Tables 4.1 and 4.2 show, respectively, guidelines of spacing of boreholes for different construction project types, as well as the minimum number of boreholes based on building and subdivision sizes.

Table 4.2 Guideline for minimum number of boreholes

Buildings		**Subdivisions**	
Area (m^2)	**Minimum Number of Boreholes**	**Area (m^2)**	**Minimum Number of Boreholes**
<100	2	<400	2
250	3	8000	3
500	4	20000	4
1000	5	40000	5
2000	6	80000	7
5000	7	400000	15
6000	8	--	--
8000	9	--	--
10000	10	--	--

4.6.2 Depth of boreholes

The depth of a borehole depends on many factors, such as foundation type (shallow or deep foundation), structural load, type of subsurface soils, etc. At least enough depth, for which engineering parameters are needed in the design phase, should be maintained. Some guidelines are the following:

- When the settlement computation of clayey soils is needed, the borehole depth should be deep enough so that the vertical stress increment $\Delta\sigma$ due to the new footing is about 10% or less of the stress increment at the footing base.
- Borings should penetrate through unsuitable soil strata such as unconsolidated fills, peat, organic soils, etc.
- The boring should penetrate into the supporting strata of piles with a minimum of 5 to 6 m in order to assure enough thickness of the supporting layer.
- The boring should penetrate a minimum of 3 m into rock when encountered. During the initial stage of boring practice, the termination depth should be flexible to accommodate unanticipated ground conditions that might be encountered.

4.7 Soil sampling

The objective of soil sampling is to obtain soils of satisfactory size with minimum disturbance for observations and laboratory tests. Standard Penetration Test (SPT) samples are unsuitable for determining critical soil parameters, necessitating undisturbed specimens typically obtained using thin wall Shelby tubes, which have diameters ranging from 50 to 150 mm, with the 50 to 75 mm sizes being most common. To prevent disturbance, the wall of the tube should maintain a specific strength-to-thickness ratio, ideally ensuring that the ratio of the tube section area to the soil area is below 0.10. The sampling process involves the tube being pushed into the ground smoothly at the desired depth, with both ends sealed to preserve moisture during transport to the laboratory for testing. Alternative techniques such as piston samplers and pitcher samplers exist, the former effectively suited for soft clays by minimizing wall friction during sample extraction, and the latter designed for use in stiff clays and cemented sands, adapting to different material conditions encountered (Figure 4.2). Despite being termed "undisturbed," these samples may still experience some disturbance due to unavoidable wall friction, in-situ stress relaxation post-extraction, and additional factors that can compromise the integrity of the specimens.

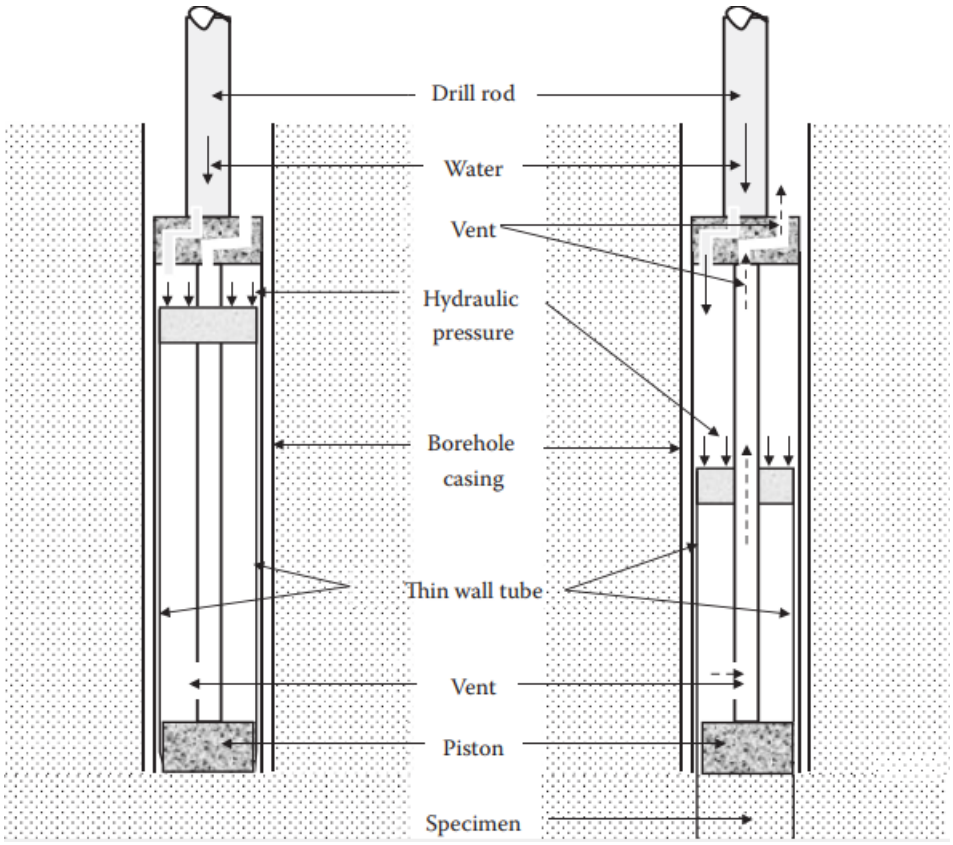

Figure 4.2 schematic diagram of a piston sampler

4.8 Groundwater Conditions

The groundwater table information is essential for foundation design. It affects the computations of unit weight (total versus submerged) and hence effective stress (Chapter 7). It also influences the construction process. Groundwater is monitored during the boring process. Observation wells and piezometer monitoring are very common.

An ***observation well*** is usually installed in a borehole with a slotted section of smaller diameter PVC (polyvinyl chloride) pipe. The level of the water table is measured by dropping a tape in the well.

A ***piezometer*** consists of porous stone at the tip that is connected to a plastic standpipe in the borehole and can be used for continuous monitoring of water pressure change at the tip section. The void in the borehole should be sealed by bentonite cement grout. This is also often used to monitor water pressure monitoring in a confined aquifer.

In both cases, it may take a few hours for highly permeable soils to several weeks for low permeable soils to obtain a stable reading. Continuous monitoring of the groundwater table is needed to obtain its seasonal variation.

4.9 Soils laboratory tests

Soils laboratory tests involve taking samples from the field to evaluate their physical and mechanical properties for foundation design and construction material use. Disturbed samples from standard samplers are primarily used for visual inspection and physical property tests, while undisturbed samples from thin-walled samplers assess both physical and mechanical properties. The accuracy of test results, particularly for mechanical properties, can be impacted by sampling and handling disturbances, necessitating careful preservation of sample integrity, often achieved by coating samples with wax to prevent moisture loss.

4.10 Standard penetration test

The standard penetration test (SPT) was developed circa 1927 and it is perhaps the most popular field test. The SPT is performed by driving a standard split spoon sampler into the ground by blows from a drop hammer of mass 63.5 kg falling 760 mm (Figure 4.3). The sampler is driven 152 mm into the soil at the bottom of a borehole, and the number of blows (N) required to drive it an additional 304 mm is counted. The number of blows (N) is called the standard penetration number.

The word “standard” is a misnomer for the standard penetration test. Several methods are used in different parts of the world to release the hammer. Also, different types of anvils, rods, and rod lengths are prevalent. Various corrections are applied to the N values to account

for energy losses, overburden pressure, rod length, and so on. It is customary to correct the *N* values to a rod energy ratio of 60%. The rod energy ratio is the ratio of the energy delivered to the split spoon sampler to the free-falling energy of the hammer. The corrected *N* values are denoted as N_{60} and given as:

$$N_{60} = N\left(\frac{ER_r}{60}\right) = NC_E$$

where ER_r is the energy ratio and C_E is the 60% rod energy ratio correction factor.

Correction factors for rod lengths, sampler type, borehole diameter, and equipment (60% rod energy ratio correction) are given in Table 4.3. We can write a composite correction factor, C_{RSBE}, for the correction factors given in Table 4.3 as:

$$C_{RSBE} = C_R C_S C_B C_E$$

where C_R, C_S, C_B, and C_E are correction factors for rod length, sampler type, bore hole diameter, and rod energy correction, respectively.

Compactness of coarse-grained soils based on *N* values is given in Table 4.4. The corrected *N* value is:

$$N_{cor} = C_{RSBE}N$$

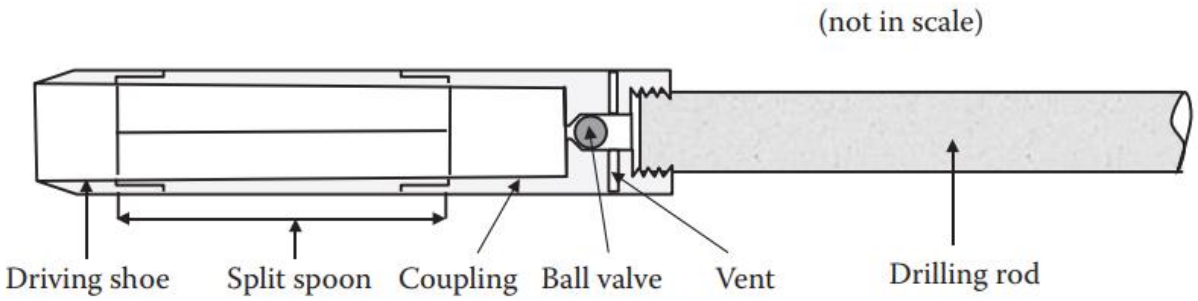

Figure 4.3 Schematic diagram of an SPT split-spoon sampler

The SPT is very useful for determining changes in stratigraphy and locating bedrock. Also, you can inspect the soil in the split spoon sampler to describe the soil profile and extract disturbed samples for laboratory tests.

The SPT is simple and quick to perform. The equipment is widely available and can penetrate dense materials. SPT results have been correlated with engineering properties of soils, bearing capacity, and settlement of foundations. SPT tests are unreliable for coarse gravel, boulders, soft clays, silts, and mixed soils containing boulders, cobbles, clays, and silts.

Table 4.3 Correction factors for rod length, sampler type, and borehole size

Correction factor	**Item**	**Correction factor**
C_R	Rod length (below anvil)	$C_R = 0.05L + 0.61$; 4 m < $L \leq$ 6 m $C_R = -0.0004L^2 + 0.017L + 0.83$; 6 m < L < 20 m $C_R = 1$; $L \geq$ 20 m L = rod length
C_S	Standard sampler	C_S =1
	U.S. sampler without liners	C_S =1.2
C_B	Borehole diameter:	
	65 mm to 115 mm	C_B =1
	152 mm	C_B =1.05
	200 mm	C_B =1.15
C_E	Equipment:	
	Safety hammer (rope, without Japanese "throw" release)	C_E = 0.7-1.2
	Donut hammer (rope, without Japanese "throw" release)	C_E = 0.5-1
	Donut hammer (rope, with Japanese "throw" release)	C_E = 1.1-1.4
	Automatic-trip hammer (donut or safety type)	C_E = 0.8-1.4

Table 4.4 Compactness of coarse-grained soils based on *N* values

N	**Compactness**
0-4	Very loose
4-10	Loose
10-30	Medium
30-50	Dense
> 50	Very dense

4.11 Cone penetration test

The cone penetrometer is a cone with a base area of 10 cm² and cone angle of 60° (Figure 4.4) that is attached to a rod. An outer sleeve encloses the rod. The thrusts required to drive the cone and the sleeve into the ground at a rate of 2 cm/s are measured independently so that

the end resistance or cone resistance and side friction or sleeve resistance may be estimated separately. Although originally developed for the design of piles, the cone penetrometer has also been used to estimate the bearing capacity and settlement of foundations.

The piezocone (uCPT or CPTu) is a cone penetrometer that has porous elements inserted into the cone or sleeve to allow for porewater pressure measurements. The measured porewater pressure depends on the location of the porous elements. A load cell is often used to measure the force of penetration. The piezocone is a very useful tool for soil profiling.

The cone resistance is influenced by several soil variables such as stress level, soil density, stratigraphy, soil mineralogy, soil type, and soil fabric. Results of CPT have been correlated with laboratory tests to build empirical relationships for strength and deformation parameters. Investigators have also related CPT results to other fi eld tests, particularly SPT.

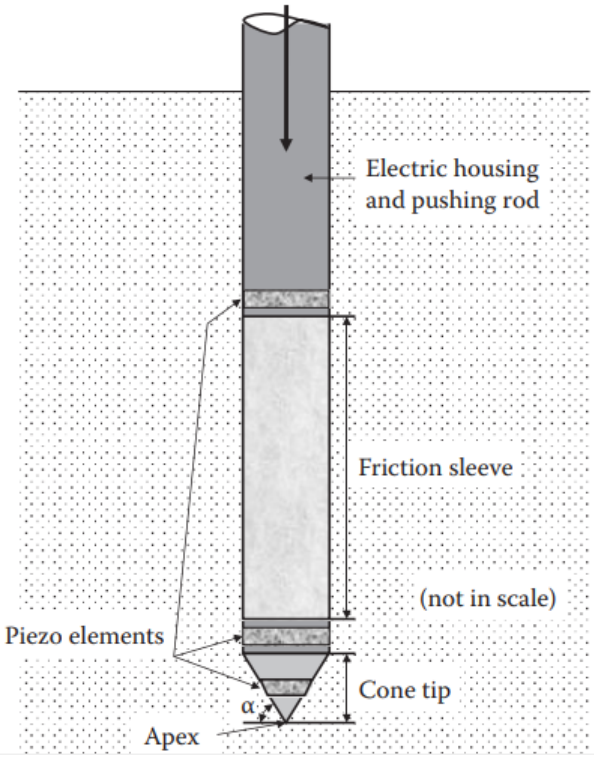

Figure 4.4 Typical cone penetrometer (piezocone)

4.12 Other in-situ tests

4.12.1 Vane shear test

For the vane shear test (VST) device, a rigid, cross-shaped vane such as seen in Figure 4.5 is often used in the field. A vane is installed on the tip of a boring rod and pushed into the soil. The shaft is then twisted to rotate the vane blades, which shear undisturbed soil around them. Torque is continuously measured until the maximum torque is obtained at failure. Shear

resistance comes from the perimeter area and the top and the bottom surfaces of the vane. The measured maximum torque T_f and the undrained shear strength C_u are related by:

$$T_f = \pi c_u \left(\frac{D^3}{8} + \frac{D^2}{2} H \right)$$

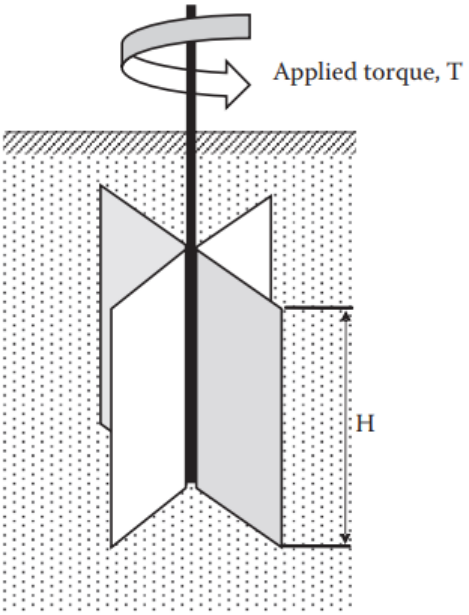

Figure 4.5 Vane shear test device

4.12.2 Pressuremeter test

The pressuremeter was developed in Europe in the 1950s as one of the in-situ test methods. The test determines stress–strain behavior and compressibility characteristics of soils in the field. A cylindrical probe with a common size of 58 mm diameter and 450 mm in length is inserted in a bored hole, as seen in Figure 4.6, or it is self-drilled into the soil with a drilling bit on its tip section (self-boring pressuremeter). The probe consists of three sections (lower guard cell, test section in the middle, and upper guard cell) with the same diameters. After the probe is placed at the desired location in a borehole, the test section is expanded by hydraulics or gas. Expansion of the test section pushes the soils around it; as a result, a relationship between the applied pressure and measured volume change can be obtained. The relationship is then interpreted to obtain soil's elastic modulus, shear modulus, compressibility, and shear strength values semi-empirically. This method is used to test soil in a field condition, and thus provides valuable data, but the results depend on semi-empirical correlations.

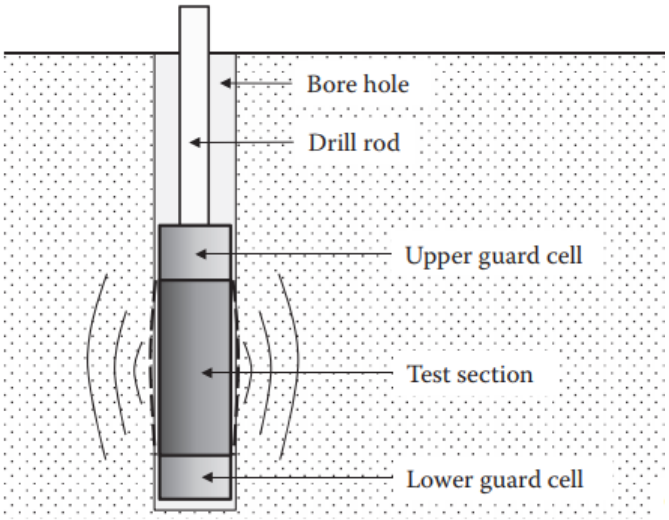

Figure 4.6 Pressuremeter

4.12.3 Dilatometer test

The dilatometer was developed in Italy in the early 1970s. The probe consists of a tapered flat blade (95 mm wide, 15 mm thick, 240 mm long) as seen in Figure 4.7. In the center section of the probe, a 60 mm diameter flexible metal membrane is installed. The probe is pushed from the bottom of the borehole into undisturbed soil. A metal membrane is then inflated by pressure and the pressure and response curve is obtained. The result is correlated to the soil's elastic modulus, lateral earth pressure coefficient, undrained shear strength, etc. This could provide valuable design parameters from in-situ tests, but the results also depend on empirical correlations as in the case of a pressuremeter.

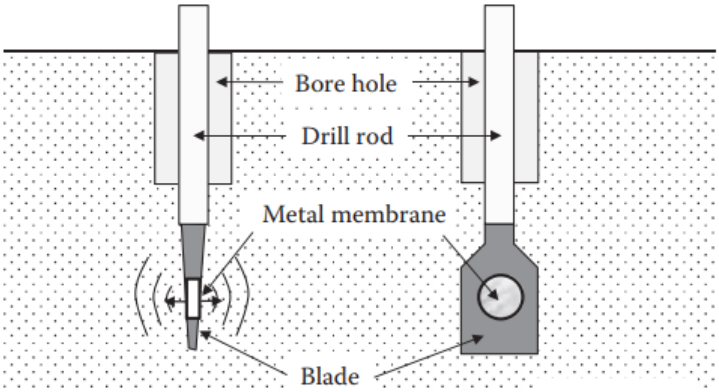

Figure 4.7 Flat plate dilatometer

4.13 Exercises

Exercise 1

In your area, choose a project under construction or a recently constructed project such as a road or a building. Obtain the soils (geotechnical) report and review it.

Exercise 2

Obtain borehole logs from a building site in your area. Describe the geology, the methods used in the soils exploration, and the type of fi eld tests used, if any.

Exercise 3

The blow counts for an SPT test at a depth of 6 m in a coarse-grained soil at every 0.152 m are 8, 12, and 15. A donut automatic trip hammer and a standard sampler were used in a borehole 152 mm in diameter.

1) Determine the *N* value.
2) Correct the *N* value for rod length, sampler type, borehole size, and energy ratio to 60%.
3) Make a preliminary description of the compactness of the soil.

Solution

1) The *N* value is the sum of the blow counts for the last 0.304 m of penetration. Just add the last two blow counts.

$N = 12 + 15 = 27$

2) Correction factors

From Table 4.3, $C_R = 0.05L + 0.61$; 4 m < L < 6 m. Therefore, $C_R = 0.91$ for rod length of 6 m, $C_S = 1.0$ for standard sampler, and $C_B = 1.05$ for a borehole of diameter 152 mm. For a donut automatic trip hammer, $C_E = 0.8$ to 1.4; use $C_E = 1$.

$$N_{cor} = C_{RSBE}N = 0.91 \times 1 \times 1.05 \times 1 \times 27 = 26$$

3) Use Table 4.5 to describe the compactness.

For $N = 27$, the soil is medium dense.

References

ASTM, Standard test method for particle-size analysis of soils. Annual Book of ASTM Standards, vol. 04.08, Designations D 422-63, 2012

Bouafia, A. Aide-mémoire de mécanique des sols. Édition OPU, Alger, pp. 415, 2016

Bowles, J.E. Foundation analysis and design, 5th ed., McGraw–Hill, New York, 1996

Braja, M.D. Advanced soil mechanics. Third edition. Taylor and Francis New York, USA, pp. 594, 2008

Budhu, M. Soil mechanics and foundations. 3rd ed., John Wiley & Sons, INC., USA, pp. 781, 2011

Casagrande, A. Classification and identification of soils. Transactions of ASCE, vol. 113, pp. 901-991, 1948

Chapuis, R.P. Predicting the saturated hydraulic conductivity of sand and gravel using effective diameter and void ratio. Canadian Geotechnical Journal, vol. 41, no. 5, pp. 787-795, 2004

Costet, J., Sanglerat G. Cours pratique de mécanique des sols. 2nd ed., Dunod, 1981

Daniel, D.E. In-situ hydraulic conductivity tests for compacted clay. Journal of Geotechnical Engineering, vol. 115, no. 9, pp. 1205-1226, 1989

Holtz, R.D., Kovacs, W.D. An introduction to geotechnical engineering. Prince Hall Paperback, pp. 746, 1981

Ishibashi, I., Hazarika, H. Soil mechanics: fundamentals and applications. CRC Press, Taylor & Francis Group, Boca Raton London New York, pp. 420, 2015

London, A.G. The computation of permeability from simple soil tests. Geotechniques, vol. 3, pp. 165-183, 1952

Magnan, J.P. Résistance au cisaillement. Techniques de l'Ingénieur, Traité Construction, Paris, C216, pp. 1-24, 1991

Magnan, J.P. Description, identification et classification des sols. Technique de l'ingénieur, traité construction, Paris, C 208, pp. 1-16, 1997

Murthy, V.N.S. Geotechnical engineering: principles and practices of soil mechanics and foundation engineering. Marcel Dekker, New York, USA, 2003

Philipponnat, G., Hubert B. Fondations et ouvrages en terres. Éditions Eyrolles, Paris, pp. 546, 1998

Peck, R.B., Hanson, W.E., Thornburn, T.H. Foundation engineering. 2nd ed., John Wiley & Sons, New York, 1974

Proctor, R.R. Fundamental principles of soil mechanics. Engineering News Record, vol. 111, nos. 9, 10, 12, and 13, 1933

Robertson, P.K. Soil classification using the cone penetration test. Canadian Geotechnical Journal, vol. 27, no.1, pp. 151-158, 1990

Schlosser, F. Éléments de mécanique des sols. Presses de l'école nationale des ponts et chaussées, Paris, pp. 280, 1989

Skempton, A.W. Notes on the compressibility of clays. Quarterly Journal of the Geological Society of London, vol. 100, 119-135, 1944

Skempton, A.W. Standard penetration test procedures and the effects in sands of overburden pressure, relative density, particle size, aging and overconsolidation. Geotechnique, vol. 36, no. 3, pp. 425-447, 1986

Sowers, G.F. Introductory soil mechanics and foundations: geotechnical engineering. 4th ed., Macmillan, New York, 1979

Terzaghi, K. Theoretical soil mechanics. John Wiley & Sons, New York, 1943

Terzaghi, K., Peck, R.B., Mesri, G. Soil mechanics in engineering practice. 3rd ed., John Wiley & Sons, New York, 1996

Appendices

Appendix 1

Point Load

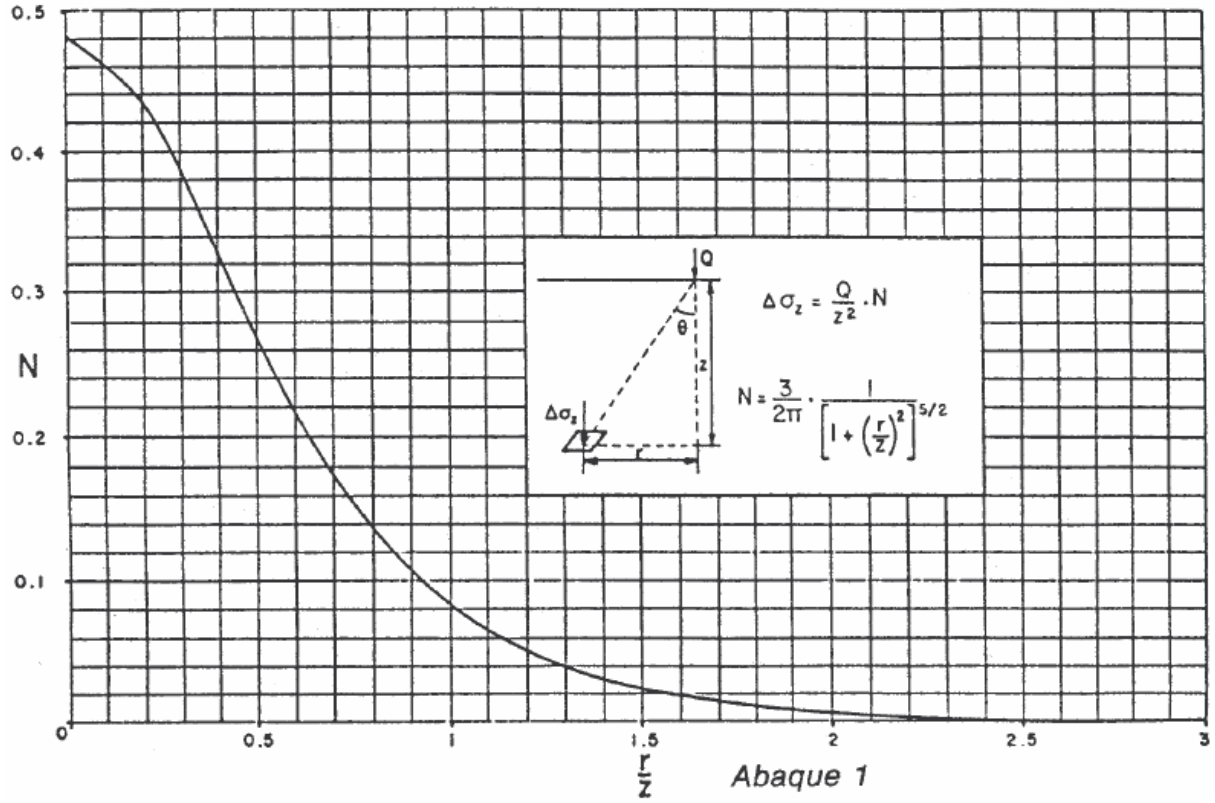

Abaque 1

Appendix 2

Uniform rectangular load

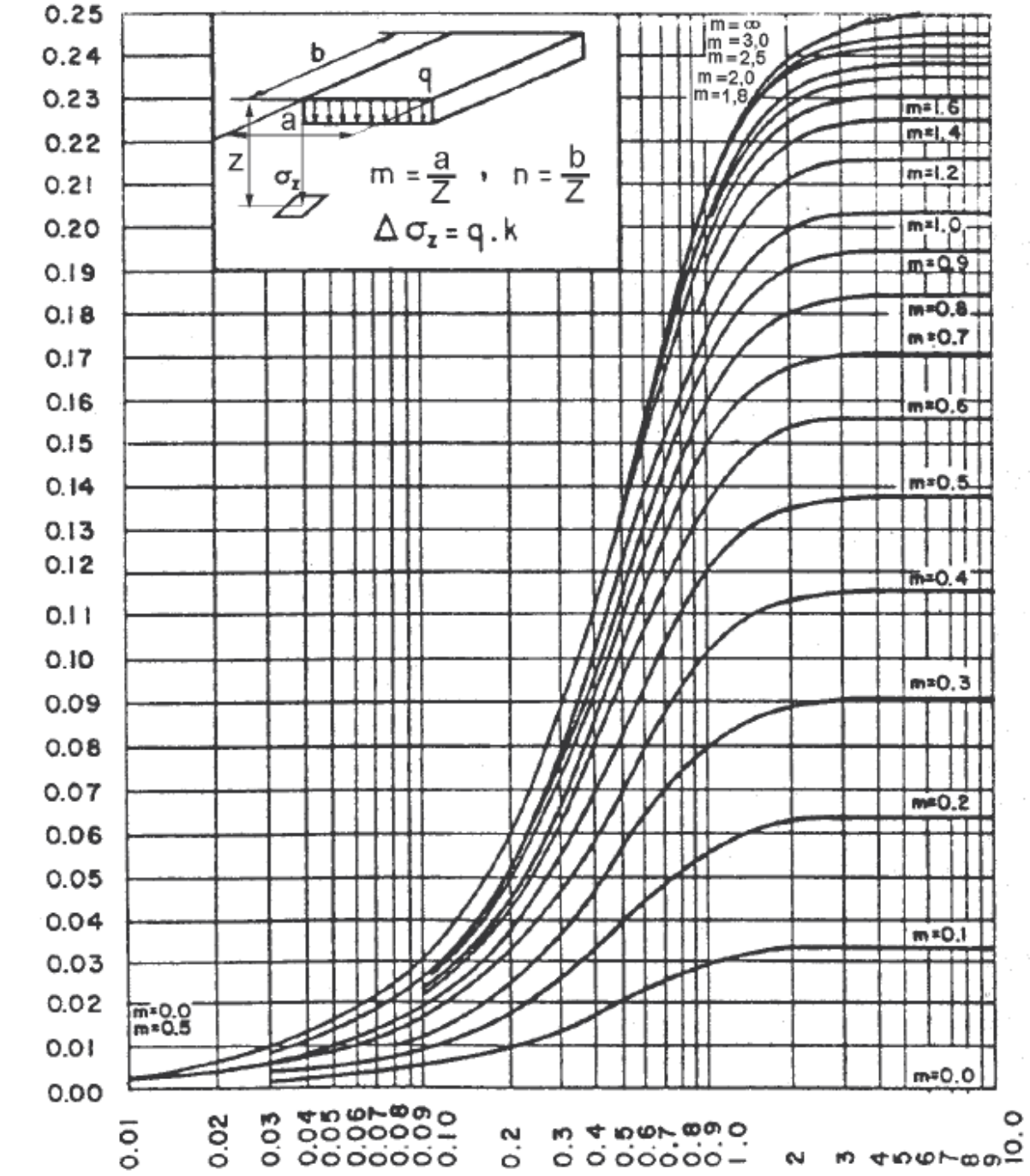

Note : m et n sont interchangeable

Abaque 2

Appendix 3

Circular load

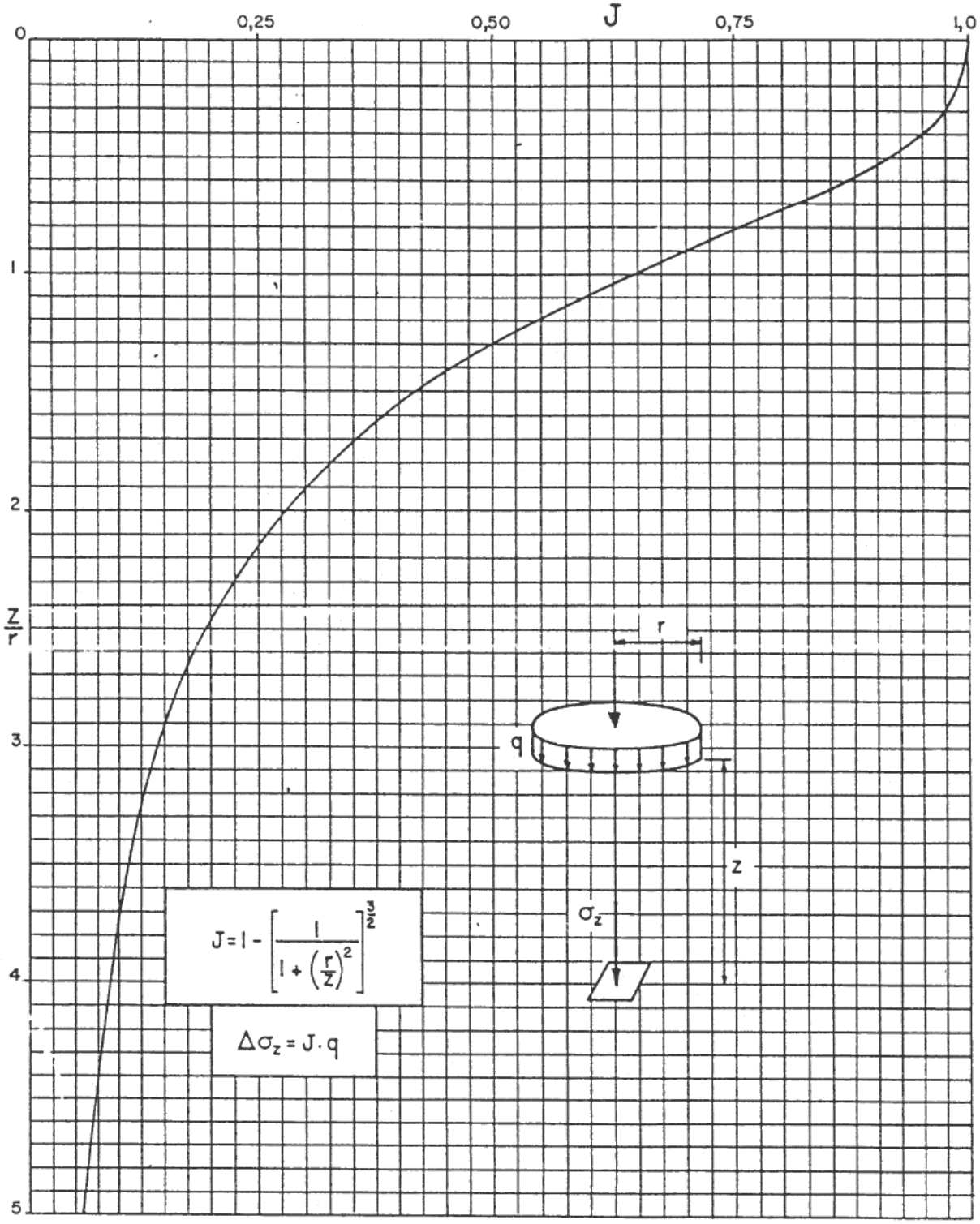

Abaque 3

Appendix 4

Embankment-shaped load of infinite length

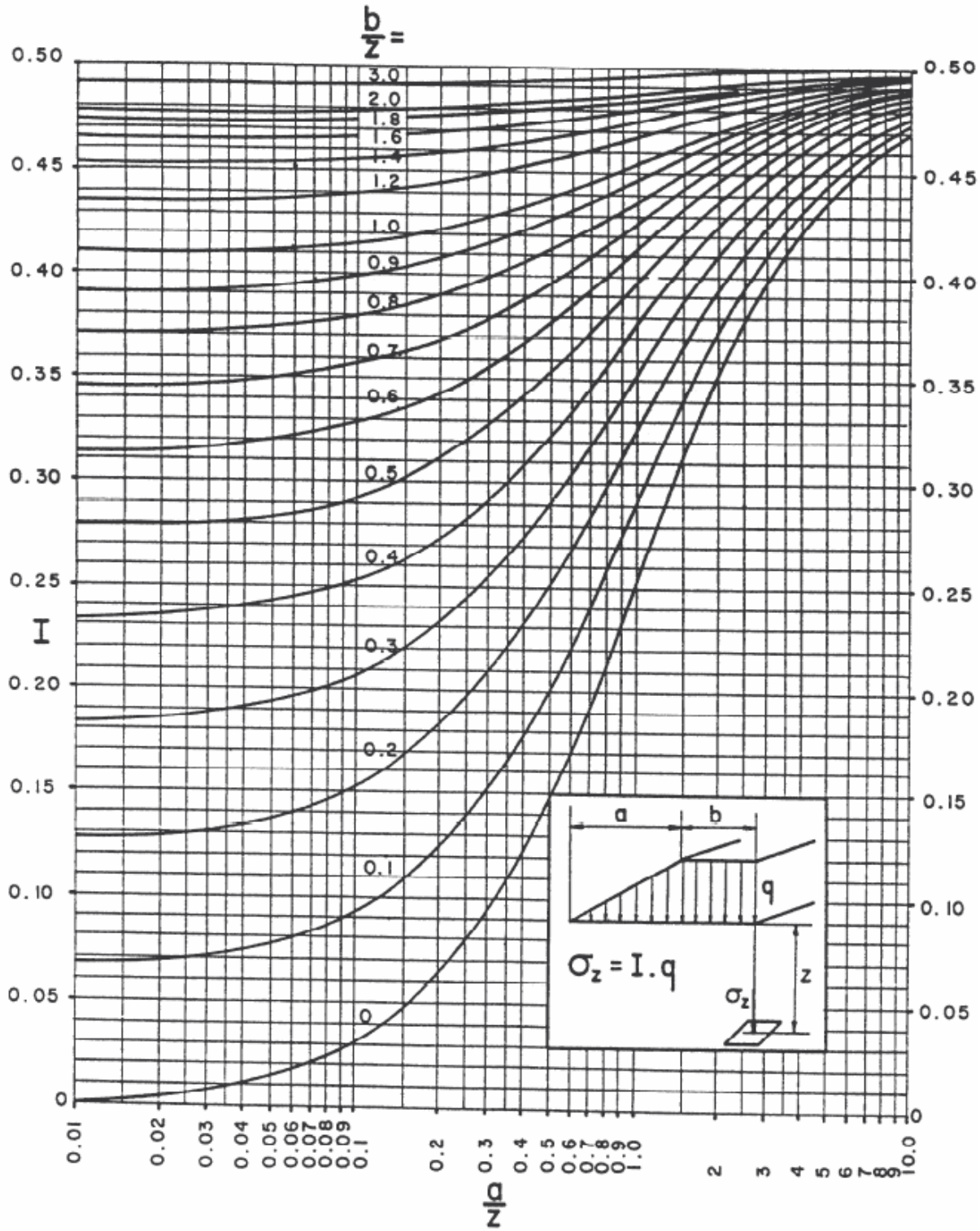

Abaque 4

Appendix 5

Some orders of magnitude for allowable angular distortions

angular distortions ω	**Comments**
Civil engineering structures with continuous beams, spans 14-15 m:	
ω = 1/350 à 1/250	Reinforced concrete structures
ω = 1/200 à 1/150	Prestressed concrete structures
ω = 1/200	Metal structures
Buildings	
ω > 1/750	Operation of mechanisms sensitive to settlements is disturbed
ω > 1/600	Defects appear in braced structures
ω > 1/500	Cracks appear
ω > 1/300	Initial cracks may appear in panel walls; problems may occur with overhead cranes
ω > 1/250	Inclination of tall and rigid buildings may become noticeable
ω > 1/150	Significant cracking can occur in panels and brick walls; structural damage is to be expected in all buildings

Appendix 6

- **Table of the function U (T_v)**

T_v	U	T_v	U	T_v	U	T_v	U
0.004	0.0795	0.060	0.2764	0.175	0.4718	0.600	0.8156
0.008	0.1038	0.072	0.3028	0.200	0.5041	0.700	0.8595
0.012	0.1248	0.083	0.3233	0.250	0.5622	0.800	0.8874
0.020	0.1598	0.100	0.3562	0.300	0.6132	0.900	0.9119
0.028	0.1889	0.125	0.3989	0.350	0.6582	1.000	0.9313
0.036	0.2141	0.150	0.4370	0.400	0.6973	2.000	0.9942
0.048	0.2464	0.167	0.4610	0.500	0.7640	∞	1.0000

- **Table of the function T_v (U)**

U	10 %	20 %	30 %	40 %	50 %	60 %	70 %	80 %	90 %	100 %
T_v	0.008	0.031	0.071	0.127	0.197	0.287	0.403	0.567	0.848	∞

$T_v = \frac{C_v}{d^2} \cdot t$ $C_v = \frac{K \cdot E_{oed}}{\gamma_w}$	T_v : time factor, U : average degree of consolidation, d : drainage length (equals the thickness of the layer if drained on one side), C_v : coefficient of consolidation.